Archaeological Investigations at Saintbury, Gloucestershire

By Duncan Wright, Scott Chaussée, Oliver Creighton, David Gould, Tim Kinnaird, Michael Shapland, Aayush Srivastava, and Sam Turner

June 2024

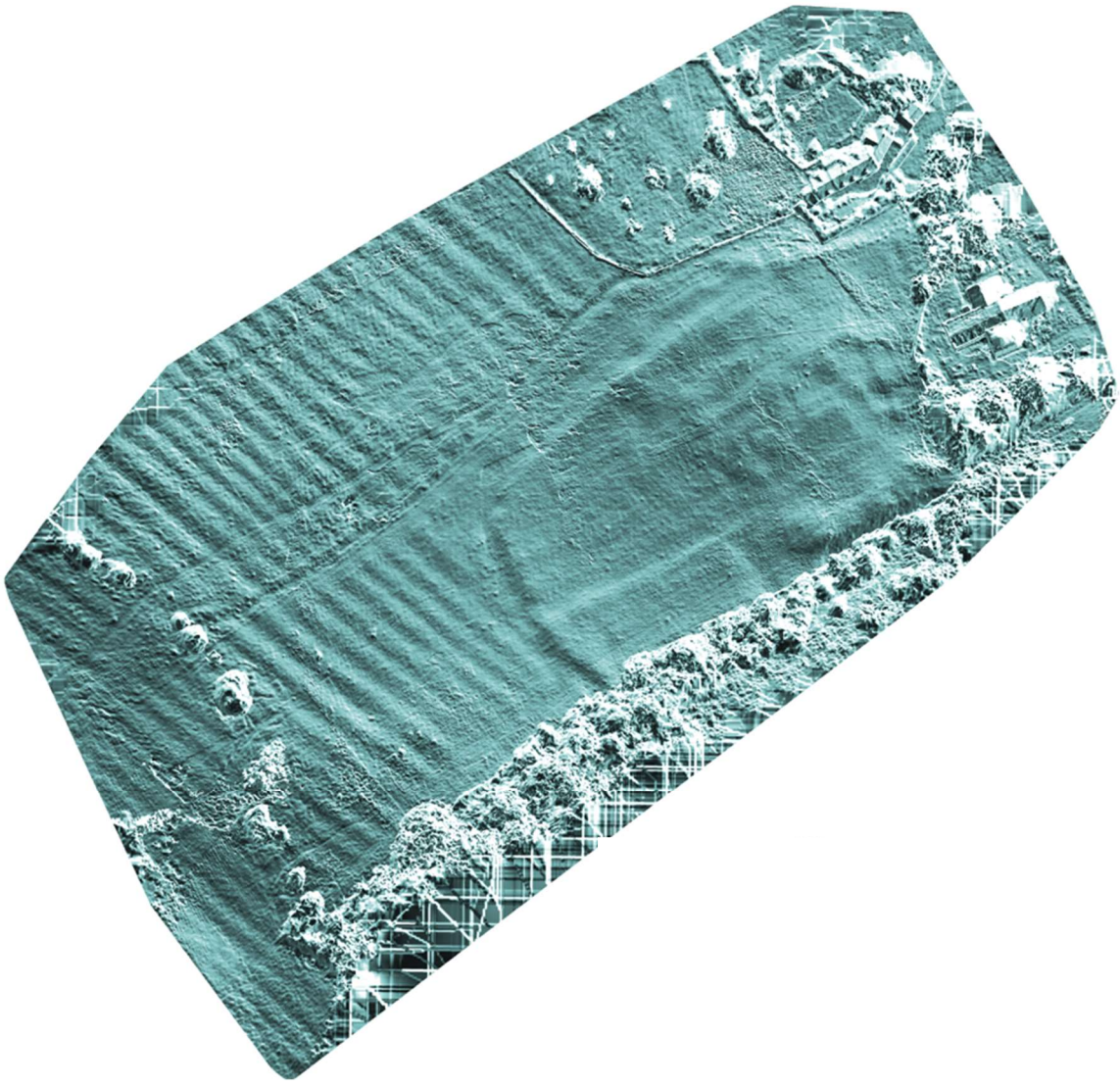

Newcastle University
University of Exeter
Portable Antiquities Scheme
www.finds.org.uk
UKRI Arts and Humanities Research Council

ARCHAEOLOGICAL INVESTIGATIONS AT SAINTBURY, GLOUCESTERSHIRE

ABSTRACT

Standing building assessment of St Nicholas' Church, Saintbury, and archaeological investigations of the surrounding landscape were conducted as part of the AHRC-funded research project Where Power Lies: The Archaeology of Transforming Elite Centres in the Landscape of Medieval England *c*. AD 800-1200*. OSL profiling and dating show the extensive earthwork complex south-west of the church probably originated in the late Iron Age, and in the Romano-British period a series of stone buildings, perhaps forming part of a villa or rural settlement, were raised. The outer earthwork defining the site was maintained into the ninth century when a lordly centre seems to have been developed: the 'S*æwine*'s burh' of the place-name. In* c.*1100 an impressive Romanesque church was built, perhaps over an Anglo-Saxon precursor, but it is unlikely that Norman tenants-in-chief perpetuated the adjacent high-status residence. Instead, they installed a motte and bailey nearby that provided oversight of the hundred meeting place and Roman road, a strategic location in a landscape that formed part of a long-lived ecotone between political groupings.*

INTRODUCTION

The parish church of St Nicholas, Saintbury, Gloucestershire, and its landscape were selected for a programme of detailed archaeological investigation as part of the AHRC-funded research project *Where Power Lies: The Archaeology of Transforming Elite Centres in the Landscape of Medieval England* c*. AD 800-1200*.[1] The project aimed to carry out a systematic assessment of the physical evidence for Saxo-Norman power centres in the English countryside, combining nationwide mapping of sites with closely juxtaposed churches and residences, with intensive fieldwork on a small number of these locations. Accordingly, it should be noted this report focuses specifically on the medieval phases (*c.*AD 400-1500) of Saintbury rather than being intended as a comprehensive account of its archaeological and historical development.

Saintbury was selected as a case study based upon its substantial archaeological potential, especially for evidence dating to the medieval period. St Nicholas' Church (NGR SP 11713 39459; HE List Entry No: 1088496) is largely medieval in date, with significant Romanesque elements and, in the field immediately to the south-west, extensive and well-preserved earthworks have been identified by previous authors as the remains of a 'manorial' complex (e.g. Bowden 2006, 181; Blair 2018, 394-5). The largely open and undeveloped character of the landscape surrounding the church, which is presently used for pastoral farming, also makes it an ideal candidate for archaeological survey (Figure 1). The site is located on a pronounced terrace of the Cotswold scarp with extensive views to the north. It forms the northern terminus of the village of Saintbury, which has an attenuated linear form suggestive of shrinkage.

A multifaceted and multi-phase programmed of fieldwork was instigated comprising geophysical and topographic survey, standing building assessment, and targeted excavation of

[1] AHRC Standard Research Grant (Award Reference: AH/W001187/1); Principal Investigator: Duncan Wright, Newcastle University; Co-Investigator: Oliver Creighton, University of Exeter.

earthwork features to gain samples for optically-stimulated luminescence (OSL) profiling and dating. Allied to desk-based archaeological and historical research, the scheme aimed to reveal new evidence to help clarify the extent, character, and chronological development of the lordly centre. The programme of fieldwork was carried out in three phases during 2023; the gradiometer survey and standing building assessment were conducted in July, excavation for OSL samples and earth resistance survey took place in September, and topographic survey, 3D modelling of the church via Unmanned Aerial Vehicle (UAV), and ground-penetrating radar (GPR) were carried out in November.

HISTORICAL AND ARCHAEOLOGICAL BACKGROUND

The historical development of Saintbury is poorly understood, largely due to a lack of previous research. The most prominent prehistoric feature in the area, situated 600m south of St Nicholas' Church, is the Iron-Age hillfort of Willersey Hill Camp (HE List Entry No: 1003327). The monument encloses an area of approximately 32ha, within its circuit is a Neolithic long barrow surviving as a rectangular mound. Further evidence for burials was identified by excavations in 1884 and 1987 (GHER No: 333), and it seems that the monument encompasses an area of perhaps quite extensive Neolithic and Bronze Age funerary activity, in a manner similar to that seen at the northern Cotswold's other large hillfort of Nottingham Hill Camp (Maddison 2021, 403). The extent to which prehistoric funerary activity extended further north from Willersey Hill Camp, towards St Nicholas' Church, has been a matter of discussion. Helen O'Neil and Leslie Grinsell (1960, 128) identify two Bronze-Age round barrows approximately 350m and 430m south of the church, but this identification is insecure, and the Gloucestershire Historic Environment Record (GHER) suggests they are natural (GHER Nos: 2775; 6987). Whether artificial or natural, the tumulus at NGR: SP 11889 39139 (GHER No: 6987) seems to have been extant by the early first millennium AD, as the Roman road here avoids the feature and deviates in its course as it heads northwards down the Cotswold escarpment. The distinctive kink in the course gives its name to the local name 'Buckle Street', part of the Roman road Ryknild Street (also spelt Ryknield Street) (Ivan Margary's rr18a) that in this southern section connected Lower Slaughter with Alcester (Margary 1955). Ryknild Street runs parallel to the eastern side of Willersey Hill Camp, and follows the initial line of Buckle Street for *c*.150m in a north-easterly direction. Whereas the route of Buckle Street then curves north, Ryknild Street retains its north-easterly orientation down the hill until it too projects north at the northern edge of Saintbury Coppice at NGR: SP 1253 3975. A single Roman coin from the fourth century AD has also been recorded by the Portable Antiquities Scheme in the north-east of Saintbury parish, and could be associated with a known Romano-British settlement at Weston-sub-Edge approximately 2km north-east of St Nicholas' Church (PAS Unique ID: WAW-F79FAB).

Although Saintbury itself is not named until Domesday Book, several tenth-century charters exist relating to neighbouring estates at Willersey and Broadway, the bounds of which mention 'Cada's Minster' (*cadan mynster*) (Sawyer 1968, nos 80, 786, 1327, 1385 & 1599). Della Hooke (1987, 96-9) locates this in the north-western corner of Willersey Hill Camp, around 600m south of St Nicholas' Church (Figure 2). The earliest phases of the church date

from the late eleventh century (see below), a provenance that broadly coincides with Saintbury's first appearance in the documentary record, in Domesday Book. The place-name derives from an Old English personal name Sǣwine and 'burh', an element that can interpreted in a number of different ways depending on context (Smith 1964, 256; Draper 2008; 2018, 306). In 1086 Saintbury is recorded as being held in chief by Hascoit Musard, who held extensive estates elsewhere in Gloucestershire as well as other parts of southern and midland England, and valued at £10, having been held in 1066 by Cynwy Chelle and valued at £10. By the time of Domesday, the manor contained 18 villagers, ten slaves and three smallholders, while there was land for 12 plough teams and a mill was valued at 5 pence (Williams and Martin 2002, 469; GDB folio 169). Saintbury remained in the Musard family until 1302, as an inquisition post-mortem of that year records how it was the principal seat of Malcolm Musard, and it seems that he held no other manors (Gloucestershire Archives D3439/1/328). Following Musard's death, the manor passed to Evesham Abbey, in the 30th year of Edward I (1301-02) (National Archives C 143/40/21).

In Domesday Book, Saintbury is documented as lying within Witley Hundred, the extents and meeting place of which are unknown, partly as the unit was subsumed into the more extensive Kiftsgate Hundred by at least 1220 (Anderson 1939, 2, 17). There are two main candidates for the meeting place of Kiftsgate Hundred, explored in some detail by John Baker and Stuart Brookes (2013, 150-6). The first, known as Kiftsgate Stone, lies 1.8km east-south-east of St Nicholas' Church on a ridgeway on the edge of the Cotswold scarp, and was the site of 'þe Kynges court' in the sixteenth century. The stone itself is a Neolithic or Bronze-Age monolith, standing to a height of about 1m, with a single round perforation through roughly its centre (HE List Entry No: 1003590). The longevity of Kiftsgate Stone as an assembly place is revealed not only by its continued use to proclaim royal coronations until William IV in 1830, but perhaps too its reputation as a place for congregation may have influenced the choice of site for the 'Cotswold Olimpick Games'; an event of games and sports established by at least 1612, and revived twice since, that takes place at Dover's Hill, 500m to the north. The second candidate for the meeting place of Kiftsgate Hundred is Kiftsgate Court, located roughly 6.5km north-east of Saintbury in Mickleton parish, for which there is a combination of place-name and topographic evidence indicating a former assembly site. The evidence for Kiftsgate Stone is certainly earlier in date, leading Olof Anderson to argue that this was the original assembly place, with Kiftsgate Court merely representing a doublet of the name (Anderson 1939, 19). The credentials for both locations are strong, however, and it seems instead that Kiftsgate Court acted as a supra-hundredal assembly point given its close proximity to a royal manor, with Kiftsgate Stone perhaps acting as the meeting place for the hundred (Baker and Brookes 2013, 156). It is notable that both locations, and indeed Saintbury itself, form part of a liminal zone at the intersection of three shires, a landscape that also represents the boundary of the Diocese of Worcester, and probably the limits of the kingdom of the Hwicce (Figure 3). Baker and Brooks (2013, 154) suggest that assembly places in areas such as these were 'occupying thresholds between different political groups within the territory', an important observation when considering the medieval development of Saintbury and its environs.

Several archaeological features of postulated medieval date have been recorded in the immediate vicinity of St Nicholas' Church, the most prominent of which are a series of well-preserved earthworks immediately to the south-west (GHER No: 26938). Commenting on the features in his *New History of Gloucestershire* Samuel Rudder (1779, 635) states that Saintbury's place-name is derived 'from the *Berg* or *Camp*, not far above the church, where the intrenchments are still visible, which the inhabitants call *Castle Bank*'. He goes on to suggest that this site was 'dependent on another very large one … raised probably by the same people…but lies in the adjoining parish of Willersey', in what is clearly a reference to Willersey Hill Camp (Rudder 1779, 635-6). In spite of this early identification, the earthworks south-west of the church have never been mapped by the Ordnance Survey, and have never been subject to scheduling. They were, however, recorded[2] and remarked upon as part of the North Cotswolds National Mapping Project by English Heritage (Stoertz 2012, 42). Despite the lack of detailed previous investigation, commentators have noted the general character of the primary features, consisting of an outer oval enclosure defined by a bank and ditch, abutting the hill scarp to the south and containing an inner series of earthworks that may represent the remains of buildings. This morphology has been considered by most as representing a 'manorial' centre (e.g. Bowden 2006, 181; Stoertz 2012, 42), with John Blair suggesting it is typical of a lordly site dating to around the period of the Norman Conquest (Blair 2018, 395). An area of ridge and furrow abuts the south-western part of the oval enclosure and also extends north-westwards from a footpath that follows its northern edge. The lack of evidence for earthworks on the line of the footpath suggests that this route may be of some antiquity, rather than a modern feature that has truncated existing ridge and furrow. To the south of the large outer enclosure, a hollow-way leads up a steep escarpment to a field containing further extensive ridge and furrow and an area that has been described as representing settlement shrinkage (GHER No: 2777). This proposed 'settlement', though, consists of only three building platforms recorded at NGRs: SP 1164 3928, SP 1166 3926 and SP 1167 3924 at the field's western edge, and the exact nature of these earthworks is unclear. A further area of proposed medieval settlement shrinkage has also been recorded at the northern end of Saintbury village in the area around Lower Farm and Middle Hill Farm (GHER No: 6883).

Two additional earthworks in the field immediately south of the church, up the steep scarp, are the remains of two pillow mounds. The features overlie an area of ridge and furrow providing a broad late medieval/post-medieval phasing, and indeed a rabbit warren is recorded in Saintbury in 1539 when *Le Conyngger* and its rabbits were leased by Evesham Abbey (Mills 1912, 658). This warren probably corresponds to the *Cony Green* field recorded on the 1841 tithe map (Glos. Archives GDR/T1/155) lying adjacent to the field containing these pillow mounds. The presence of a warren overlying ridge and furrow indicates a cessation of arable activities, possibly accompanied by settlement shrinkage or abandonment, and the subsequent adoption of pastoral farming. This agricultural regime evidently included rabbit warrening, although this was probably practiced alongside sheep farming, a common occurrence in north-east Gloucestershire (Gould 2017, 292). Indeed, the conversion of arable lands to pasture fields in this region was a particularly widespread phenomenon given the

[2] Historic England Monument Number: 1362224

continued prosperity of the Cotswold wool industry well into the post-medieval period, even after wool prices nationally had declined from their medieval heyday (Walrond 1973, 183; Dyer 1995, 156).

Situated 800m east-south-east of St Nicholas' Church is a triangular earthwork consisting of two conjoined mounds, situated within Weston Park near the crest of the escarpment (GHER No: 2434) (centred NGR: SP 1251 3903). The feature was annotated by the Ordnance Survey as early as the 1930s, and a field investigator noted not only that the ground had been artificially scarped in this area, but also observed traces of walling (Stoertz 2012, 40). It was described by Alan Saville (1980, 32) in his survey of the county's earthworks, and is suggested as a motte both by the GHER and the National Mapping Programme (Stoertz 2012, 40). The earthwork was omitted, however, from the famous castle gazetteers published by Derek Renn (1968) and David Cathcart King (1983), and was not considered a castle by Philip Davis who established the online *Gatehouse Gazetteer*.[3] Examination of LiDAR data clearly confirms the identification of a motte and bailey, although it seems to have undergone later modifications; it is heavily eroded on its western side, and the northern face has been truncated to form a more continuous slope, transforming the bailey into an unusual triangular shape (Figure 4). Some of these changes were presumably a product of continued use of the earthwork, or to make it more accessible, if indeed it did later serve as a prospect mound for the occupiers of Weston Park House. Viewshed analysis of the feature supports its interpretation as a castle, as it seems to have been located with strategic considerations in mind; a model generated using a height of 1.5m (slightly below standing height) from the top of the motte affords views over the assembly place at the Kiftsgate Stone, as well as stretches of Ryknild Street to the west and north (Figure 5).

A final archaeological feature that may be associated with Saintbury's medieval elite is an angular, half-oval, double-banked earthwork flanking the northern side of a stream 220m east of the village cross centred at NGR: SP 11962 40270 (GHER No: 2801). Although located roughly 800m north-east of the conjectured early lordly centre at St Nicholas' Church, it does lie in close proximately to a later medieval moated site (see below), and probably represents the remnants of a mill. The feature lies within a field named *The Neights* on the tithe map (Glos. Archives GDR/T1/155), which corresponds to a mill named *Ye Mill Naights* recorded in a 1683 record of charitable gifts belonging the church warden and minister of Saintbury (*ibid.*, D2202/2/4/2). Although therefore considerably later than the period of primary interest here, it is noteworthy that a mill is recorded in the manor of Saintbury at Domesday and *The Neights* could well perpetuate the approximate site of this medieval forerunner.

THE CHURCH OF ST NICHOLAS: STANDING BUILDING ASSESSMENT

Michael Shapland

Introduction

[3] https://www.gatehouse-gazetteer.info/English%20sites/1231.html

An analytical record of the standing structure of St Nicholas' Church was undertaken, aimed at better understanding the earliest phases of the building and to allow its relationship with the alleged medieval residence adjacent to be established. The church has been the subject of relatively little previous scholarship; the only published discussion of its fabric is in the regional Pevnsner Architectural Guidebook (Verey and Brooks 1999). Also useful are the detailed Listing description (HE List Entry No: 1088496), and a recent thorough gazetteer of the church furnishings (Church Recording Society 2022). A guidebook was published in 1960 (McCormick 1960).

Description

The present church is cruciform in plan, with an aisle-less nave, a relatively long square-ended chancel, a square northern transept, and a substantial southern tower topped by a spire (Figures 6-8). It is almost entirely of local limestone construction, with no evidence for re-used Roman brick and tile. The earliest extant phase is the nave (Figures 9-13). This generally consists of small and un-coursed rubble construction, with some ironstone amongst the limestone, the character of which is sufficiently rough as to indicate that it was originally plastered. In contrast, the quoins are well dressed, of side-alternate type: the western corners of the nave are clearly visible, whilst the original eastern quoins can be glimpsed where the tower and north transept meet the present chancel. The wall rests upon a low, chamfered plinth. Its upper levels were heightened when the present low, pitched roof was added in the fifteenth century: one stone corbel remains from the original roof, above the tower arch in the southern wall. The level of this corbel coincides with a clear break of construction visible externally. It is square with a rounded front, but otherwise undecorated. The internal elevations of the structure are plastered, and uninformative (Figures 14-15).

The outstanding surviving feature of the Norman nave is the north doorway, which lies mid-way along the nave wall (Figure 16). This is round-headed, of two orders, and constructed from well-dressed stone. The outer order is flanked by a pair of engaged columns with volute cushion capitals and round shafts: the shaft of the western column is richly ornamented with chevrons interspersed with roundels, whilst the eastern shaft is plain. The square column-bases were formerly gently stepped, and topped by a thick torus. The columns support a bulky roll-moulding between the outer order of voussoirs and the inner, which springs from a pair of chamfered imposts. The doorway's inner order has a semi-circular tympanum bearing incised lozenges. Above the doorway is a contemporary grotesque male face with prominent eyes, cheeks and nose (Figure 17). The opposing south doorway to the nave is also original, and of comparable design, although much plainer (Figure 18). It is round-headed, of two orders, but lacks the engaged columns of its northern counterpart. The outer order of voussoirs spring from a pair of chamfered imposts, and the shallow inner order has another tympanum, very similar to its northern counterpart, bearing incised lozenges. The doorway is surmounted not by a grotesque face but a circular sundial, which may not be original to the fabric of the wall (Bryant 2012).

In terms of windows, the only coherent example known from the church was removed in antiquity, and was reported in 1963 as being in the gable end of a nearby cottage (Figure 19) (Mackay 1963, 94). Efforts to locate this window in the village were unsuccessful. It took the form of a two-light window cut from a single block of stone: each light is round-headed, and bears a continuous chamfer. Single-light windows cut from single large stones are a feature of the area, with some dating to the sixteenth century, although this two-light example is less common, and convincingly early. A comparable two-light window with splayed jambs and round heads is known in the county at Daglingworth; rebuilt into a later medieval phase of the Church of the Holy Rood, the piece is formed from a re-used Roman altar (Mackay 1963, 81; Taylor & Taylor 1965, 189). Neither window is included in *The Corpus of Anglo-Saxon Stone Sculpture*, although the Daglingworth example has been suggested as pre-Conquest. Indeed, megalithic and through-stone windows are particularly characteristic of Anglo-Saxon architecture, especially where both the head and jambs are formed this way (Taylor & Taylor, 1965, 189; Taylor 1978, 836, 847). Further potential evidence for an early window takes the form of a possible column capital and drum, re-used high up in the building's western gable end, which was rebuilt in the fifteenth century (Figure 20). These stones are uncertain and not especially diagnostic, but are plausible as the remnant of a two-light window separated by a column — a style particularly characteristic of eleventh- and twelfth-century architecture (Stocker & Everson 2006, 36-44). A fragment of early Norman chevron ornament can also be seen built into the fourteenth-century chancel, but its origin is unknown (Figure 21).

One other early feature is a small stone figure with a tiny body, a large head, and stubby arms and legs, and – plausibly – the remains of a cloak or wings (Figure 22). It is re-set into the southern window of the fourteenth-century chancel, where it was deliberately defaced before concealment. It is of undoubtedly early – but uncertain – date, and has been taken as evidence for the existence of a previous stone church on this site (Bryant 2012). Alternatively, the figure may actually be of Roman origin, rather than medieval in date. A second figure of similar type is apparently re-set into the later medieval tower, although this could not be located (McCormick 1960). The remainder of the church (chancel, tower, north transept and porch) are of late thirteenth-century and later date, and will not be discussed here.

Interpretation

The earliest part of the church can be dated to *c*.1100 on the following grounds. The majority of its limited sculptural work, such as the south doorway and the two tympana, are quite plain in their character, which is generally taken as an indication of late eleventh-century work. The exception is the eastern jamb of the north doorway, which has volute cushion capitals and a richly ornamented chevron column, which is more generally associated with the early twelfth century and later. The fact that the north doorway's western jamb seems never to have been decorated in this way appears to be the very definition of the transition between these two decorative approaches (Clapham 1934). The sundial above the south door does not appear to be *in-situ*, but is of late eleventh-century type (Bryant 2012). The Phase 1 nave is relatively sizeable, and is consistent with a church intended for congregational use rather than as a private chapel, although its patron is nevertheless likely to have been the local lord —

conceivably the Norman Hascoit Musard, who held the manor in 1086. The nave conforms to the two-square layout typical of post-Conquest parish churches (Clapham 1934, 102-4), excepting the cross-passage between the north door and the south, which elongates the nave still further. It is unknown whether it originally had a chancel, but given its size this seems likely.

There is little physical evidence for an earlier church on the site, aside from a possible window and a single piece of *ex-situ* figurative carving, although it is plausible that the present church replaced a timber structure. Whether or not the eleventh-century phase of St Nicholas' represents the first church on the site, or whether there was an earlier building, a possible context for construction may be provided by the charter evidence for 'Cada's Minster' outlined by Hooke (see above). A well-understood phenomenon of the tenth to twelfth centuries in England is the proliferation of local churches, whereby the large territories of Middle Saxon minsters were fragmented into what would become parishes. This was due to the growth in ownership of private estates and the construction of private ('proprietary') churches to minister them, primarily as the result of lordly agency. This provides a ready context for Hascoit Musard or his kin building a generous new church adjacent to the suspected lordly residence at Saintbury, potentially utilising fragments taken from the old Cada's Minster within its fabric.

Summary

St Nicholas' Church, Saintbury, appears to have been constructed *c*.1100, comprising a relatively capacious nave and probably also a chancel. It is a well-built but quite simple structure with limited decorative work, consistent with the status and resources of a local lord such as the Norman, Hascoit Musard. The idea is postulated later in this report that the building may have had no direct early medieval predecessor, but was instead built to supplant a much older minster church thought to have been located within the Iron Age hillfort of Willersey Hill Camp *c*.600m to the south.

TOPOGRAPHIC SURVEY VIA UNMANNED AERIAL VEHICLE (UAV)

Scott Chaussée

Aims, methods, and objectives

Topographic survey via UAV was carried out with due regard to the CIfA standard and guidance for archaeological field evaluation (CIfA 2014). The broad aims of the survey were to:

- Provide information about the archaeological potential of the site; and
- Inform either the scope and nature of any further archaeological work that may be required or form a management strategy.

In order to achieve the above aims, the general objectives of the UAV photographic survey are to:

- Establish, within the constraints of the UAV photographic survey, the extent, character, and condition, of surviving archaeological remains within the specified area;

- Place any identified archaeological remains within a wider historical and archaeological context in order to assess their significance;
- Make available information about the archaeological potential of the site by reporting on the results.

It was hoped that through these methods the survey would allow greater characterisation of archaeological features already detectable on the Digital Terrain Models (DTMs) generated by Environment Agency-provided Light Detection and Ranging (LiDAR) data (Figure 23). All works were undertaken in compliance with the standards outlined in CifA (2014) and Historic England (2015) guidance. The methods are given in detail below. The survey was conducted using a Da-Jiang Innovations (DJI) Mavic 2 Pro UAV equipped with a Hasselblad 20-megapixel CMOS camera for capturing aerial imagery. The flight was pre-programmed using DroneDeploy software on a OnePlus 9 mobile phone which also served as the UAV flight controller. One pre-programmed 'Crosshatch 3D' flight was undertaken at a height of 44m above ground level (AGL), at a speed of 4m per second, totalling 18:32 minutes. Front (forward) and side (swath) overlap were 70% producing a survey corpus of 296 images covering approximately 2 hectares. Digital Terrain Models (DTMs) and Digital Surface Model (DSM) datasets in .tiff format were created using OpenDroneMap (2024) software. The raster files were processed in Relief Visualisation Toolbox (RVT) software (Kokalj and Somrak, 2019; Zakšek et al., 2011). The following topographic visualisations are presented in Table 1 below.

Visualisation	**Description**
Shaded relief topographic visualisation (Hillshade)	A visualisation technique which produces a pseudo-3d representation of terrain based on a virtual light source, combined with the slope and aspect of the elevation surface.
32 Multi-directional Hillshade	Image comprising multiple shaded reliefs combined to create a composite hillshade illuminated from multiple directions to enhance ephemeral topographic features.
Slope Severity	A visualisation that conveys the maximum rate of change in height between neighbouring cells in the DTM and DSM raster image.
Local Relief Model	A visualisation that removes large-scale features, such as landforms, and emphasises smaller-scale features.
Sky View Factor (SVF)	A visualisation that identifies light on any 'positive' (upstanding) feature and 'negative' (depression) features which receive less light.
Principle Component Analysis (PCA)	A visualisation that emphasises variation and spatial patterns in the data.

Table 1: Types of topographic visualisation

Results

David Gould and Duncan Wright

DTMs generated via the UAV topographic survey provide a far greater resolution of archaeological features than discernible through models derived from publicly accessible LiDAR data (Figures 24-26). An attempt here is made to characterise the most obvious components of the site, especially the positive features (earthwork banks) easily detectable on DTMs and through field observation. The lettering system in the text relates to annotations to the model made in Figure 25.

The most prominent topographic feature of the site is the outer enclosure bank extending along its north and west sides for *c*.195m in total. Most of the DTM models produced by the project (though contra Figure 26) suggest this is not a coherent, unbroken, oval as suggested by LiDAR models. Rather, the northern circuit seems to be made up from several intersecting, angular banks, hinting at modification over time or perhaps construction phases. The western limit of the outer enclosure is distinct in character, and may represent a less heavily altered section, consisting of broad, curving, banks (A, B) separated by a coherent break/entrance (C) that may be original. Earthwork A measures *c*.27m N-S and is *c*.9m wide; earthwork B measures *c*.29m N-S and is *c*.9m wide. At the northern edge of bank A, the outer enclosure turns eastward for *c*.40m (D) and there is a break between these two lengths of banks, with bank D being considerably less broad than banks A and B, measuring *c*.5m wide. The northern edge of the outer enclosure has a break at point E, which separates bank D from a further length of bank (F) that runs eastwards for *c*.45m. The north-eastern corner of the extant enclosure earthworks is particularly complex — the 'inner core' of the site immediately south-west of St Nicholas' churchyard — where there are several different lengths of banks: section G measures *c*.24m E-W and runs parallel to the exterior of the main outer enclosure, a curving bank (H) measuring *c*.54m E-W forms the north-east corner of the outer enclosure, while section I measures *c*.17m E-W and runs parallel to the interior of the main outer enclosure.

A rectilinear feature (J) lies at the south-west corner of the main enclosure measuring *c*.25m N-S and *c*.52m E-W; its southern edge is formed by a natural escarpment that overlooks the site and its western edge is formed by bank B, although that earthwork has a considerably broader profile than its northern and eastern sides, suggesting different phases of construction. Running parallel to the northern edge of this rectilinear feature is a further earthwork (K) that measures *c*.57m E-W; these two parallel features form a central hollow way leading from the break in the western edge of the outer enclosure (C) towards the eastern inner enclosure.

A series of features are present within the eastern end of the outer enclosure. A bank at the north-west corner of this group of features (L) measures *c*.22m N-S before turning eastwards at its northern end for *c*.25m. Three sides of a square feature (M) lay to its east, measuring *c*.11m by *c*.13m. To the east of this square feature is a bank (N) that runs *c*.26m N-S before turning westwards for *c*.9m. To its east are two further banks (O and P) that follow the same alignment as bank N but display a more curving line, with bank O measuring *c*.16m N-S and *c*.7m E-W, and bank P measuring *c*.11m N-S and *c*.5m E-W. At the south-eastern corner of the outer enclosure is a linear bank (Q) constructed parallel to the escarpment, measuring *c*.38m

E-W before turning northwards at its western edge for *c*.10m. Observation in the field clearly identifies Q as a spoil heap, probably derived from relatively recent quarrying or landscaping.

GRADIOMETER SURVEY

Scott Chaussée and Duncan Wright

Aims, methods, and objectives

The gradiometer survey was undertaken by Scott Chaussée (GeoTechnê) and Duncan Wright in dry weather conditions. An overall coverage of 1.1 hectares was achieved with tall grass, nettles, and thistles causing a reduction in the surveyable area (Figure 27). The methods and standards employed throughout the geophysical survey conformed to current good practice and guidance as outlined by the Chartered Institute for Archaeologists (CIfA 2014) and European Archaeologiae Consilium (Schmidt et al. 2015). The survey was designed to meet three main aims. These were to:

- Conduct a detailed survey covering as much of the specified area as possible, allowing for obstructions;
- Clarify the presence and/or absence and extent of any buried archaeological remains within the surveyed area; and
- Determine the general character of the archaeology present.

Individual survey grid nodes were established at 30m intervals using a Leica Viva RTK GNSS rover instrument, which is precise to approximately 0.02m and therefore exceeds European Archaeologiae Consilim recommendations (Schmidt *et al*. 2015). The detailed gradiometer survey was conducted using two Bartington Grad601-2 fluxgate gradiometer instruments, which has vertical and horizontal separation of 1m between sensors. Data were collected in the zig-zag methodat 0.25m intervals along transects spaced 0.5m apart with an effective sensitivity of 0.03 nanotesla (nT). Data from the survey were subject to minimal data correction processes. These comprise a zero mean traverse function applied to correct for any variation between the two sensors, and a de-step function to account for variations in sample location along traverses due to varying ground cover and topography. These two steps were applied throughout the survey area. Interpolation was then applied for clarity.

Results and interpretation

The geophysical survey has identified a number of features that are likely to be representative of archaeological remains (Figures 28-29). The data are displayed at -4 nT (white) to +4 nT (black) for the greyscale plots. The interpretation of the datasets highlights the presence of potential archaeological features as well as deposits of ferrous, burnt, or fired objects which may or may not be archaeological in nature. There are anomalies consistent with disturbance from known and modern sources (such as fences) throughout the dataset. These are not referred to further in this report, unless considered relevant to the archaeological interpretation. It should be noted that small, weakly magnetised features may produce responses that are below the detection threshold of the instrument used. It may be the case

that more archaeological features may be present than have been identified through the present gradiometer survey.

Area A: south-west of the church

Area A is dominated by several strong positive and negative linear anomalies of archaeological origin (Figure 30). The rectilinear arrangement of strong magnetically positive and strong magnetically negative responses at location m4000 is suggestive of structural remains, whose size and form are unresolved in the present results, but occupy an area a minimum of 21m x 14m. The purported structure appears to be partially enclosed to its west by a rectilinear strong magnetically positive feature m4001 which forms a right angle with one arm oriented north-east to south-west and is 13m x 3m. The other arm is oriented north-west to south-east and is 12m x 3m. The area of purported structural remains is enclosed to its north by a curvilinear strong magnetically positive ditch feature at m4002. The ditch feature arcs west to east and is 44m long (though truncated by the survey boundary limit) and is 3m wide. Adjacent strong magnetically negative features indicate the presence of banking material on either side of the interpreted ditch cut. It is significant that the line of this curving bank and ditch has not been located by any other of the geophysical survey methods, nor is it preserved as an earthwork. Indeed, its curving profile is distinct from the overwhelmingly rectilinear form of banks and ditches in this area, and is suggestive of a different phase. To the south-west of the purported structure at m4000, a strong magnetically positive right-angled ditch feature at m4003 forms an additional element of interior enclosure. One arm is oriented north-north-west by south-south-west and is 20m x 3m. The ditch turns south-west and extends a further 29m. The weak magnetically positive linear anomaly at m4004 is indicative of further banking material 34m x 3m after an intervening break of 19m the external enclosure appears to continue at m4005 with a weak magnetically negative linear anomaly, 26m x 1m, oriented north-east to south-west. Despite being truncated by the survey boundary extent, it is conceivable that the weak magnetically negative linear anomaly at m4006 is a continuation of the purported 'external' enclosure formed by those banks. Finally, the three sides of a rectilinear, weak magnetically negative anomaly at m4007 in the centre of the 'outer' enclosure is suggestive of attempts at levelling, to produce a platform, though no remains of a potential structure are observable in the present results.

Area B: north-east of the church

Area B is also dominated by several magnetically positive linear anomalies of archaeological origin (Figure 31). In the north-east of the survey area, a weakly magnetically positive linear 'L'-shaped anomaly at location m4050 measures 13.6m north-west to south-east before turning east for a distance of 4.6m. The full extent of this anomaly is unknown as it is truncated by the survey boundary. Two offshoot linear features extend to the south-west from its main length. The longer of the two is 8.5m and the shorter 5.8m. Dominant in the north-west of the survey area is the strongly magnetically positive complex angular arrangement of linear anomalies at location m4051. This anomaly is 3.8m at its widest and forms a right angle from a 38.8m length oriented north-east to south-west joined to a north-south oriented length that

measures 19.7m. Towards the southern end of this length, it appears to return to its north-east to south-west alignment; it is unknown for how far, as the full extent of this segment is truncated by the survey boundary. An approximately north-south arrangement of strongly magnetically positive linear anomalies at m4052, m4053, and possibly m4054, produce a seemingly coaxial association with the other linear anomalies in this survey area. The linear feature at m4052 measures 26.8m long and 2.7m wide; m4053 is 14.9m long and 2.9m wide; m4054 is 2.5m wide and at least 9.1m long but its true length is unknown due to truncation by the survey boundary. To the west of this linear arrangement at location m4055 is a much thinner (1.1m) extent of a weakly magnetically positive 13.3m long linear anomaly at that appears on a similar alignment to those discussed above.

Within the purported coaxial arrangement posited above, the north-south aligned magnetically positive linear anomaly at location m4056 appears to have been based on a differing alignment to the majority of linear anomalies apparent in this area, oriented due north-south. The linear anomaly here forms a 'T' shape with the long side measuring 16.5m by 1.8m. A short east-west aligned offshoot from this measures 4.2m by 2.1m. To the extreme west of the survey area is a magnetically positive penannular feature with a central discrete deposit at location m4057. Although truncated by the survey boundary, the southern segment of this penannular feature measures 13.6m x 2.4m. The northern segment measures at least 3.6m by 2.4m. The central deposit appears 2.9m by 1.8m. The form and scale of this feature is consistent with the remains of a windmill, probably of post-medieval date; the distinctive cross-shaped anomaly at its centre (most clearly seen in Figure 28) seems to be the footing, while the surrounding circular anomaly is the remains of the surrounding ditch of the mound. Across survey Area B, a series of positive discrete deposits are present, all of which are similar in measurement, ranging from 2.4m by 1.1m to 3.1m by 2.1m. These may represent a series of burials, either from a former extension of the graveyard, or from another phase of activity altogether.

Summary

The gradiometer survey was successful in identifying significant anomalies of probable archaeological origin in both areas investigated (Figure 32). Immediately to the south-west of the church a series of enclosures was located in what topographic evidence suggests is an inner core of activity, as well as at least one potential structure, roughly aligned with the standing church. The great complexity of the data in this zone suggests a range of features, probably spanning numerous phases, and thus was the target of further geophysical surveys (see below). Additional features consisting of a series of enclosure boundaries, a windmill footing, and several possible burials were located to the north-east of the church, an area in which there are fewer upstanding earthworks; the only prominent topographic feature of archaeological origin here is the angular course that seems to be a former field boundary or lynchet (Figure 23). Perhaps significantly, the north-west to south-east orientated anomalies on either side of the church both have a break in their extent which may be indicative of former entranceways. These breaks in the enclosures, although situated almost 200m apart, are aligned with each other, which suggests they might be contemporary features. If this is

the case, then the church seems to represent a later insertion into the existing enclosure complex. While comprehensive excavation is the only method that will fully clarify the chronological sequence of these features, the density and complexity of the anomalies identified by the gradiometer is strongly suggestive of prolonged or intensive activity, or perhaps both. Given the especially impressive results from Area A, and the zone closest to St Nicholas' Church in particular, GPR and earth resistance survey was undertaken to generate further data on the archaeological remains.

EARTH RESISTANCE SURVEY: AIMS, METHODS, RESULTS AND INTERPRETATION

Oliver Creighton

An earth resistivity survey, conducted using a Geoscan RM85, sampled an area immediately south-west of the western extent of St Nicholas' churchyard, in order to further characterise this area of high archaeological potential (Figure 33). The survey covered an L-shaped area on an approximate east-west orientation with maximum dimensions of 45m x 30m.

The survey located a series of clear rectilinear features surviving as high-resistance anomalies, on approximately the same orientation as the church (Figure 34). At the eastern end of the surveyed area, a rectilinear feature was identified, measuring *c*.8m E-W x 20m N-S, and lying *c*.20m west of the church (Figure 35: A). The boundaries of the feature are distinct and are made up of four regular high-resistance bands *c*.2-3m wide, suggesting the presence of a stone building. A rectilinear area of high resistance near the centre of this feature perhaps represents a subdivision within the building, or another collection of structural remains (Figure 35: B). Immediately west of this probable building is another feature, also formed by four bands of high-resistance anomalies *c*.2-3m wide (Figure 35: C). Together the four bands create an almost regular square, measuring *c*.22m N-S and 22m E-W in total, and enclosing a low-resistance core of roughly 10m in both directions. Again, the high-resistance bands that make up this feature are suggestive of a building, perhaps built of stone. There is a suggestion of an annexe-style arrangement or entranceway on the south side of the feature. A further, less distinct N-S band of high resistance lies to the west of this feature, in the westernmost part of the surveyed area (Figure 35: D).

Without excavation, the date and purpose of the features located by the earth resistance survey will remain, to some extent, conjectural. Nevertheless, the rectilinear arrangements of possible stone structures is reminiscent of Roman buildings of various types, an interpretation supported by the form of the rectilinear earthwork surrounding the complex, the north-eastern corner of which exhibits a distinctive 'playing card' shape usually associated with military installations (cf. Collins 2013, 31-2). The presence of a temple, villa, or other type of rural settlement cannot be discounted, however, and the clear potential for phasing suggests that any blanket interpretation may be insufficient to capture the complex history of the site. Indeed, a medieval origin for some of the features located by the earth resistance is also plausible, especially given their apparent orientation with the eleventh-century church. With an aim of unpicking at least some of the phasing on site, a final phase of geophysics consisting of a GPR survey, was undertaken.

GROUND PENETRATING RADAR SURVEY (GPR): RESULTS AND INTERPRETATION

Aims, objectives, and methodology

GPR survey was carried out in the same area targeted by the earth resistance survey, immediately south-west in what was clearly an area of concentrated archaeological activity. The primary aim of the GPR survey was to establish, where possible, phases within this activity, with the expectation that this could provide some relative chronology to the site sequence. This is possible by establishing basic stratigraphic relationships through analysis of individual radar profiles, and resultant interpolated time-slice visualisation.

The GPR survey was conducted using a Leica DS2000 dual-antenna ground penetrating radar. This GPR system uses separate low frequency (250 MHz) and high frequency (700 MHz) shielded transmitter and receiver antennae placed in perpendicular, broadside arrangement that allows for them to be pushed simultaneously across the survey area. Traverses were collected every 1.0m in an east-west direction using the zig-zag method. The data were recorded every 3cm with a horizontal profile spacing of 0.5m within a time window of 100ns. Baselines were established using a GNSS RTK instrument, which is precise to approximately 0.02m and therefore exceeds European Archaeologiae Consilium recommendations (Schmidt et al, 2015). Data from the survey were subjected to common radar signal correction processes using the software RGPR. These processes include amplitude and wobble correction of the radar profile to correct for variance in temperature and moisture content, and background and bandpass filtering to remove noise in the data and the surrounding area.

It is possible to determine the average velocity of the GPR pulse through the ground more precisely if excavated features at a known depth can be identified in the data. To determine velocity of the radar pulse, radargrams were analysed for suitable hyperbolic reflections which were then used to determine the velocity of the GPR pulse through the subsurface deposits. Resultant approximate depth conversions are given.

Results

For the low frequency antenna, the propagation velocity was established to be 0.1m/ns (Table 1). Time-slice (TS) 03 and 07 returned data consistent with probable archaeological features. A series of anomalies has been identified in TS03, located between 0.4m and 0.6m below the ground surface. These anomalies comprise a complex, coaxial arrangement of linear features which reflect alignment and positioning of earthworks visible in the UAV survey, and the magnetic anomalies observed in the gradiometer survey (Figures 36-37). The most prominent of these features is a central rectilinear feature, enclosing an area with internal dimensions of 9.15m x 8.40m. This clearly correlates with feature ‘C’ located by the earth resistance survey. The responses in TS03 also closely resemble the extent and morphology of the observed magnetic anomalies observed in the gradiometer data. The rather uneven distribution of the anomalies that make up this feature suggests that it may be a spread of rubble, rather than coherent walls as indicated by earth resistance. Even so, the rectilinear form of the anomalies

— perhaps representing one of more walls and/or enclosures — again encourages comparison with Roman structures. As argued above, it is only through excavation that the identity of these features, and indeed whether they are Roman in origin at all, will be verified.

Table 2: Time-slices, time range, and corresponding depths for the LF antenna, assuming a propagation velocity of 0.1 m/ns

Time-slice #	Time (ns)	Depth (m)
1	0.0 – 4.0	0.0-0.2
2	4.0 – 8.0	0.2-0.4
3	8.0 – 12.0	0.4-0.6
4	12.0 – 16.0	0.6-0.8
5	16.0 – 20.0	0.8-1.0
6	20.0 – 24.0	1.0-1.2
7	24.0 – 28.0	1.2-1.4
8	28.0 – 32.0	1.4-1.6
9	32.0 – 36.0	1.6-1.8
10	36.00 – 40.0	1.8-2.0

Table 2: Time-slices, time range, and corresponding depths for the LF antenna, assuming a propagation velocity of 0.1 m/ns

Beneath the assemblage of reflectors visible in TS03 is another set of responses in TS07, representing a depth of between 1.2m and 1.4m below ground surface (Figures 38-39). The overall picture of the presumed associated features in TS07 is a lack of definition perhaps due to perhaps varying lithology within the surrounding sediment matrix showing broad contrast visible as a single rectilinear arrangement of possible rubble, or perhaps platform banking material visible in the UAV survey as earthwork remains. The overall picture of the limits of the disturbance in TS07 is, however, a rectilinear enclosure-type feature curving at its short ends, oriented north-east to south-west and with internal dimensions of 17.76m x 10.26m. This feature is best interpreted as a building or structure of unknown origin and function.

The trend of this somewhat messy but clearly coherent responses in TS03 and TS07 is counterbalanced with apparently *in-situ*, arguably structural remains as discrete high amplitude reflector is visible in both Lines 4 and 5 at this depth.

Summary

The GPR builds upon the results of the topographic, gradiometer, and earth resistance surveys, confirming the presence of one or more buildings or enclosures at the core of the inner complex immediately south-west of St Nicholas' Church. Crucially, the large stratigraphic gap between the two sets of anomalies of up to 1m is clearly suggests distinct phasing, with the features at TS03 presumably representing a more recent episode than those of TS07 below. If the features visible at TS03 do indeed represent Roman remains, then the structure at TS07 must be from an earlier phase, perhaps prehistoric in date or an earlier Roman phase. If the

identification of Roman archaeology at a depth of between 0.4m and 0.6m is correct, then any medieval deposits present will lie between this interface and the ground surface. The absence of clear anomalies in the time-slices of possible medieval date may be due to the more ephemeral character of the archaeology from this period. Stratigraphic deposits may also have been negatively impacted from more recent landscaping, if indeed the spoil heap to the south does represent upcast from such activity. Nevertheless, the premise that the complex archaeological evidence at Saintbury located by topographic and geophysical survey methods represents an accumulation from perhaps a significant span of chronological phases is given further, final, backing by the results of the OSL profiling and dating.

OPTICALLY-STIMULATED LUMINESCENCE (OSL) PROFILING AND DATING

Tim Kinnaird, Aayush Srivastava, and Sam Turner

OSL profiling and dating was undertaken to provide chronological constraints for the development of earthworks south-west of St Nicholas' Church. Five trenches were opened: Trenches 1 and 2 sectioned the northern arm of the south-west to north-east projecting earthwork that is part of the outer enclosure; Trench 3 the abutting north-west to south-east projecting earthwork that also forms part of the outer enclosure; Trench 4 the system of ridge and furrow to the south-west; and Trench 5 the bank and ditch of the most prominent earthwork of the complex immediately south-west of the church (Figure 40-41). Section drawings were made of each trench, and a small find of pottery was made in the west-facing section of Trench 1 (Figure 42). Full details of the multi-stage methodologies used both in the field and in the lab can be found in Appendix 1. The consistency between the datasets, and the spatial (and temporal) correlations observed in the OSL signal intensities across the investigated sediment stratigraphies, suggest the following chronological sequence:

- A phase of soil formation, with some zeroing of the luminescence, at 3.26 ± 0.18 ka (1230 ± 180 BC)
- Construction of earthwork(s) between 2.38 ± 0.22 ka (360 ± 220 BC) and 1.91 ± 0.11 ka (AD 110 ± 110). A *terminus ante quem* is provided by the weighted combination of the ages obtained for <504>, the basal fill of the ditch, which is cut into the slope above the earthwork(s). The earlier constraint is provided by the weighted combination of ages obtained for the sediment at the base of the earthwork in trenches 2 and 3.
- Continued management of the earthwork(s) into the seventh and ninth centuries AD (1.40 ± 0.15 ka (AD 630 ± 150) and 1.14 ± 0.11 ka (AD 890 ± 110), respectively)
- Development of the ridge and furrow between the thirteenth and seventeenth centuries AD (0.77 ± 0.16 ka (AD 1260 ± 160 and 0.33 ± 0.13 (AD1690 ± 130), respectively)

This sequence is of fundamental significance for interpretating the origins and evolution of the earthwork complex at Saintbury, and will be considered in detail alongside the other evidence in the discussion (see below).

PORTABLE ANTIQUITIES SCHEME (PAS) DATA

David Gould

Very few finds of any date have been recorded within Saintbury or its neighbouring parishes within the PAS database and no finds are directly associated with the manor-church complex of Saintbury itself. The nearest find to the site is a jetton dated to between 1497-1521 that was found approximately 380m north of the parish church. Only two potentially pre-1066 finds, recovered from the same findspot, have been recorded within the 5km search radius of the lordly complex on the Saintbury-Weston-sub-Edge border approximately 1.2km NE of Saintbury's church: a ninth- to eleventh-century buckle and a harness fitting from *c*.1000-1100. The sole potentially pre-1200 find within the 5km search area is a buckle found approximately 3.8km SE of the parish church, although its date range in fact falls between *c*.1175 and c.1400.

DISCUSSION

The multifaceted programme of original fieldwork, lab analyses, and desk-based investigation undertaken by *Where Power Lies* and partners has generated a series of crucial insights, allowing an unprecedented understanding of Saintbury's archaeological development. The results of OSL profiling and dating suggests that the key components of the earthwork complex, extending south-west of St Nicholas' Church, was constructed between 360 ± 220 BC and AD 110 ± 110: either during the late Iron-Age or Romano-British period. Significantly, the *terminus ante quem* for this phasing comes from the basal fill of enclosure ditch m4002 identified by the gradiometer survey. This enclosure was not located by any other geophysical survey method, and is not visible as an earthwork; existing only as a buried feature, then, the enclosure appears to be a distinct, probably earlier phase from the rectilinear arrangement of geophysical anomalies and standing earthworks, that otherwise characterise the complex immediately south-west of the church. The south-western terminus of the outer enclosure earthwork has a similar curving profile which may be of comparable provenance, although the form of the enclosure to the north – made up of a series of angled linear banks and ditches rather than a coherent singular curving feature as previously believed — hints at modification, an premise supported by the evidence from OSL. The coherent character of the hollow way that enters through the south-western extension of the outer enclosure, continuing north-eastwards into the interior, suggests that it is contemporary with construction rather than a later feature. If inner and outer enclosure are of Iron-Age provenance as the OSL suggests, and the hollow way an original feature too, then these conceivably represent the remains of a banjo enclosure, albeit one subject to alteration (Figure 43). If this identification is correct, then the existence of a high-status settlement in such close proximity to Willersey Hill Camp is clearly significant, indicating a clustering of broadly contemporary Iron-Age activity in this scarp-edge landscape. The concept of Iron-Age agglomerations is well-established in the literature (e.g. Moore and Fernández-Götz 2022), including elsewhere the Cotswolds (Moore 2020), and at Saintbury we can now identify for the first time two substantial sites located only *c*.600m apart.

Occupation may have continued into the Romano-British period, or perhaps the site was

reused following a period of abandonment; either way, many of the features that make up the inner network of earthworks and geophysical anomalies seem Roman in origin, possibly representing a villa or other rural settlement, although a military installation or temple cannot be discounted entirely. That the sites of banjo enclosures were reutilised in the Romano-British period is well established, although in such cases the Iron-Age features are consistently abandoned to be replaced by new buildings and enclosures (see Lang 2016, 348-51). We could also be seeing this at Saintbury, where the inner ditch of the curving banjo enclosure seems to be truncated by later rectilinear features, although the large outer earthwork was clearly retained. It is notable that there are several excavated of villa complexes built in the immediate vicinity of banjo enclosures (e.g. Harding 2007) in England and south Wales, which perhaps strengthens the case for a high-status rural settlement at Saintbury in the Romano-British period, over the other possible interpretations offered above. Whatever the character of the Roman activity, it is important not to study the dense, well-preserved archaeology south-west of the church in isolation; further features of similar character, albeit not standing as earthworks, are present north-east of the church signifying contemporary occupation. The structural remains south-west of the church could therefore represent a westerly concentration of a far more extensive complex, much of which lies under St Nicholas' (Figure 43).

OSL data suggests that the earthworks of the outer enclosure remained in use during this period, and it continued to be maintained throughout much of the first millennium AD. For what purpose the site was being used in the earliest medieval centuries, or by whom, is obscure, but if Cada's minster was an early foundation, then it may have been the community of the nearby church who kept the earthworks in order. An alternative, perhaps more likely scenario, is that Saintbury is in fact the site of the minster itself; lying only 600m north of where Hooke's documentary analysis located the church, the confirmation of Middle Saxon activity by St Nicholas' raises the distinct possibility that Cada's minster was instead situated half-way down the Cotswold scarp rather than inside Willersey Hill Camp (Figure 43). Further support for this theory is the character of the outer enclosure, which gained its final, curving form between the seventh and ninth centuries. There are a number of Middle Saxon monastic sites in England with compounds of similar size and shape, but perhaps the best-known example is Jarrow, Durham, where a combination of excavation and geophysics allows reconstruction of an enclosure closely comparable to Saintbury (see Turner et al. 2013, 136).

The outer earthwork enclosure at Saintbury eventually ceased to be added to after the ninth century AD at the latest, as in all likelihood a secular lord appropriated the former minster site in order to develop a private power centre. A lack of embanked material after the Middle Saxon period does not necessitate that the enclosure system was abandoned; the earthworks could have continued to be modified in less visible ways, enhanced instead through planation of hedges or construction of a wooden palisade, as encountered regularly at comparable sites of the period (e.g. Wright *et al*. 2023). A strikingly similar arrangement, consisting of an outer horseshoe-shaped enclosure surrounding an inner complex, is located at Middleton Stoney, Oxfordshire, where excavation between 1970 and 1982 revealed a Late Saxon lordly centre also built over Romano-British buildings (Figure 44) (Rahtz and Rowley 1984). Sections

through the ditch of what was dubbed 'the eastern enclosure' of the inner complex — and what would later become part of the inner bailey of the castle — was phased to the late Saxon period through stratigraphic relationships, and confidently placed the in a 'pre-castle' phase (i.e. before the twelfth century). Interpreted as a lordly residence preceding the castle, it is notable that recovery of Middle Saxon pottery at Middleton Stoney points towards more prolonged, if less visible occupation, comparable to the situation at Saintbury (Rahtz and Rowley 1984, 52-3). As for the outer horseshoe enclosure, this was not sectioned, and there was no stratigraphic relationship between the earthwork and any of the excavated features; it therefore remains undated. As at Saintbury, however, it would be unwise to assume Middleton Stoney's outer enclosure is the product of a single construction episode, and it too may be a composite feature shaped by several phases of use.

At Saintbury, exactly when the place came to be called Sæwine's burh, and whether this was attached to a real or imagined individual is unclear. Unfortunately the 'burh' element is not a reliable indicator of a lordly centre, even when combined with a personal name, as it was also applied to prehistoric enclosures, Roman sites, and monastic compounds (Draper 2008). While 'burh' could equally reference Saintbury's prehistoric, Roman, or early medieval phases, the personal name was probably coined when this already ancient site was transformed into a secular power centre around the end of the first millennium AD through. The relative dearth of archaeological evidence for the high-status residence and church that would have been the key components of this enclave is again probably a product of visibility. Residential buildings will have been constructed entirely of turf and timber; ephemeral materials usually rendered invisible to methods of prospection employed here. Any pre-Conquest church is more likely to have been built of stone but this building, if extant, probably lies under or close to its early Norman successor (Figure 43). Again, Middleton Stoney provides an invaluable parallel; here nothing in the church fabric pre-dates the twelfth century, although the results of excavation clearly locate a late Saxon lordly focus (Rahtz and Rowley 1984). At Saintbury, the present church and graveyard certainly give the impression of being intrusive features into the complex, and indeed can now be shown as being relative latecomers in the site chronology. The possibility of burials extending to the north-east hint that the current churchyard may represent truncation of a larger unit, although these internments may equally belong to a pre-church phase.

If Sæwine was the first lord of this nascent power centre, then he may have taken advantage of the changing tenurial conditions of the ninth and particular tenth centuries, as the fragmentation of extensive Church estates, such as that probably belonging to Cada's minster, rapidly proliferated. The development of lordly centres on former Church lands is a well-recognised phenomenon of the increasingly avaricious elite of the late Saxon period, but is most famously demonstrated at Barton-upon-Humber, Lincolnshire. Here, a tower-nave and residence, built upon territory formerly belonging to the minster at Barrow, was divided amongst secular lords from the late tenth century (Rodwell and Atkins 2011. 45). Little is known of Saintbury's lord in 1066, Cynwy Chelle, although Domesday Book lists other holdings in Arlington in Gloucestershire, Ash in Oxfordshire, and Ashton in Wiltshire (Williams and Martin 2002). It will have either been the first Norman tenant-in-chief, Hascoit Musard, or one

of his immediate successors who commissioned at Saintbury's lordly centre an impressive new church around the year 1100; the size of the early Norman building demonstrates that it was intended to house a large congregation from the outset, rather than being an entirely proprietary enterprise. In contrast, there is doubt whether an elite residence next to St Nicholas' was retained after the Conquest, as little archaeological evidence recovered thus far indicates prolonged occupation. Early Norman lords may instead have based themselves at the motte and bailey in Weston Park, some distance from the church, but strategically placed to overlook the meeting place at Kiftsgate Stone and extensive stretches of Ryknield Street. This represents a divergence from those lordly centres where castles were superimposed upon precursors, as seen elsewhere in the Cotswolds at Hillesley, Gloucestershire, where a ringwork was built over a late Saxon site (Figure 44) (Ellis 1984; Williams 1987; Longman 2005). At Middleton Stoney too, a motte and inner bailey was constructed next to the church, and the pre-existing enclosure retained as an outer bailey (Rahtz and Rowley 1984, 156-7). The reasons why Saintbury did not follow this course of evolution is debatable, but in a landscape that may still have been an ecotone between different political groups, proximity to an assembly place, and indeed the ability to observe movement along the Roman road, may have taken priority over perpetuating the existing seat of lordly power.

By the later medieval period, the settlement focus at Saintbury shifted down the slope to the area of the crossroads where a cross of fourteenth-century date still stands (HE List No: 1014396). That this relocation included a manorial component is evidenced by an L-shaped moated enclosure at Lower Farm, immediately south-east of the crossroads (GHER: 26917). It is to this residence that the unusual earthworks of the mill, in a field later known as 'The Neights', will have been attached. On the hill above the small, dispersed village, post-medieval alterations to the motte and bailey has resulted, until now, in uncertainty around its interpretation. In contrast, and somewhat ironically, the earthworks by St Nicholas' Church were prominent enough (and more frequently encountered by those using the church?) to be named 'castle bank' by locals by at least the late eighteenth century. The apparently rapid transformation in the medieval period from a place of prolonged activity over many centuries, to one used exclusively for pastoral farming, explains the exceptional preservation of the site that continues into the present day. It is only through the series of investigations outlined here, however, that the incredibly deep and complex history of the site is now being realised.

CONCLUSIONS

The landscape immediately surrounding St Nicholas' Church is clearly an area of extremely high archaeological potential, with activity spanning the late prehistoric to medieval period. As with many sites investigated by *Where Power Lies*, it is clear that the lordly centre formed but one phase of a far longer and more complex history, and future research must consider more fully the role of antecedent landscapes in shaping the decisions of elites in developing their enclaves. Although at Saintbury a sound idea of the broad chronological development of the site has been achieved, it is only through detailed excavation that this sequence will be understood more fully. Any intervention should at first seek to assess the archaeological evidence across the site, through a programme of open area excavation of the inner zone

combined with targeted evaluation or small open area trenches of other feature of interest.

ACKNOWLEDGEMENTS

Sincere thanks are extended to Barry Brogan, Cerian Brogan, Anne Thomas, and their family who have supported our work in every way possible throughout. Isobel Sinclair kindly gave her time in joining the OSL dating and earth resistance survey phase of the fieldwork. The *Where Power Lies* team are grateful to Tim Kinnaird, Aayush Srivastava, and Sam Turner for their involvement in delivering the OSL profiling and dating, the results of which hugely benefit our understanding of the site.

BIBLIOGRAPHY

Primary Sources

Gloucestershire Archives

D2202/2/4/2 *Deeds of Durham family at Willersey & Saintbury, including terrier of estate. 1635-1757.*

D3439/1/328 *Hockaday Abstracts volume 328: ecclesiastical records relating to St George, Bristol, from the year 1678, to St Briavels from the year 1256, and to Saintbury from the year 1282, compiled by F S Hockaday in the early 20th century.*

GDR/T1/155 *Saintbury tithe map and apportionment*, 1841.

The National Archives

C 143/40/21*. Malcolm Musard to grant the manor of Saintbury to the abbot and convent of Evesham. Glouc.*

Secondary Sources

Anderson, O. S. 1939. *The English Hundred-Names: The South-Western Counties*. Lunds Universitets Arsskrift, 35.5. Lunds Universitet: Lund.

Baker, J. and Brookes, S. 2013. 'Monumentalising the political landscape: a special class of Anglo-Saxon assembly site', *The Antiquaries Journal* 93, 147-162.

Blair, J. 2005. *The Church in Anglo-Saxon Society*. Oxford: Oxford University Press.

Blair, J. 2018: *Building Anglo-Saxon England*. Princeton and Oxford: Princeton University Press.

Bowden, M. 2006: 'The Medieval Countryside' in N. Holbrook and J. Jurica (eds*) Twenty-five Years of Archaeology in Gloucestershire: A Review of New Discoveries and New Thinking in Gloucestershire (Bristol and Gloucestershire Archaeological Report 3*). Cirencester: Cotswold Archaeology, 167-187.

Bryant R. 2012. *Corpus of Anglo-Saxon Stone Sculpture. Volume X: The Western Midlands.* Oxford: Oxford University Press.

Church Recording Society 2022: *Record Of Church Furnishings Of St. Nicholas, Saintbury, Gloucestershire*. Unpublished report: Gloucestershire Record Office ref. ACC 16298.

CIfA 2014: *Standard and Guidance for Archaeological Geophysical Survey*. Unpublished guidance document.

Clapham, A. W. 1934. *English Romanesque Architecture After the Conquest*. Oxford: Oxford University Press.

Collins, R. 2013. 'Soldiers to warriors: renegotiating the Roman frontier in the fifth century', in F. Hunter and K. Painter (eds) *Late Roman Silver: The Traprain Treasure in Context*. Edinburgh: Society of Antiquaries of Scotland.

Draper, S. 2008. 'The significance of Old English *burh* in Anglo-Saxon England', *Anglo-Saxon Studies in Archaeology and History* 15,240-53.

Draper, S. 2018. 'The 'burys' of Almondsbury and Saintbury', *Bristol and Gloucestershire Notes and Queries* 136, 304-306.

Dyer, C. 1995. 'Sheepcotes: evidence for medieval sheep farming', *Medieval Archaeology* 39, 136-164.

Ellis, P.J. 1984. 'Earthwork surveys of three sites in Avon', *Transactions of the Bristol and Gloucestershire Archaeological Society* 102, 204-205.

Gould, D. 2017. *Rabbit Warrens of South-West England: Landscape Context, Socio-Economic Significance and Symbolism*. Unpublished PhD thesis for Exeter University.

Harding, P. 2007. 'Two possible Iron Age 'banjo' enclosures and a Romano-British villa and settlement at Beach's Barn, Fittleton, Salisbury Plain', *The Wiltshire Archaeological and Natural History Magazine* 100, 83-90.

Historic England, 2015. *Metric Survey Specifications for Cultural Heritage*. Swindon: Historic England.

Hooke, D. 1987. 'Two documented pre-Conquest Christian sites located upon parish boundaries', *Medieval Archaeology* 31, 96-101.

King, D.J.C. 1983. *Castellarium Anglicanum*, 2 vols. London: Kraus.

Kokalj, Ž., and Somrak, M. 2019. 'Why not a single image? Combining visualisations to facilitate fieldwork and on-screen mapping', *Remote Sensing* 11(7), 747.

Lang, A.T.O. 2016. 'Defining banjo enclosures: investigations, interpretations, and understanding in the Iron Age of southern Britain', *Proceedings of the Prehistoric Society* 82, 341-361.

Longman, T. 2005. 'The excavation of an early medieval field system at Hillesley Farm, Hillesley, Gloucestershire, 1997', *Transactions of the Bristol and Gloucestershire Archaeological Society* 123, 95-119.

Mackay, T. F. 1963. 'Anglo-Saxon architecture and sculpture in the Cotswold area', *Transactions of the Bristol and Gloucestershire Archaeological Society* 82, 66-94.

Maddison, S. 2021. 'The spatial distribution of hillforts in Britain and Ireland', in F. Delrieu, C. Féliu, P. Gruat, M-C. Kurzaj, and É. Nectoux (eds) *Les espaces fortifiés à l'âge du Fer en Europe: Actes du 43e colloque international de l'Association française pour l'étude de l'âge du Fer*. Collection AFEAF (3), AFEAF, 393-407. https://hal.science/hal-03260887/document [accessed 06/06/24].

Margary, I.D. 1955. *Roman Roads in Britain*. London: Phoenix House.

McCormick, J. 1960. *St. Nicholas Church*. Unpublished Guidebook.

Mills, H. J. (ed.) 1912. *Index to the Charters and Rolls in the British Museum, Vol. II Index Locorum (1882-1900*). London: J. Frances.

Moore, T. 2020. *A Biography of Power: Research and Excavations at the Iron Age 'Oppidum' of Bagendon, Gloucestershire (1979-2017)*. Oxford: Archaeopress.

Moore, T. and Fernández-Götz, M. 2020. 'Bringing the Country to Town: 'Rurban' Landscapes in Iron Age Europe', *Journal of Urban Archaeology* 5, 101-125.

Morris, R. 1989. *Churches in the Landscape*. London: J. M. Dent & Sons.

O'Neil, H. E. and Grinsell, L. V. 1960: 'Gloucestershire Barrows, Lists: Round Barrows, Gloucestershire', *Transactions of the Bristol and Gloucestershire Archaeological Society* 79, 100-138.

Rahtz, S. and Rowley, T. 1984. *Middleton Stoney: Excavation and Survey in a North Oxfordshire Parish 1970-1982*. Oxford: Oxford University Department for External Studies.

Renn, D. 1968. *Norman Castles in Britain*. London: John Baker.

Rodwell, W. and Atkins, C. 2011. *St Peter's, Barton-upon-Humber, Lincolnshire: A Parish Church and its Community*. Oxford and Oakville: Oxbow Books.

Rudder, S. 1779. *A New History of Gloucestershire*. Cirencester: Samuel Rudder.

Sawyer, P. H. 1968. *Anglo-Saxon Charters: An Annotated List and Bibliography*. London: Royal Historical Society.

Schmidt, A.R., Linford, P., Linford, N., David, A., Gaffney, C.F., Sarris A. and Fassbinder J. 2015: *EAC Guidelines for the use of Geophysics in Archaeology: Questions to Ask and Points to Consider*. EAC Guidelines 2. Namur, Belgium: Europae Archaeologia Consilium (EAC), Association Internationale sans But Lucratif (AISBL).

Smith, A.H. 1964. *The Place-Names of Gloucestershire, Part 1: The River and Road-Names - The East Cotswolds*. Cambridge: Cambridge University Press.

Stoertz, C. 2012. *The North Cotswolds: A Highlight Report for the National Mapping Programme*. Swindon: English Heritage.

Stocker, D. A. and Everson, P. 2006. *Summoning St Michael: Early Romanesque Towers in Lincolnshire*. Oxford: Oxbow Books.

Taylor, H. M. and Taylor, J. 1965. *Anglo-Saxon Architecture* (2 vols). Cambridge: Cambridge University Press.

Taylor, H. M. 1978. *Anglo-Saxon Architecture* (volume three). Cambridge: Cambridge University Press.

Turner, S., Semple, S. and Turner, A. 2013. *Wearmouth and Jarrow: Northumbrian monasteries in an historic landscape*. Hatfield: University of Hertfordshire Press.

Verey, N. and Brooks, A. 1999. *The Buildings of England. Gloucestershire 1: The Cotswolds*. London & New Haven: Yale University Press.

Walrond, L. F. J. 1973. 'Wool, woolmen and weavers', in C. Hadfield and A.M. Hadfield (eds) *The Cotswolds: A New Study*. Newton Abbot: David & Charles, 178-203.

Williams, A. and Martin, G.H. 2002. *Domesday Book: A Complete Translation*. London: Penguin Books.

Williams, B. 1987. 'Excavation of a medieval earthwork complex at Hillesley, Hawkesbury, Avon', *Transactions of the Bristol and Gloucestershire Archaeological Society* 105, 147-164.

Wright, D.W, Bromage, S., Shapland, M.G., Everson, P. and Stocker, D., 2023. 'Laughton en le Morthen, South Yorkshire: evolution of a medieval magnate core', *Landscapes* 23, 140-165.

Zakšek, K., Oštir, K., and Kokalj, Ž. 2011. 'Sky-view factor as a relief visualization technique', *Remote Sensing* 3(2), 398-441.

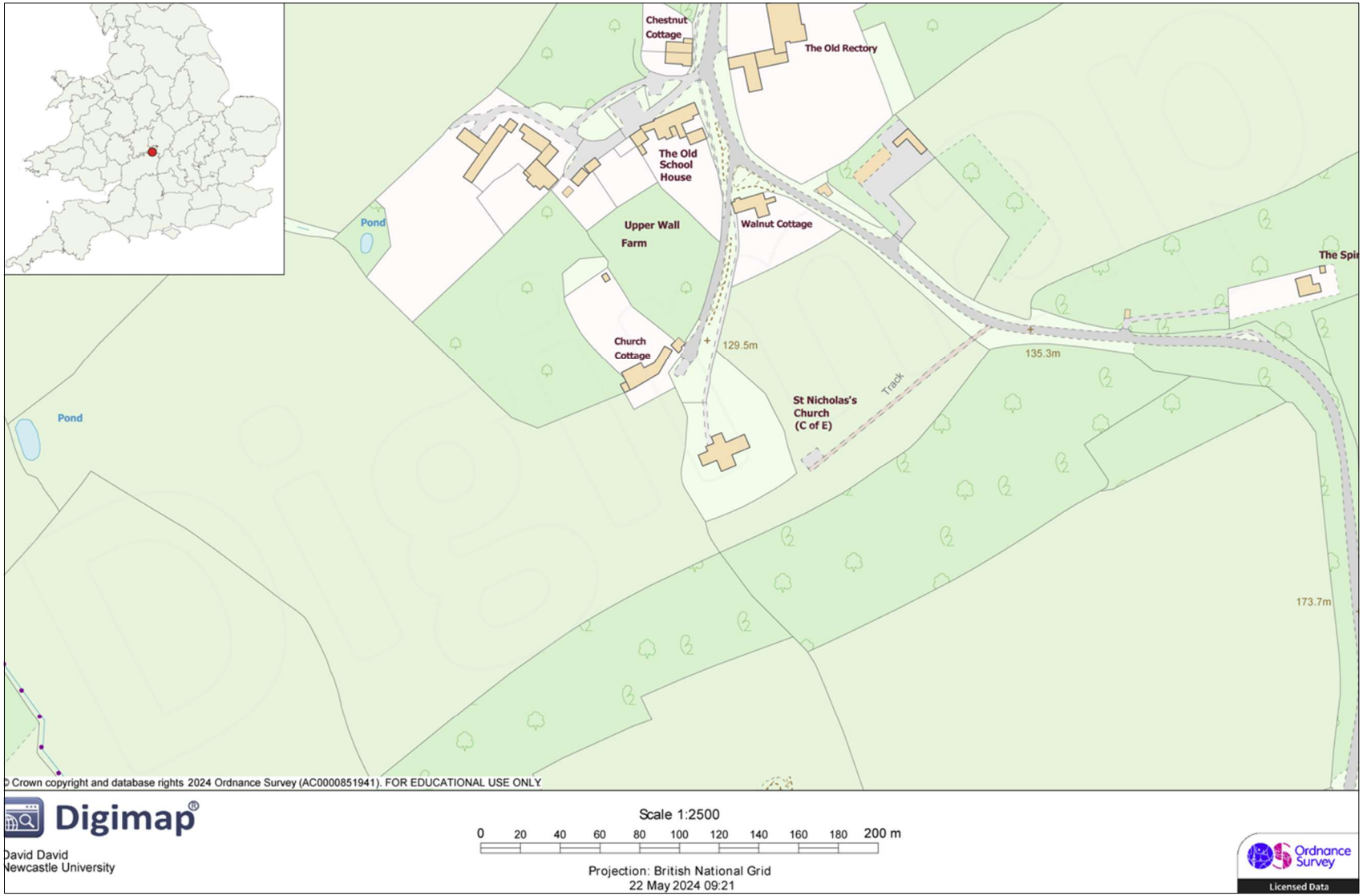

Figure 1: Modern OS map of St Nicholas Church, Saintbury, and the survey area. The location of Saintbury in central southern Britain is inset. Source: © Crown Copyright and Database Rights. Ordnance Survey (Digimap Licence).

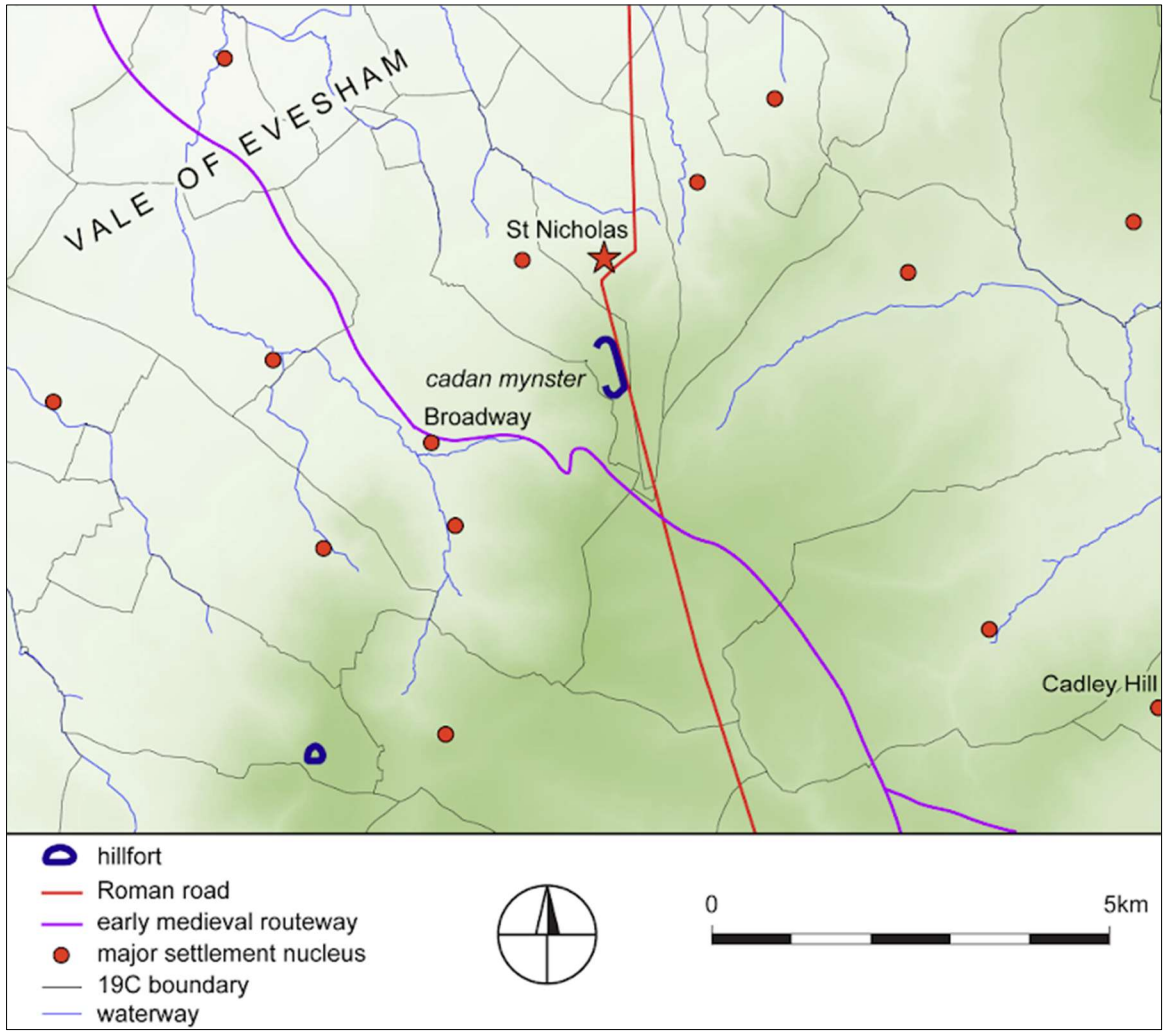

Figure 2: Della Hooke's reconstruction of the landscape around Saintbury, based upon the evidence from Old English charter bounds (Hooke 1987, 96-9).

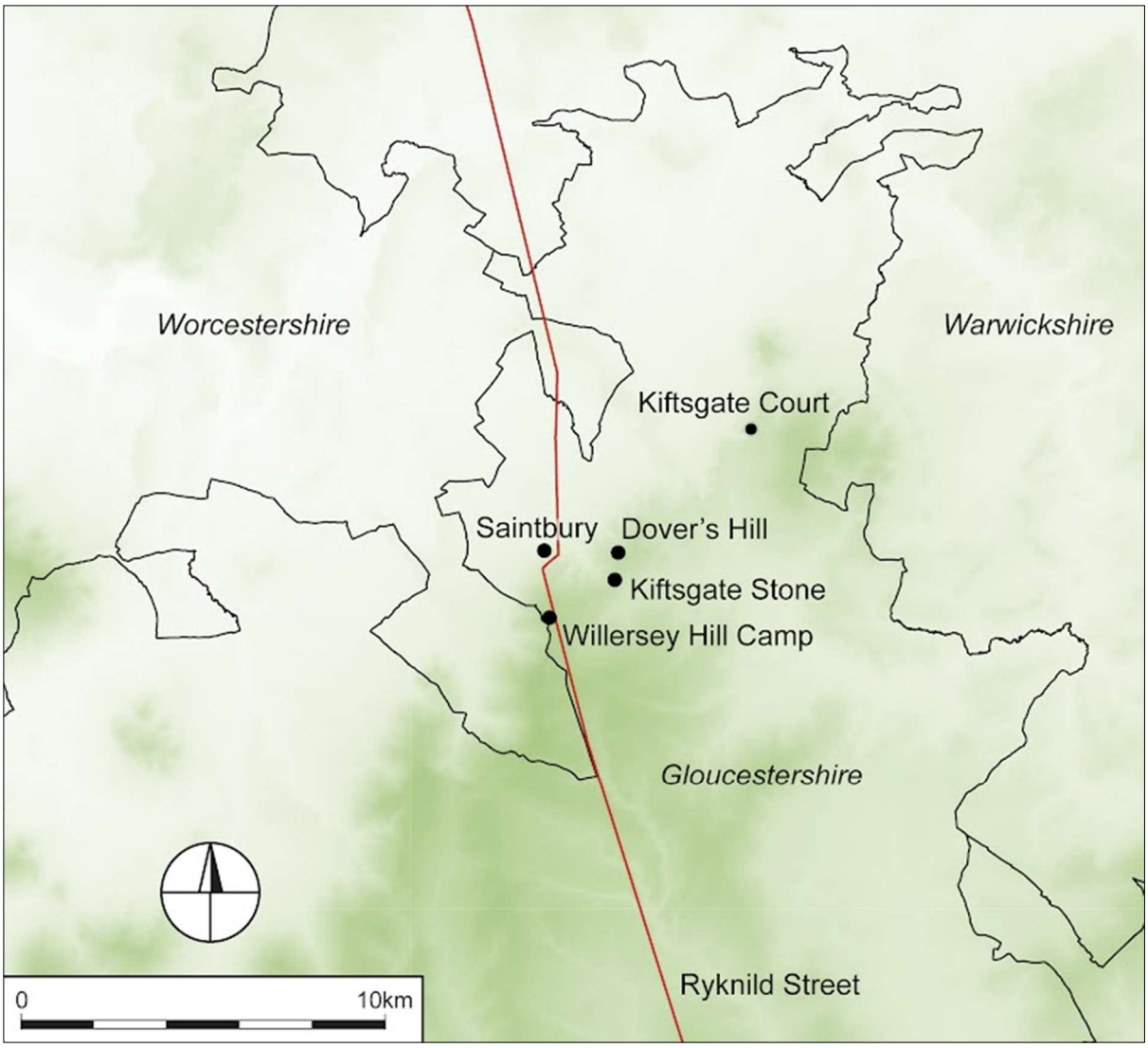

Figure 3: A landscape of early medieval assembly in northern Gloucestershire. The meeting places of Kiftsgate Stone and Kiftsgate Court, and other locations mentioned in the text.

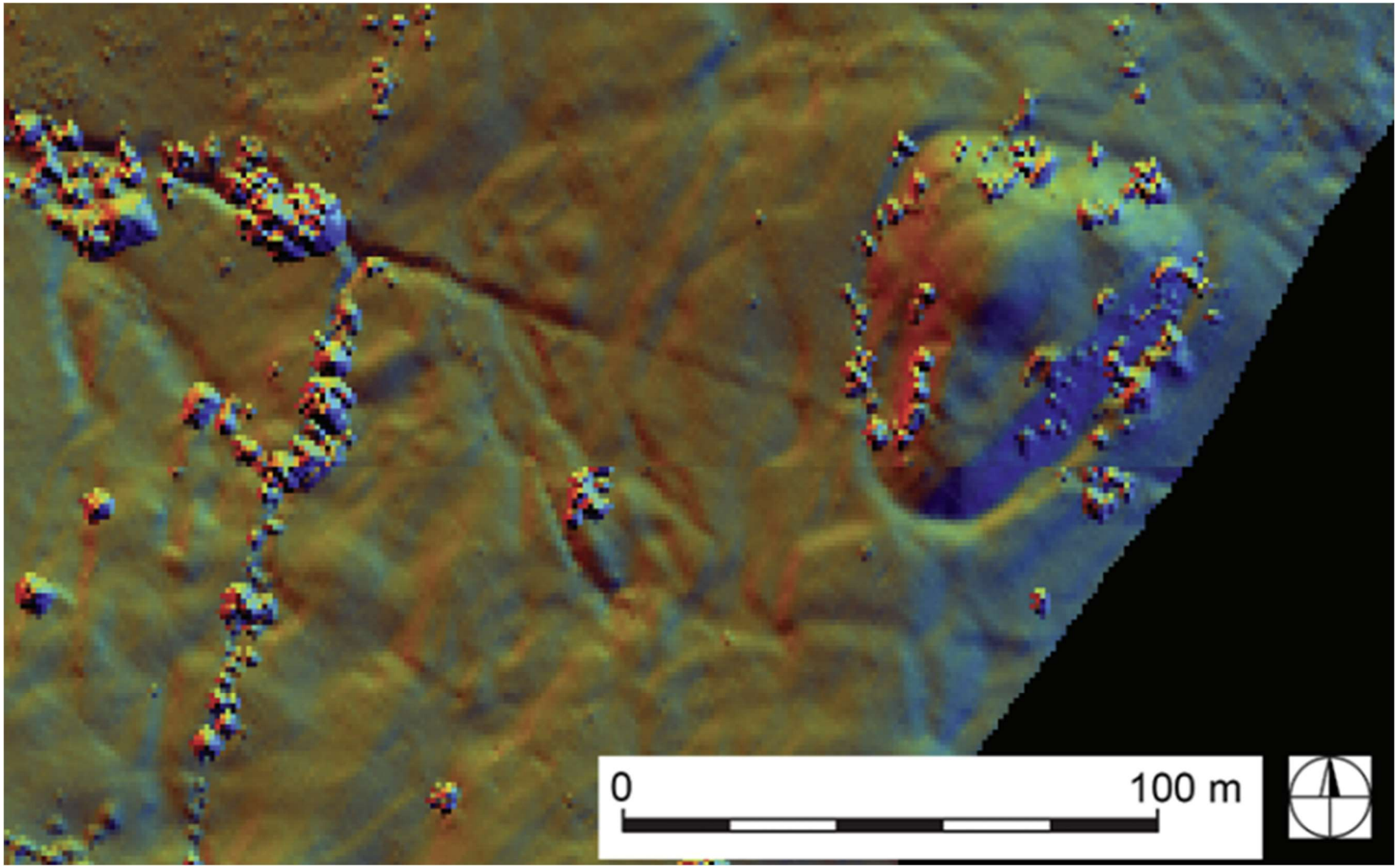

Figure 4: The motte and bailey castle in Weston Park, Saintbury. The earthwork has been truncated on its northern side in particular, probably when it was adapted for use as a prospect mound by the occupiers of the house.

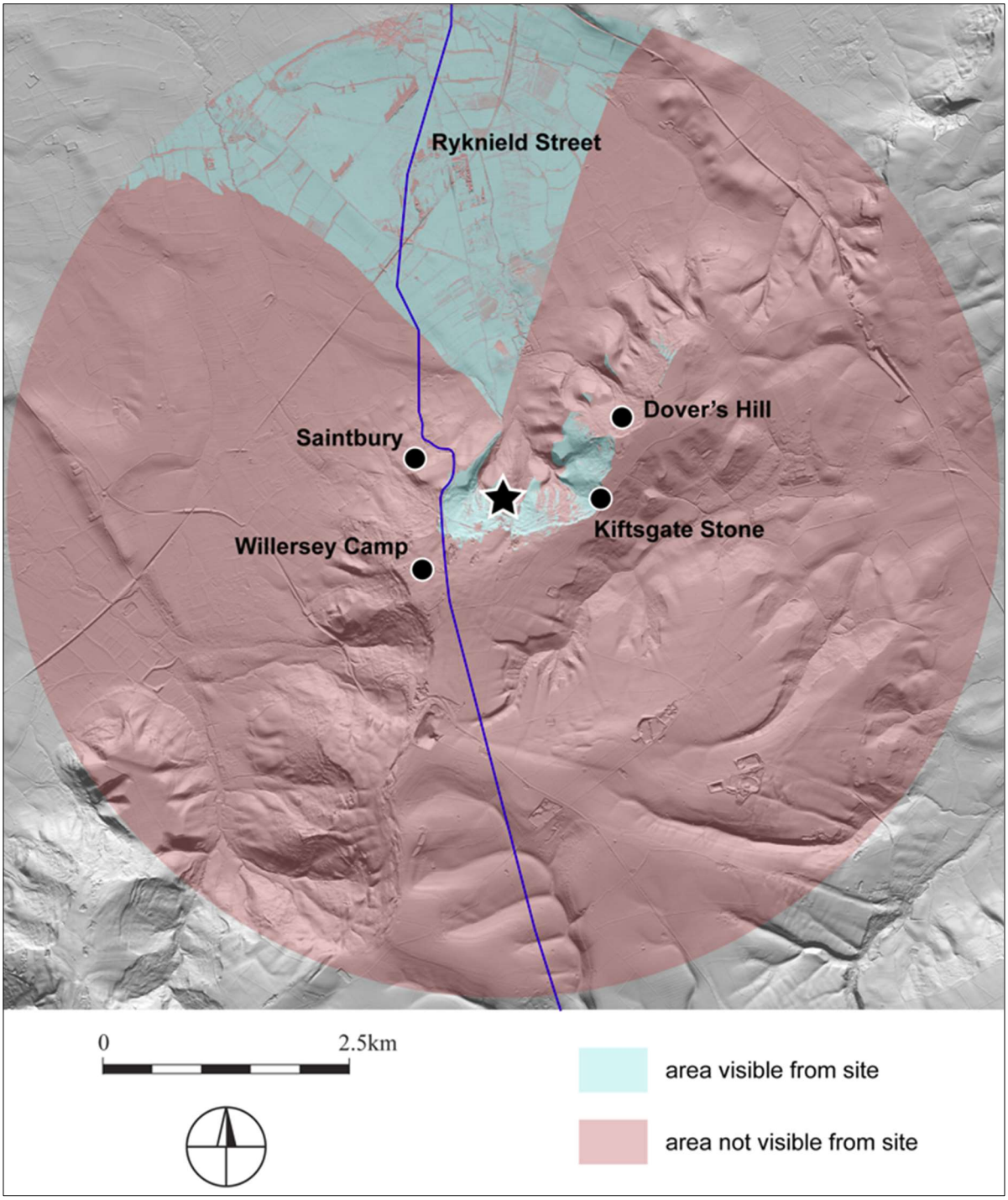

Figure 5: Viewshed model from the castle in the grounds of Weston Park, Saintbury, based upon a 1.5m height from the highest point of the motte. The star represents the castle, with other features mentioned in the text also labelled.

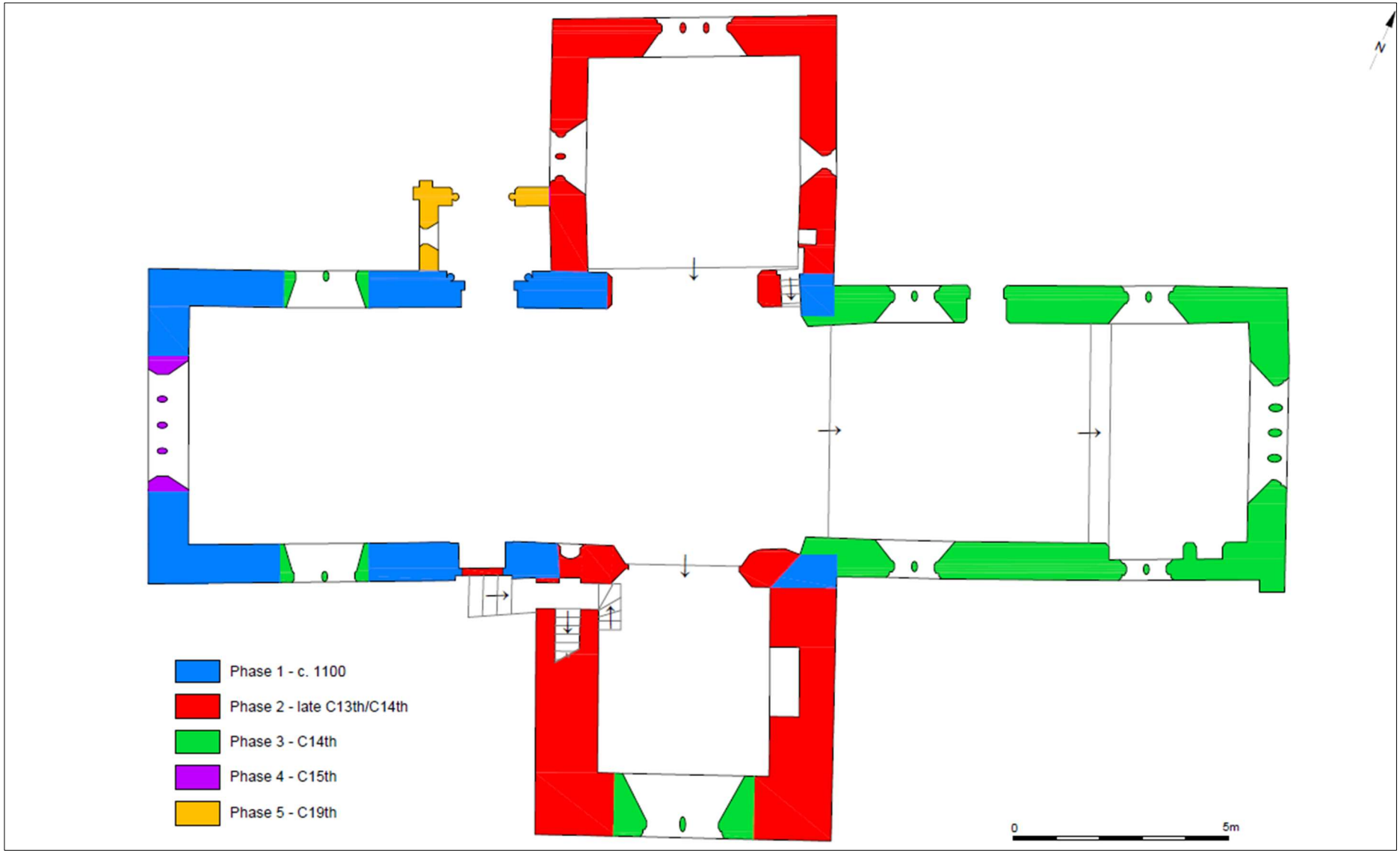

Figure 6: Indicative phase plan of St Nicholas' Church, Saintbury.

Figure 7: General view of the church, looking south-west.

Figure 8: General view of church, looking north-west.

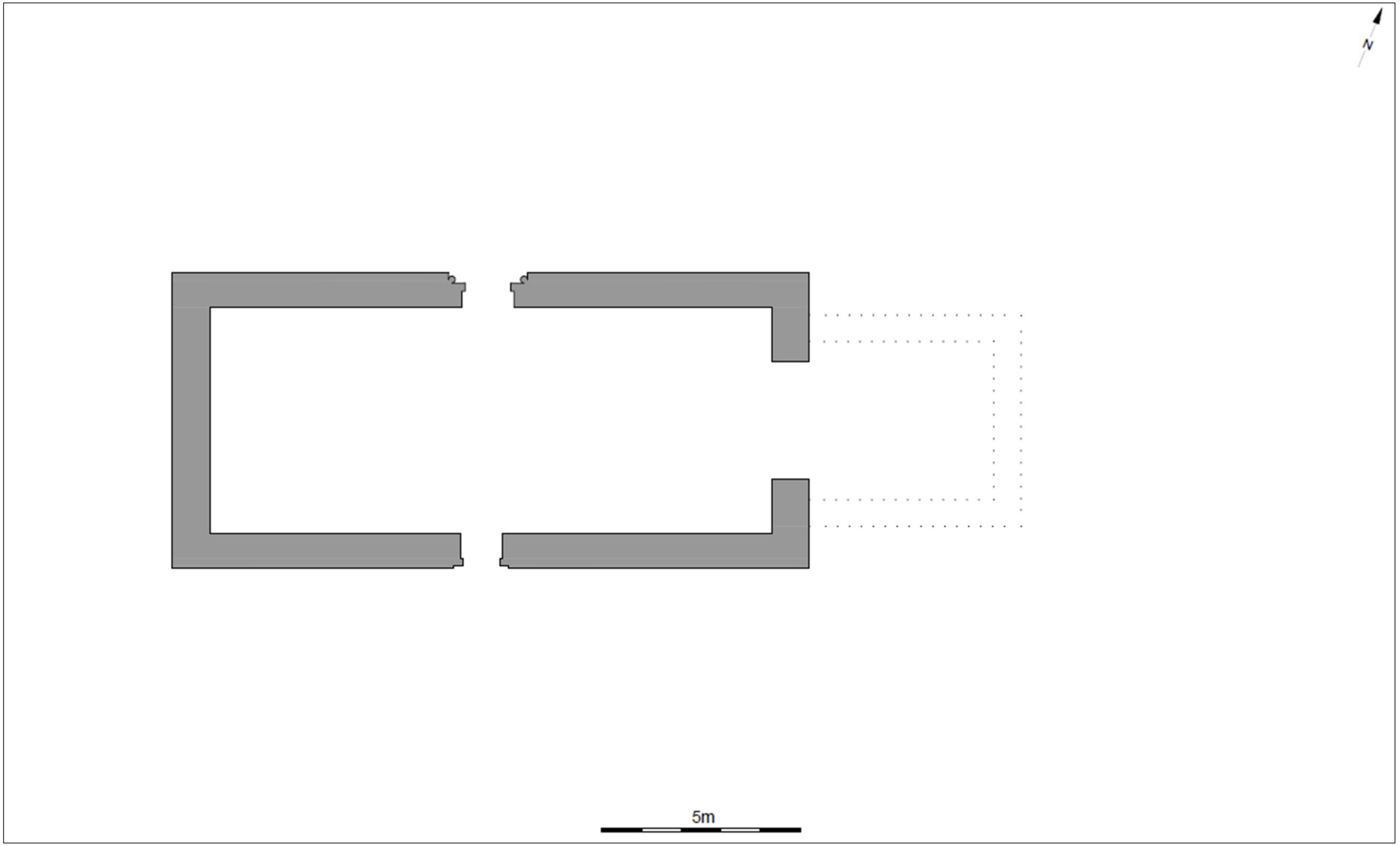

Figure 9: Reconstruction plan of Phase I of St Nicholas' Church, Saintbury.

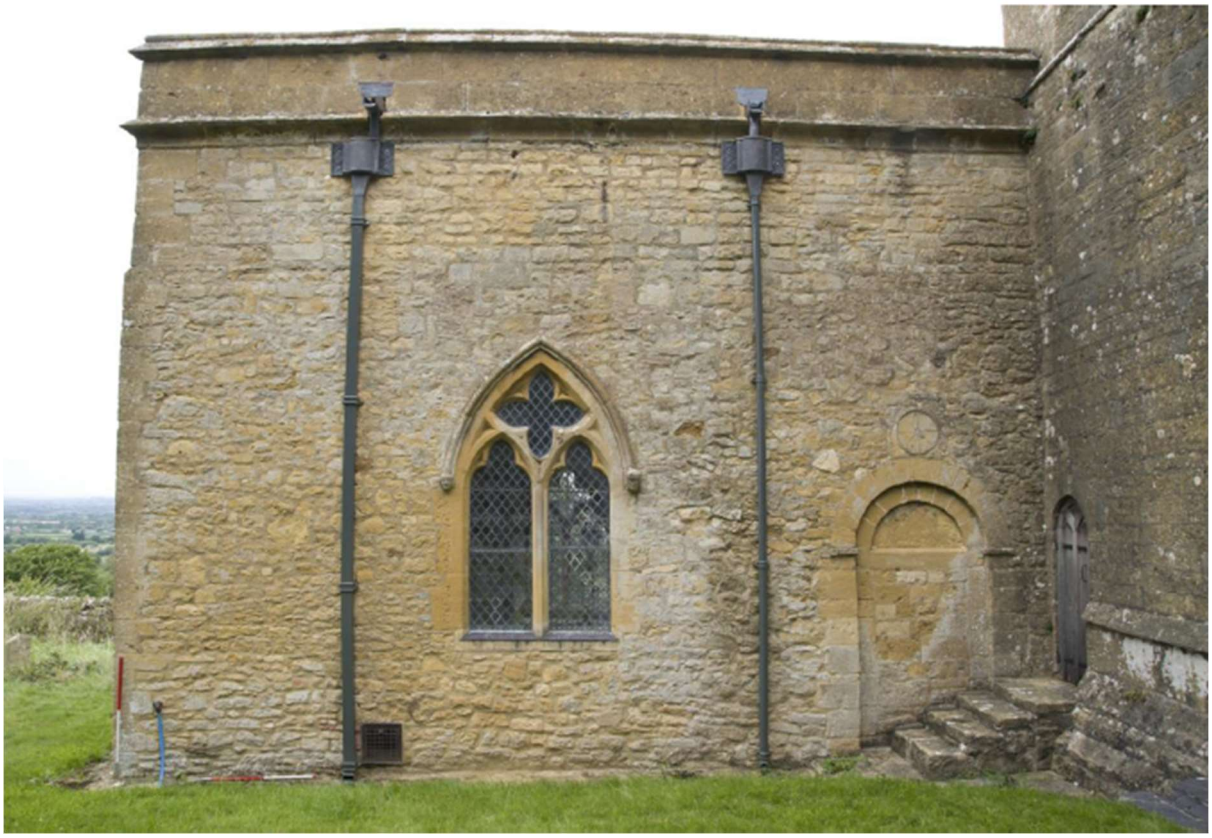

Figure 10: The Norman nave, external south elevation looking north.

Figure 11: The Norman nave, external north elevation looking south.

Figure 12: The Norman nave, external west elevation looking east.

Figure 13: The Norman nave, former external north elevation, looking south from within the later medieval north transept.

Figure 14: The Norman nave, general view looking east.

Figure 15: The Norman nave, general view looking west.

Figure 16: North doorway, general view looking south.

Figure 17: Detail of grotesque about the north doorway.

Figure 18: South doorway, looking north.

Figure 19: Two-light megalithic window formerly located within the church (Mackay 1963). The current location is unknown.

Figure 20: Remnant of possible former column re-set into the western gable end of the church.

Figure 21: Remnant of chevron ornament re-set into the southern external wall of the chancel.

Figure 22: Possible early figurative sculpture re-set into the southern internal wall of the chancel.

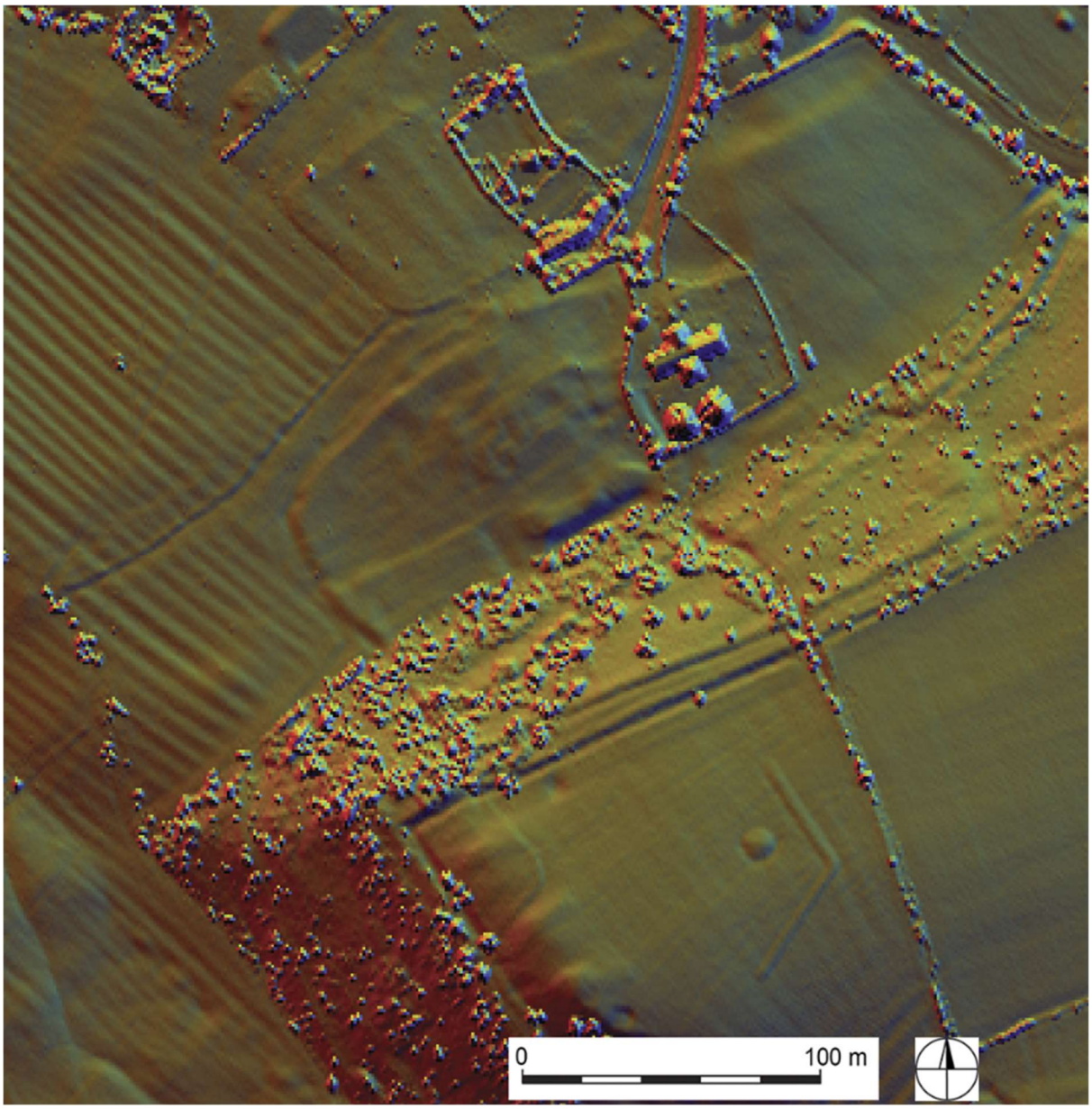

Figure 23: DTM of St Nicholas' Church and the surrounding landscape derived from Environment Agency LiDAR data. © Environment Agency copyright and/or database right 2022. All rights reserved.

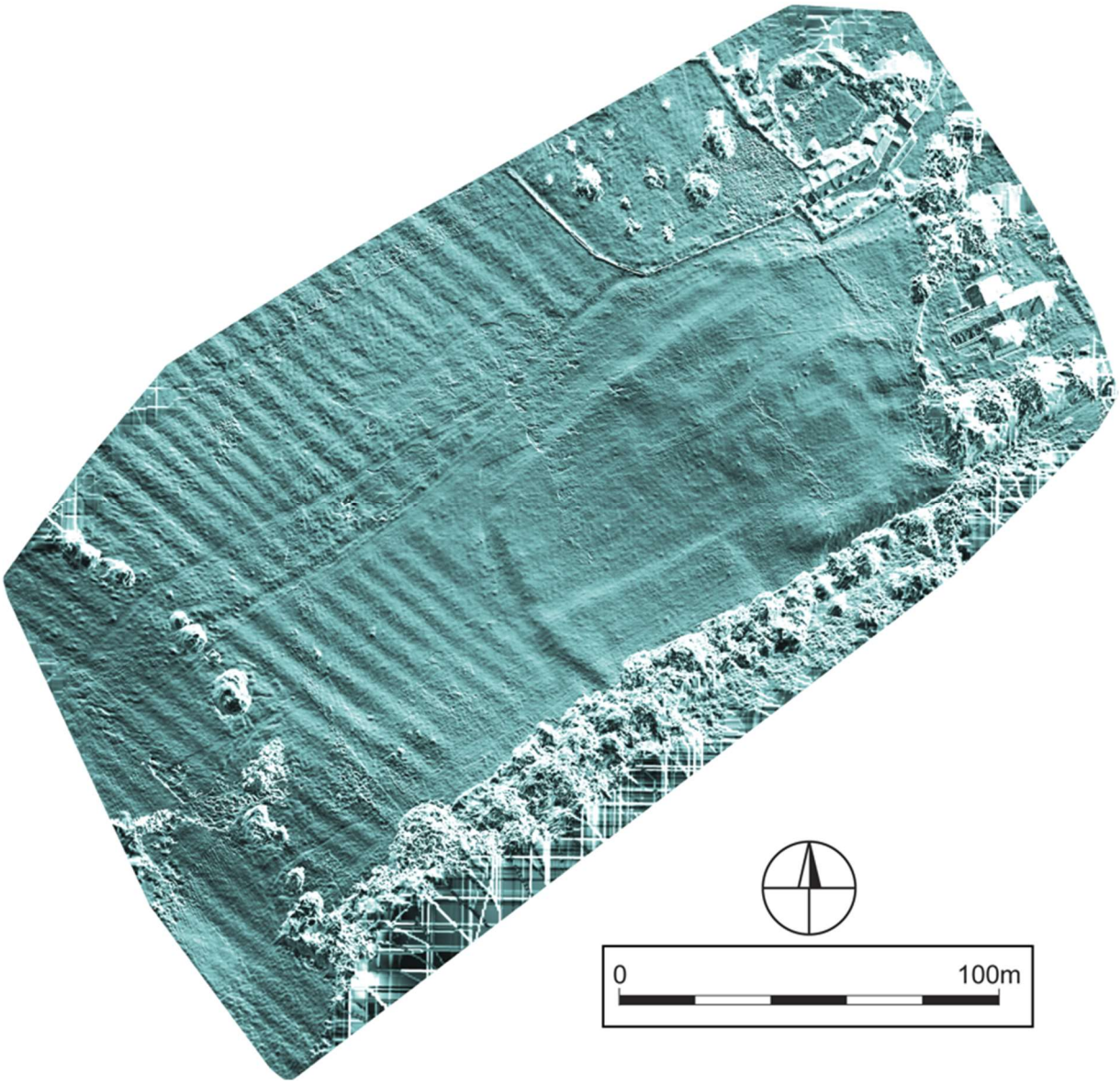

Figure 24: Digital Terrain Model of earthworks south-west of St Nicholas' church.

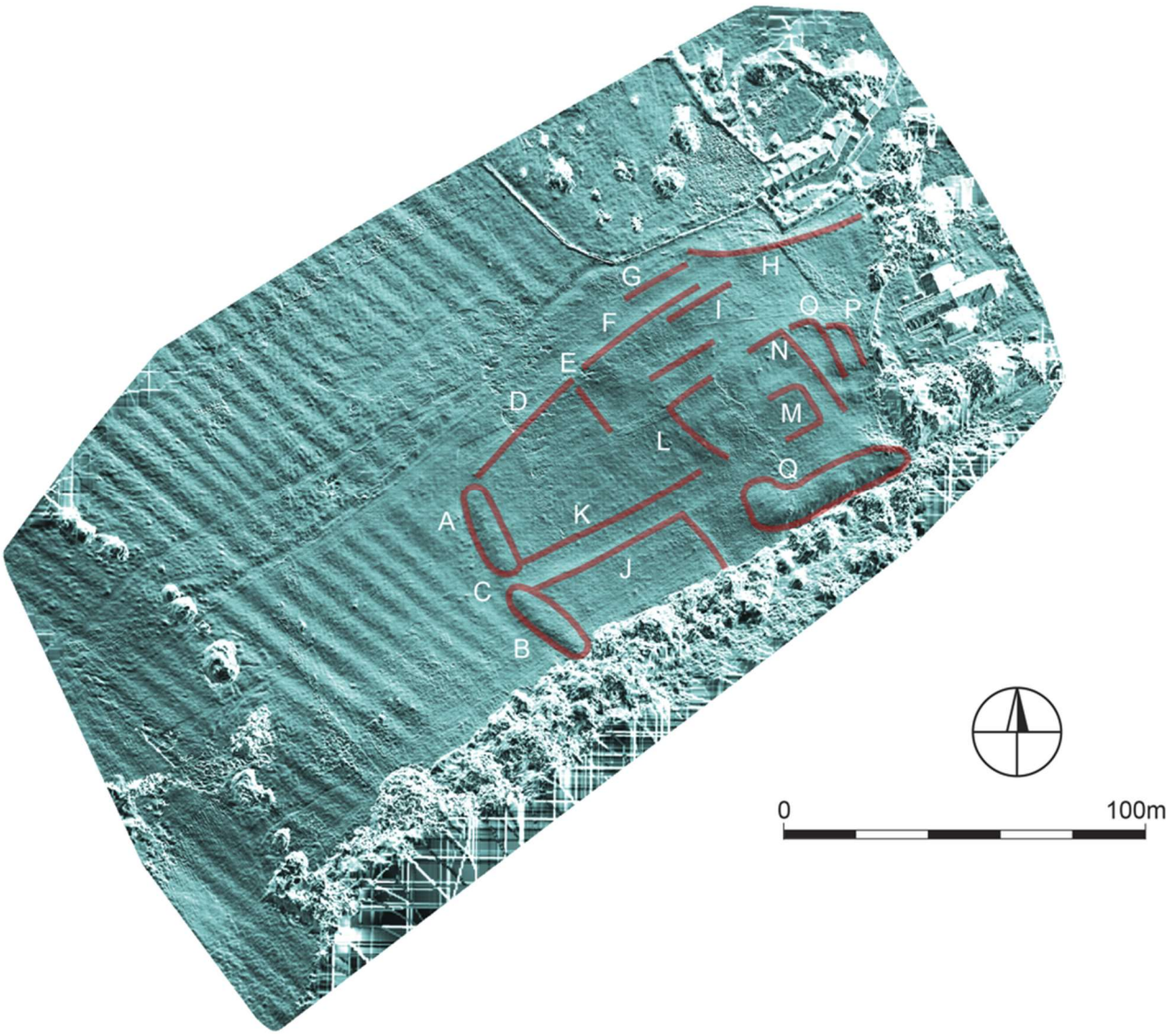

Figure 25: Annotation of positive earthwork features (i.e. banks) identified on the DTM generated by UAV survey.

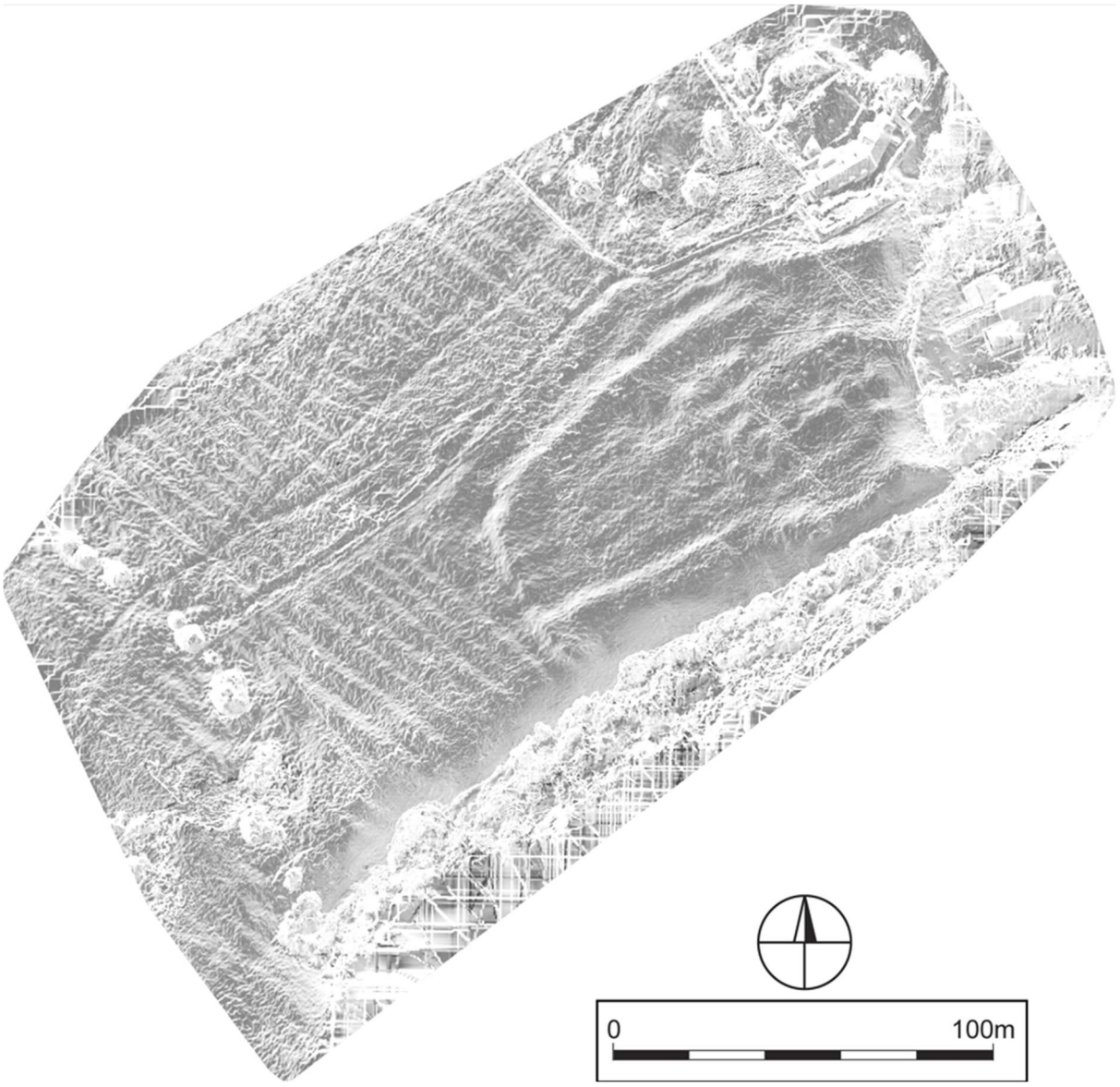

Figure 26: Greyscale DTM with accentuated slope profile. This processing has the advantage of rendering key features more visible, although more subtle variations in the topography can be harder to detect.

Figure 27: Gradiometer survey being undertaken in Area A, south-west of St Nicholas' Church.

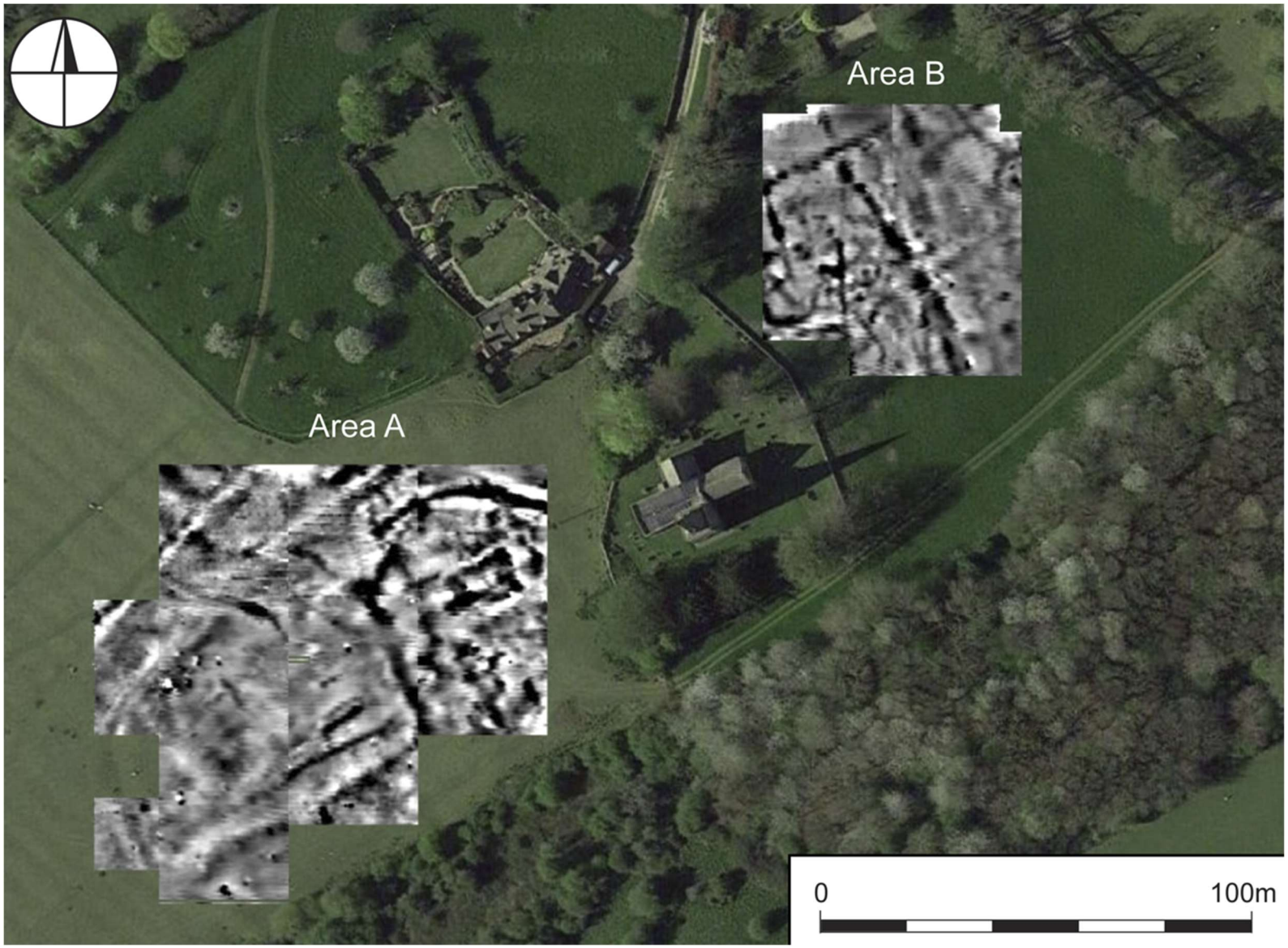

Figure 28: Processed gradiometer plot of the two survey areas either side of St Nicholas' church (centre).

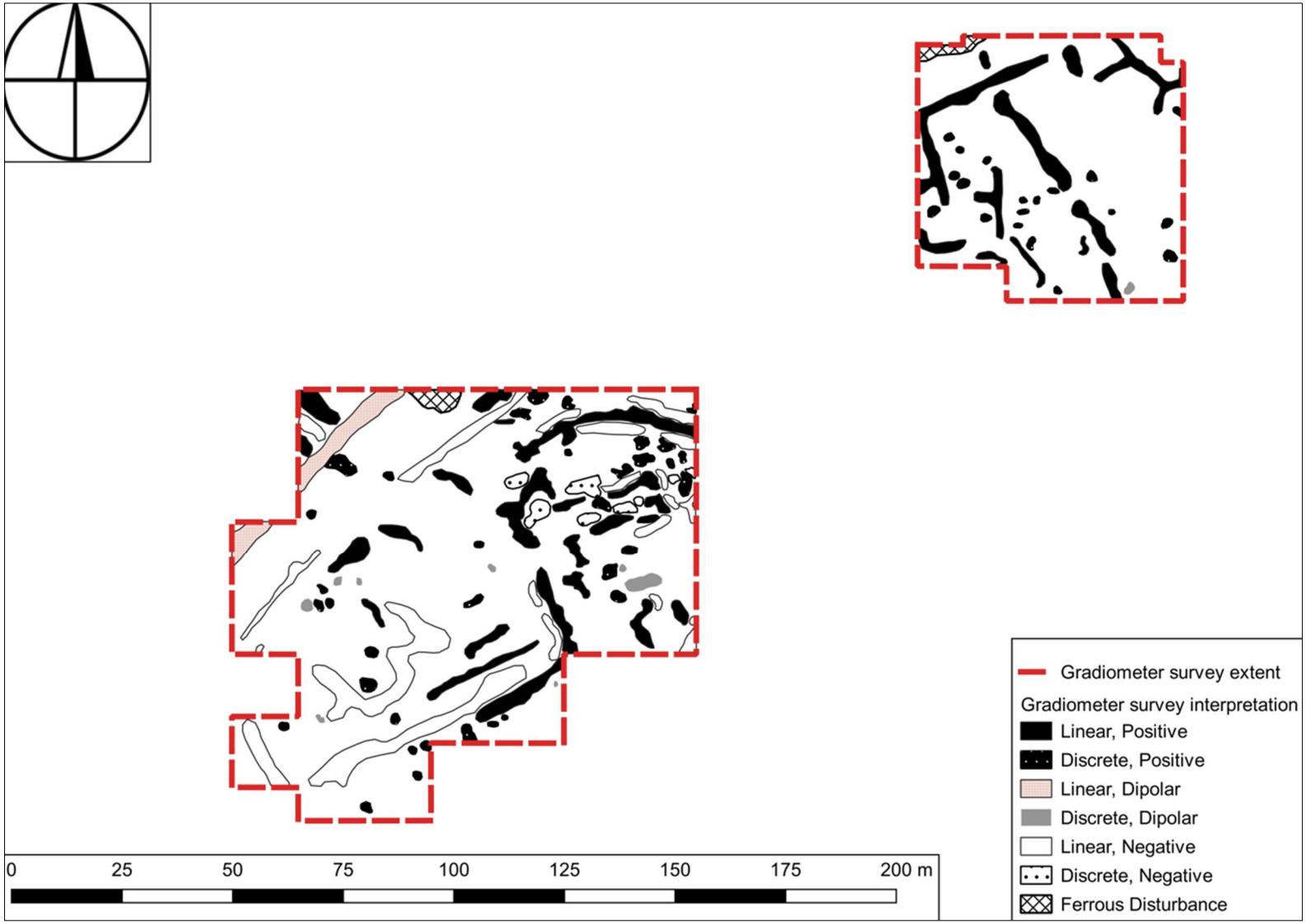

Figure 29: Interpretation of anomalies identified in the gradiometer data.

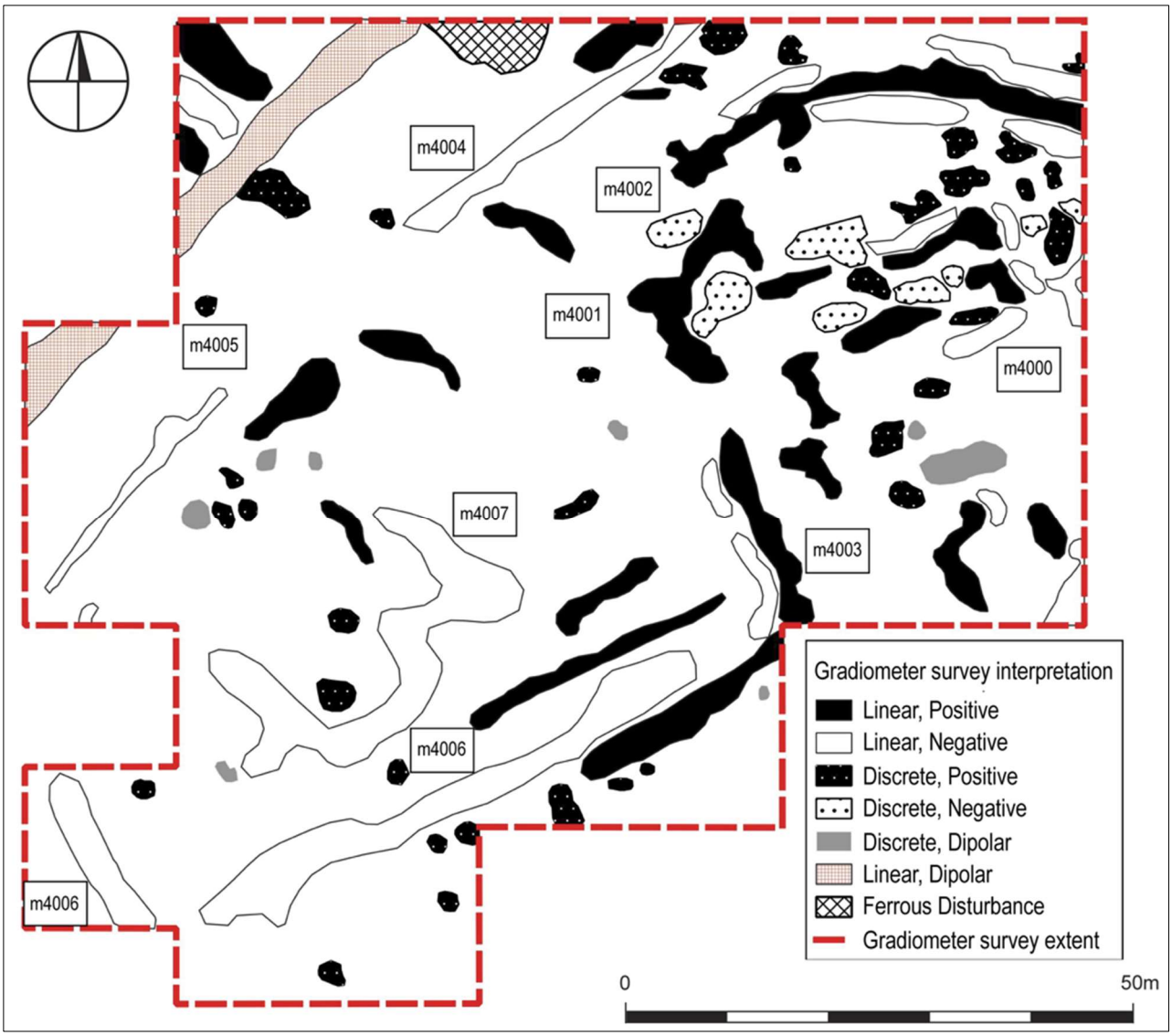

Figure 30: Annotated interpretation of gradiometer survey Area A, south-west of the church.

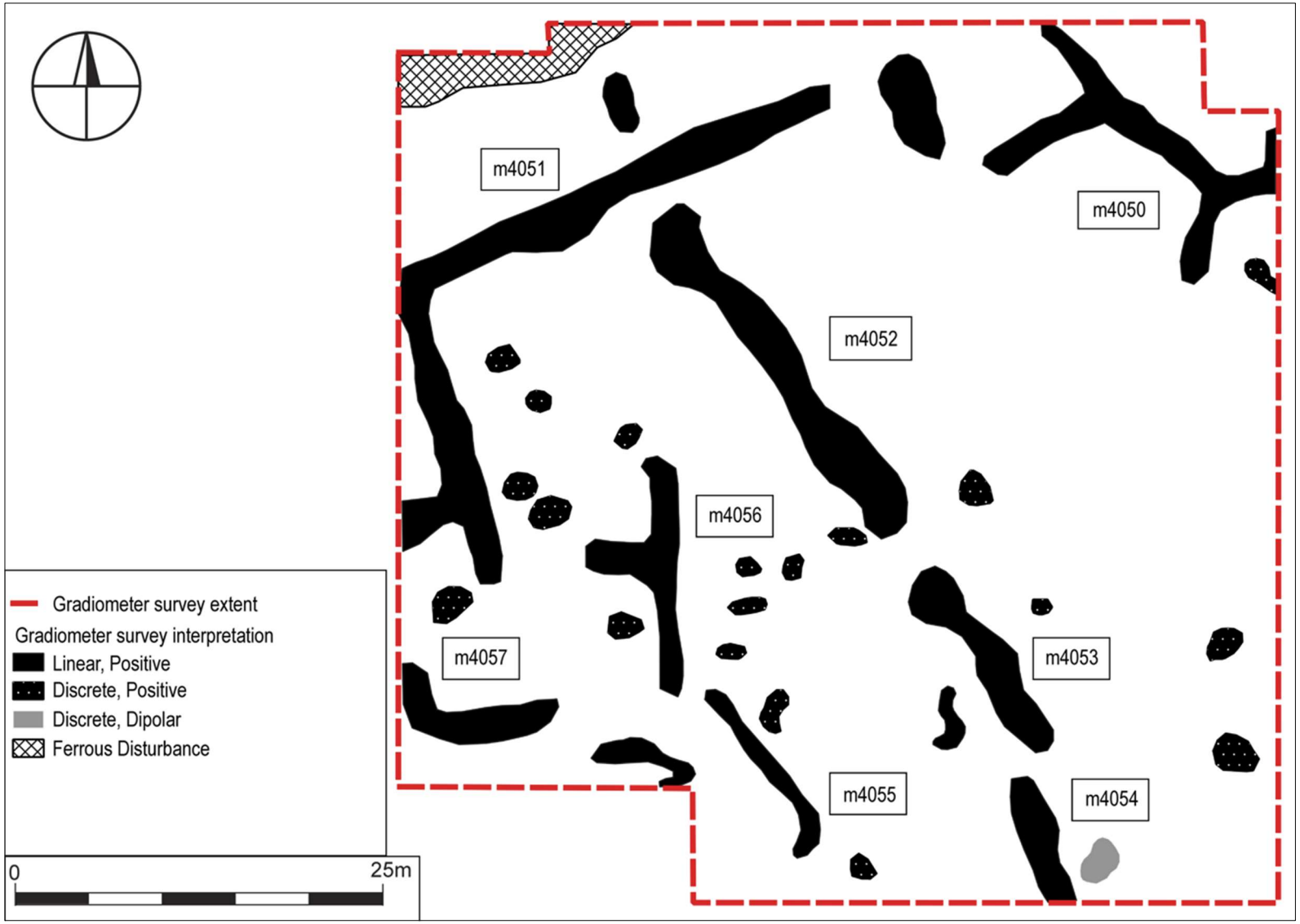

Figure 31: Annotated interpretation of gradiometer survey Area B, north-east of the church.

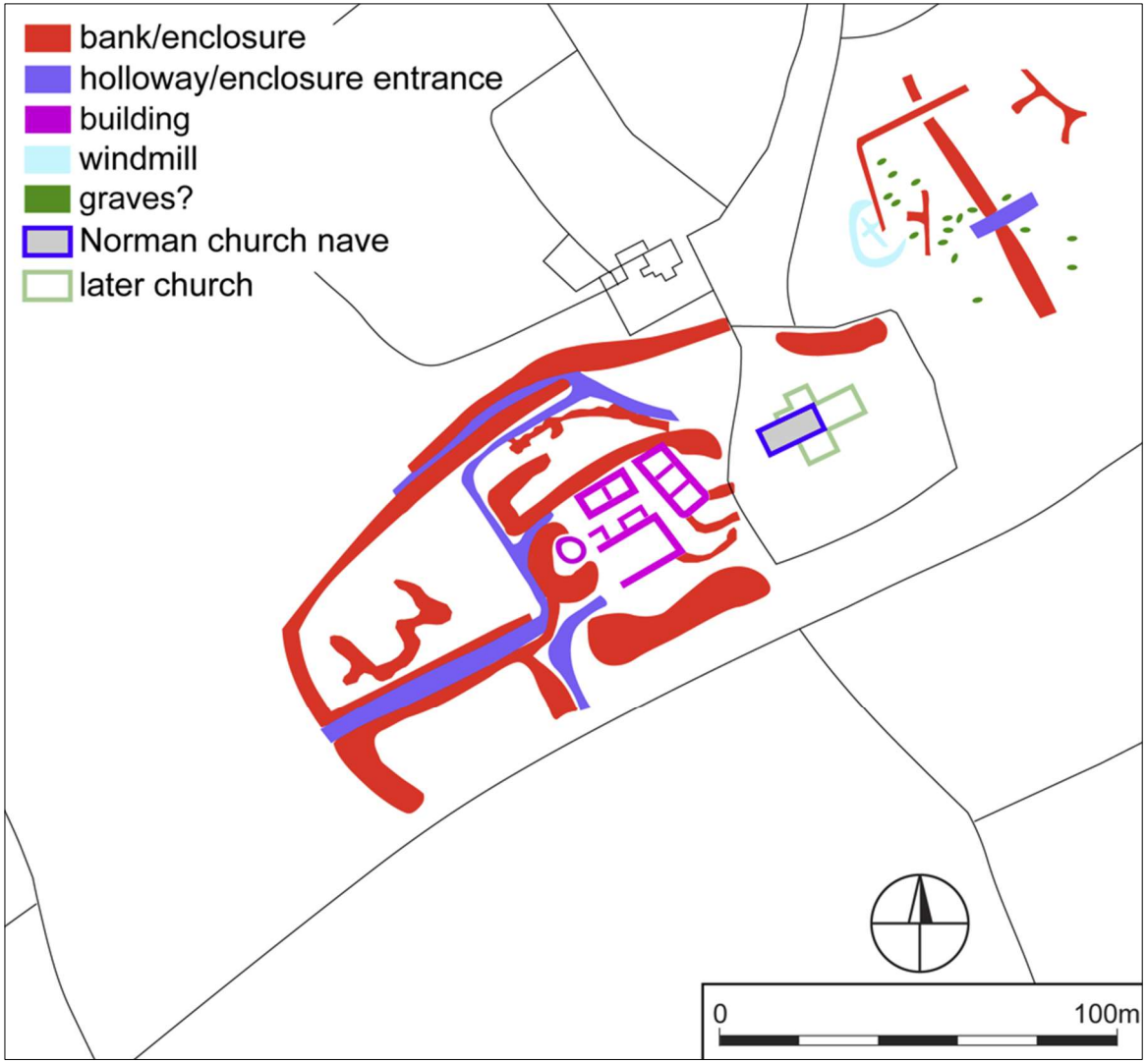

Figure 32: Schematic plan of features identified by topographic and gradiometer surveys, including conjectured interpretations. © Crown Copyright and Database Rights. Ordnance Survey (Digimap Licence).

Figure 33: Earth resistance survey being carried out in Area A, immediately west of St Nicholas' churchyard.

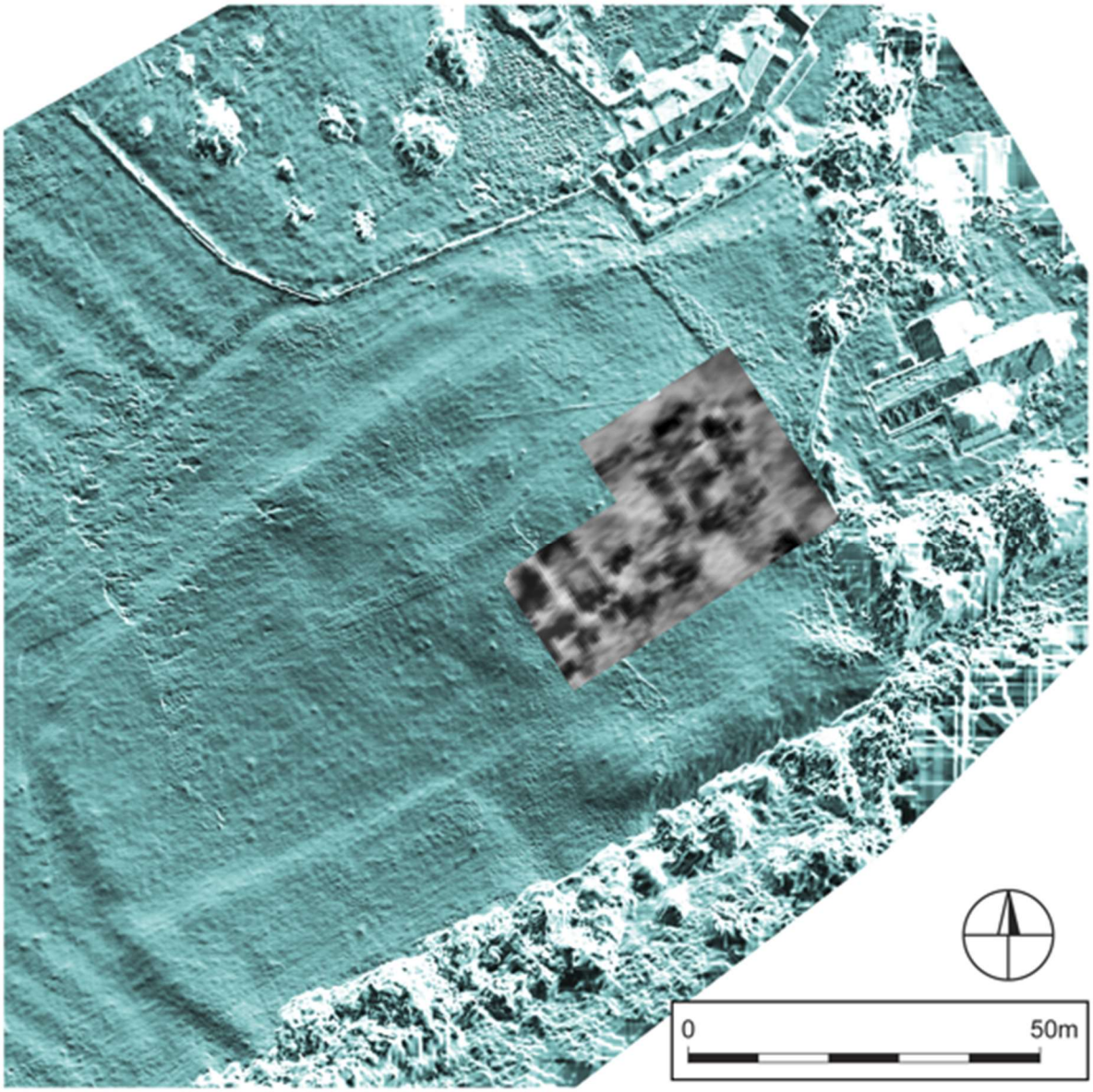

Figure 34: Plot of earth resistance data. Dark areas represent high resistance anomalies, and light areas low resistance anomalies.

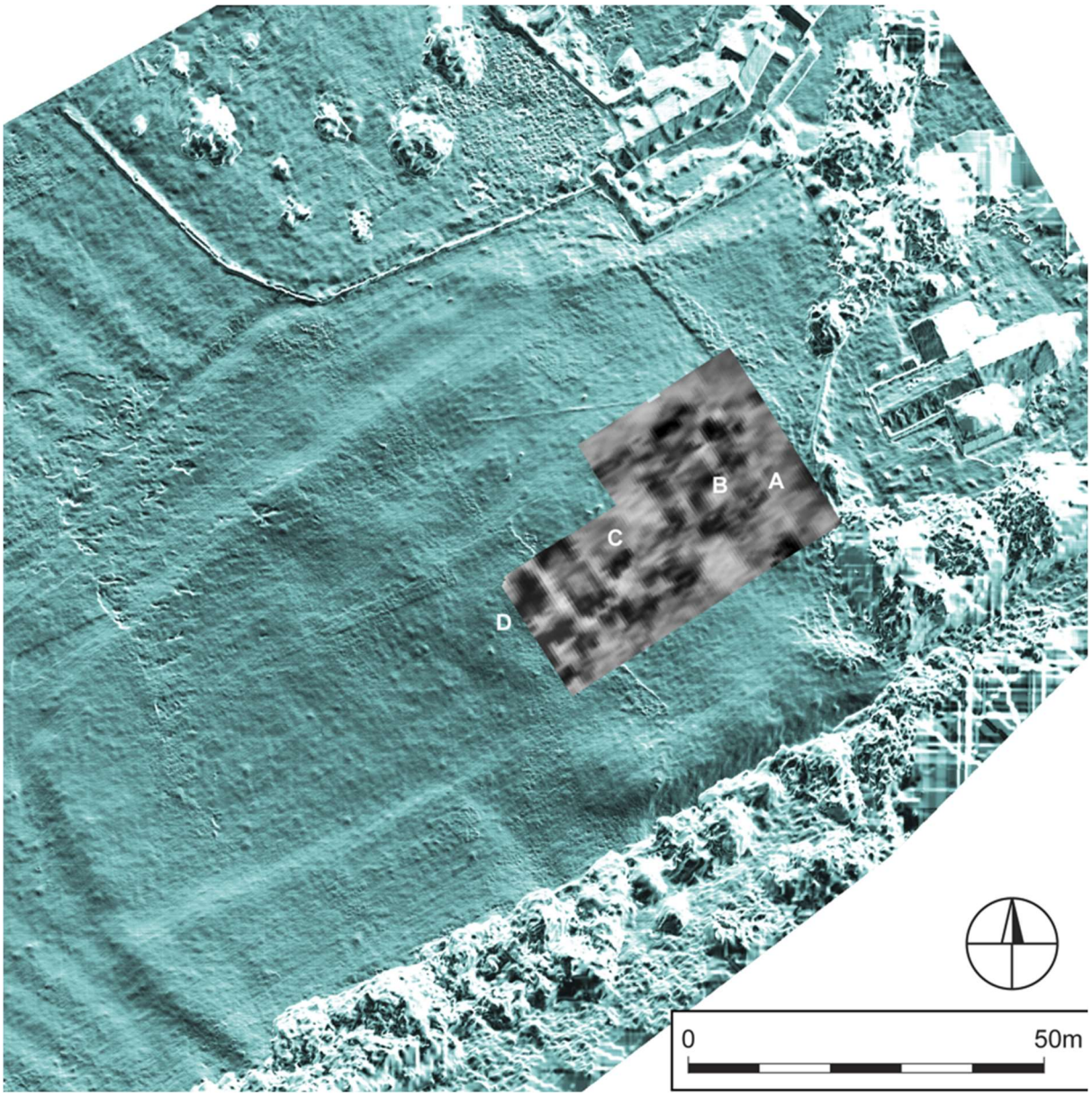

Figure 35: Annotation of anomalies identified by the earth resistance survey.

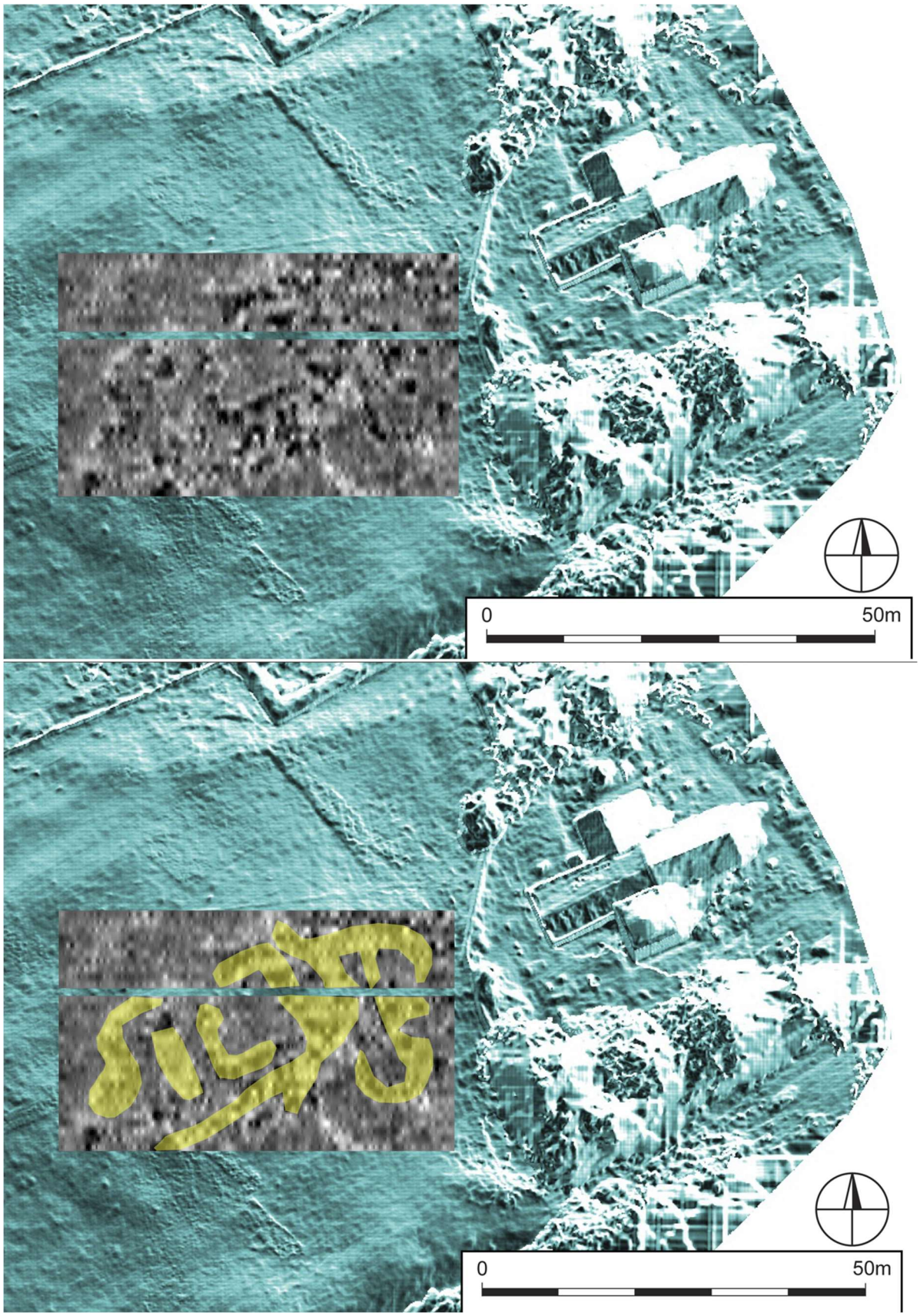

Figure 36: Raw plot of anomalies at TS03 (above) and interpretation (below) located by the GPR. These features are located at a depth of *c*.0.4-0.6m below ground surface.

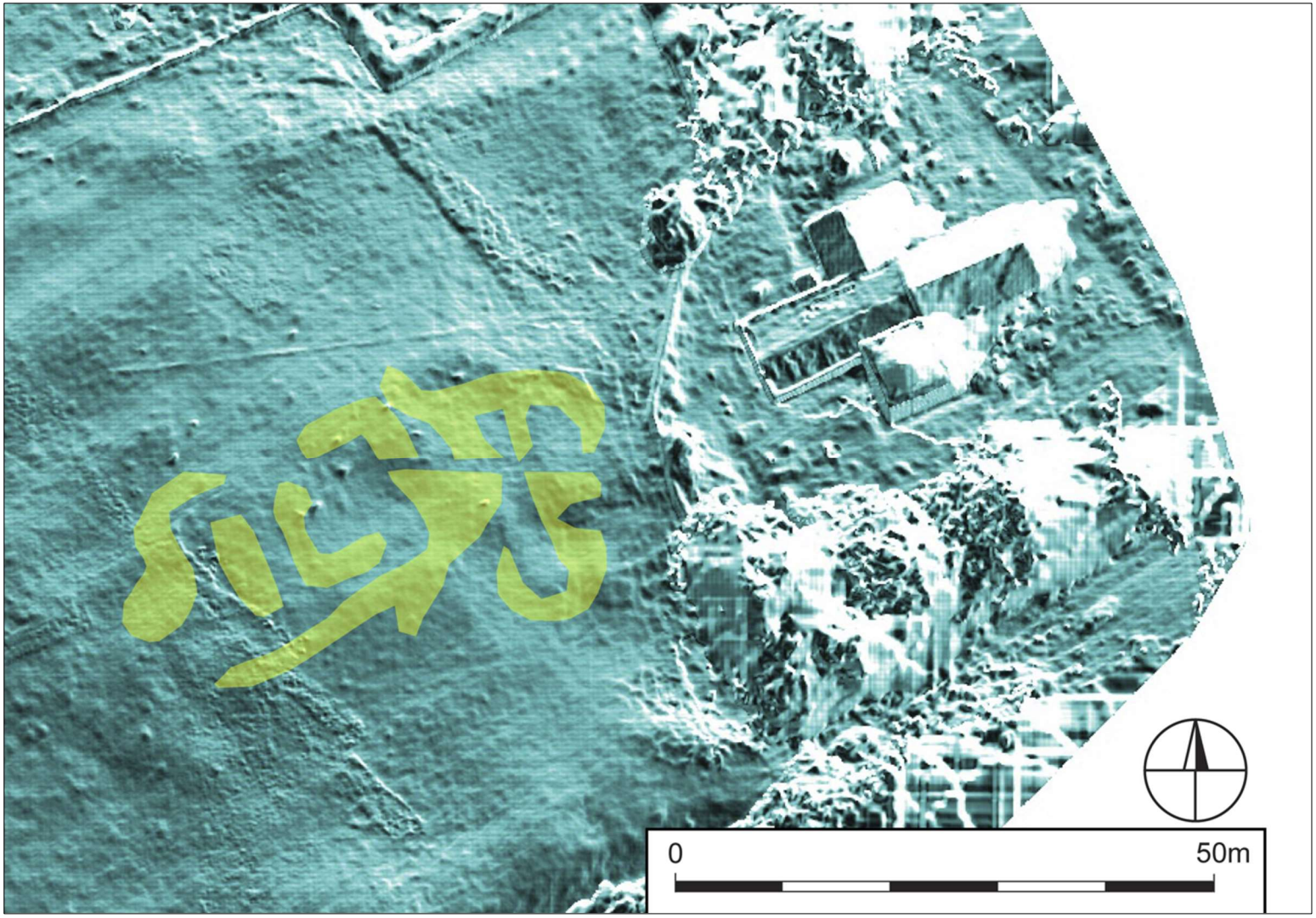

Figure 37: Interpretation of anomalies at TS03, overlaid on the DTM model. Several of the anomalies clearly correlate to upstanding earthworks.

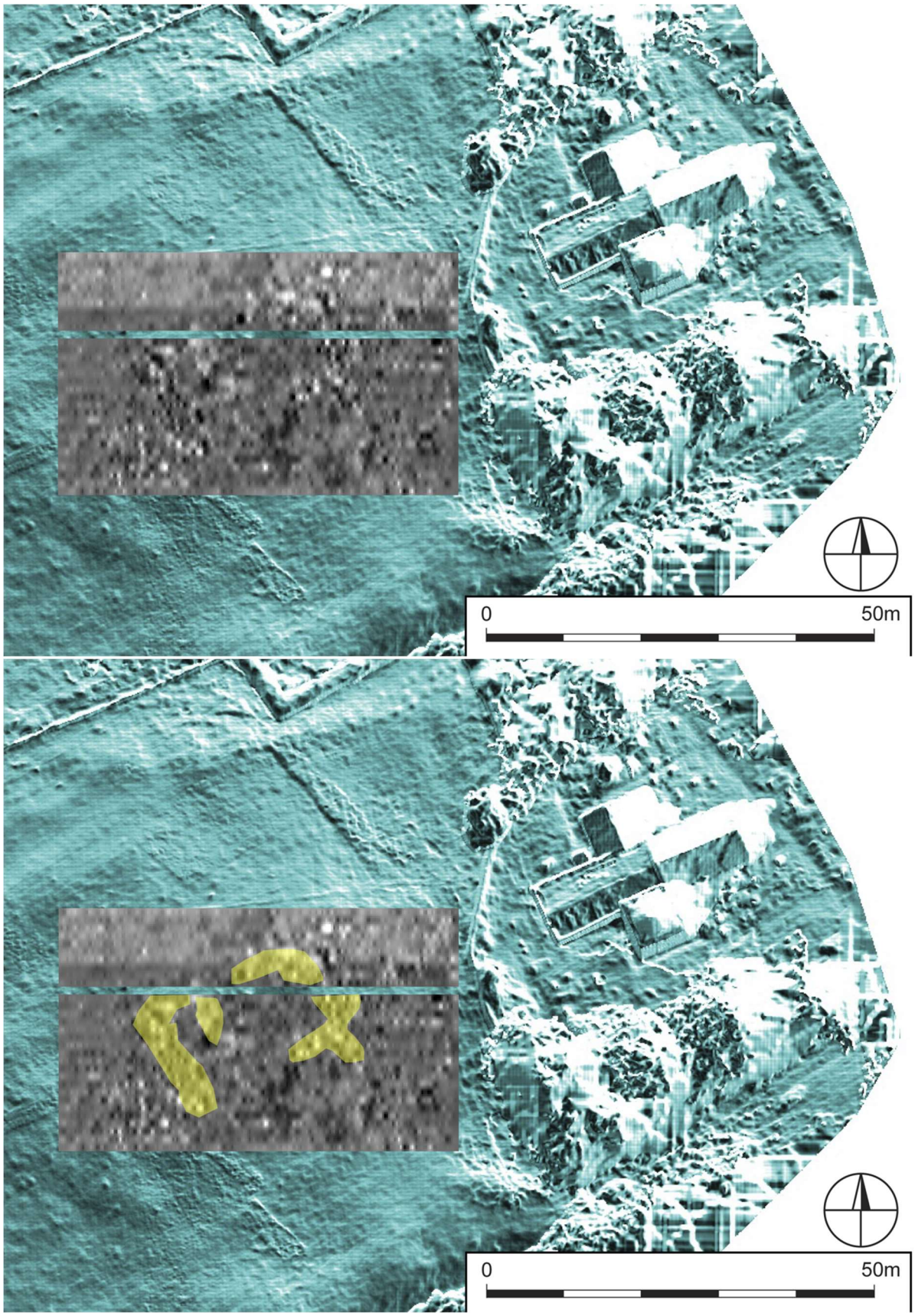

Figure 38: Raw plot of anomalies at TS07 (above) and interpretation (below) located by the GPR. These features are located at a depth of *c*.1.2-1.4m below ground surface.

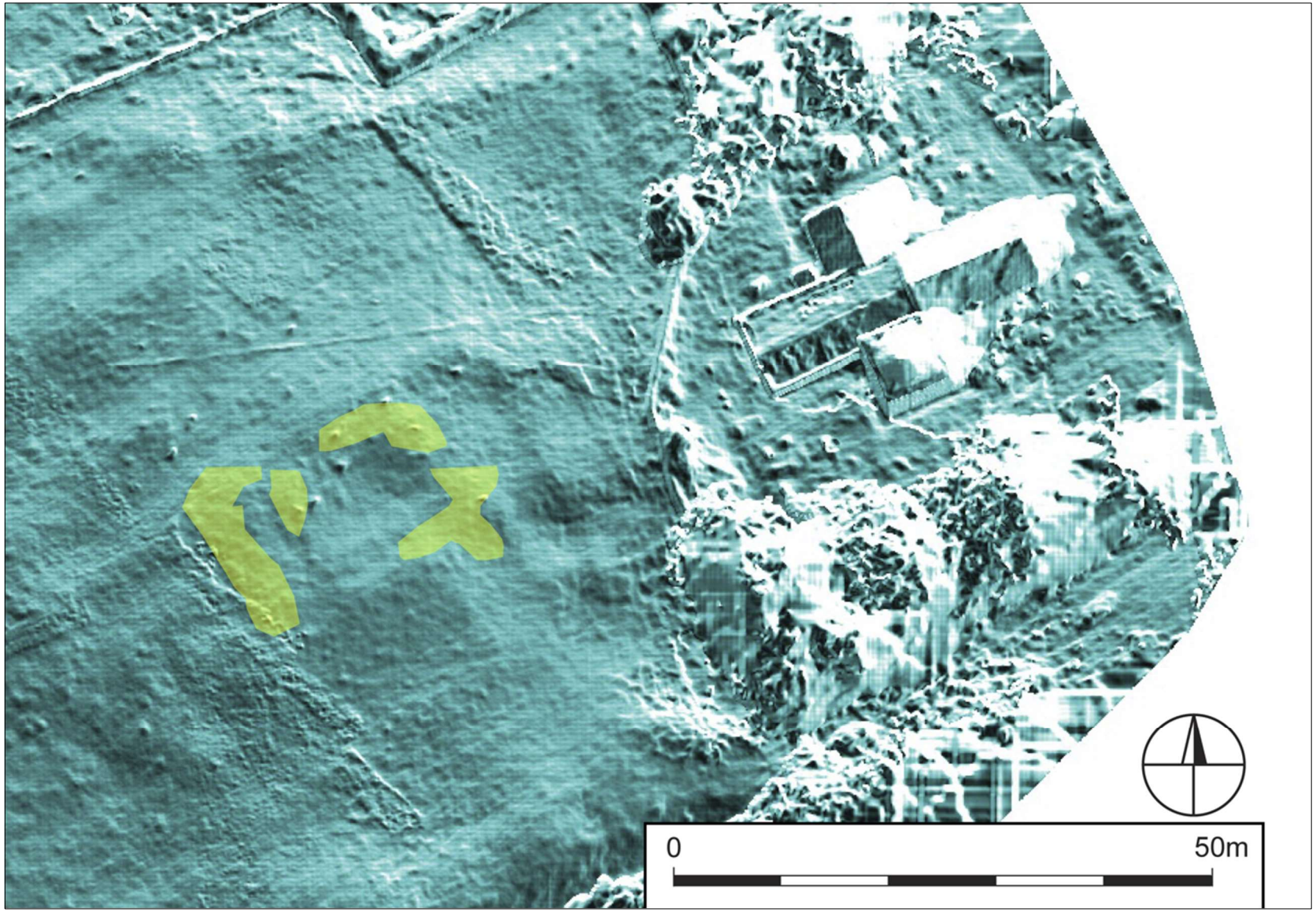

Figure 39: Interpretation of anomalies at TS07, overlaid on the DTM model.

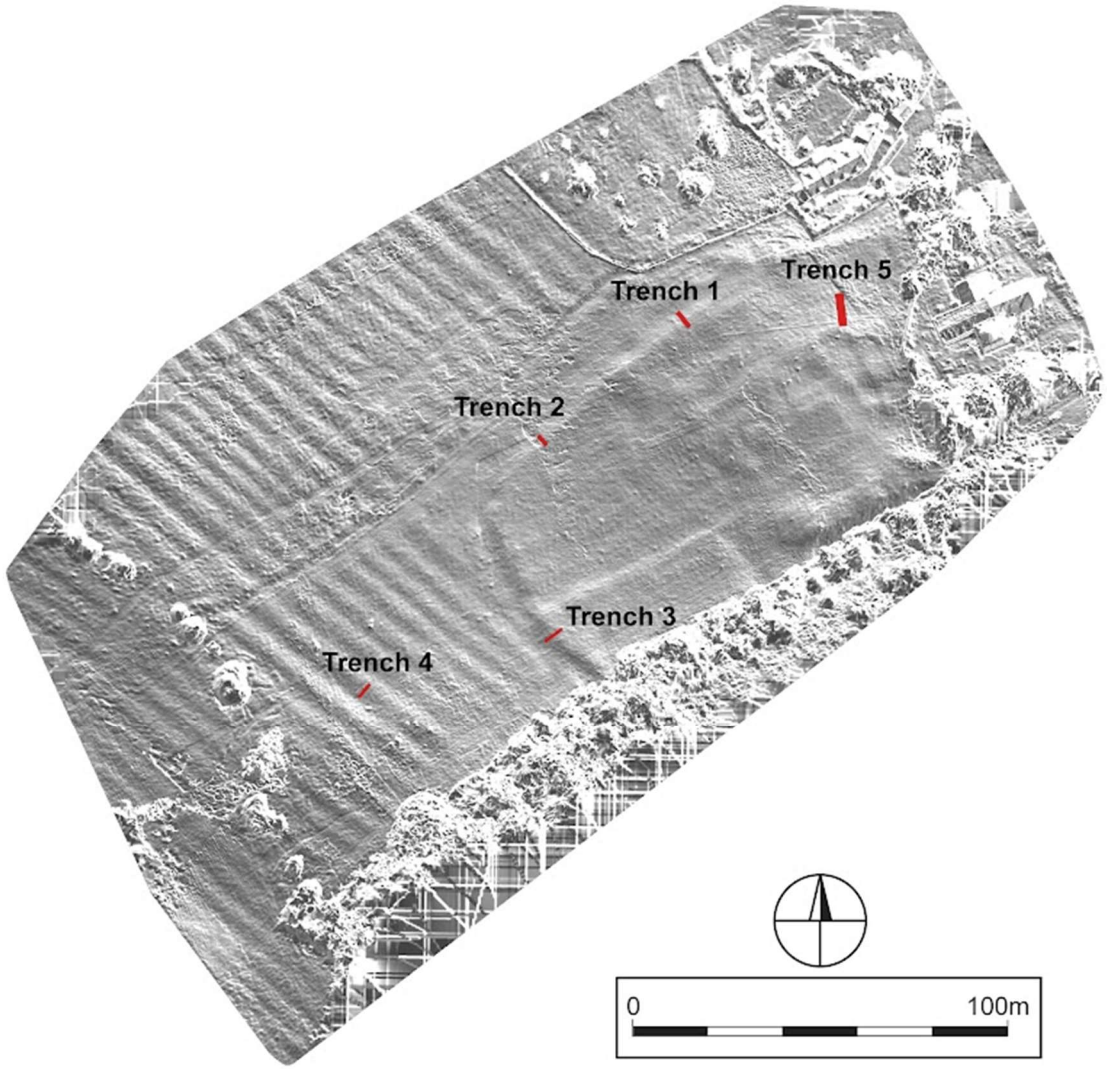

Figure 40: Location of trenches excavated to obtain samples for OSL profiling and dating.

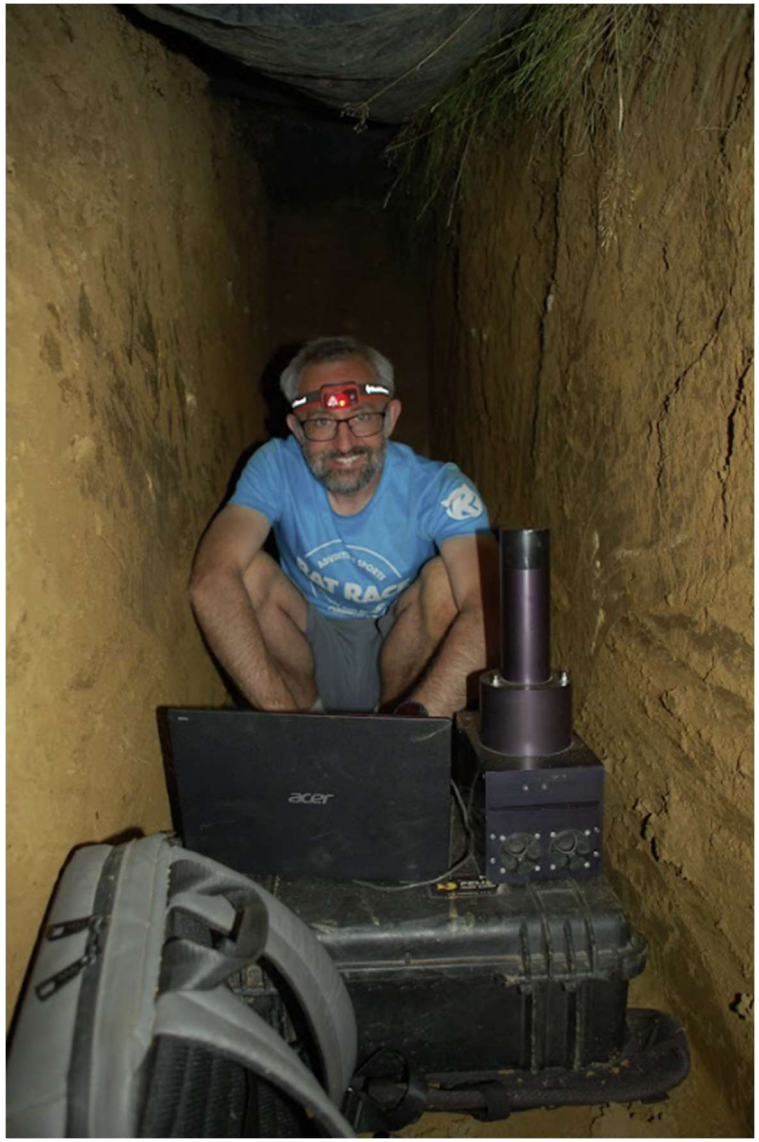

Figure 41: Retrieval of OSL samples, and profiling using portable equipment.

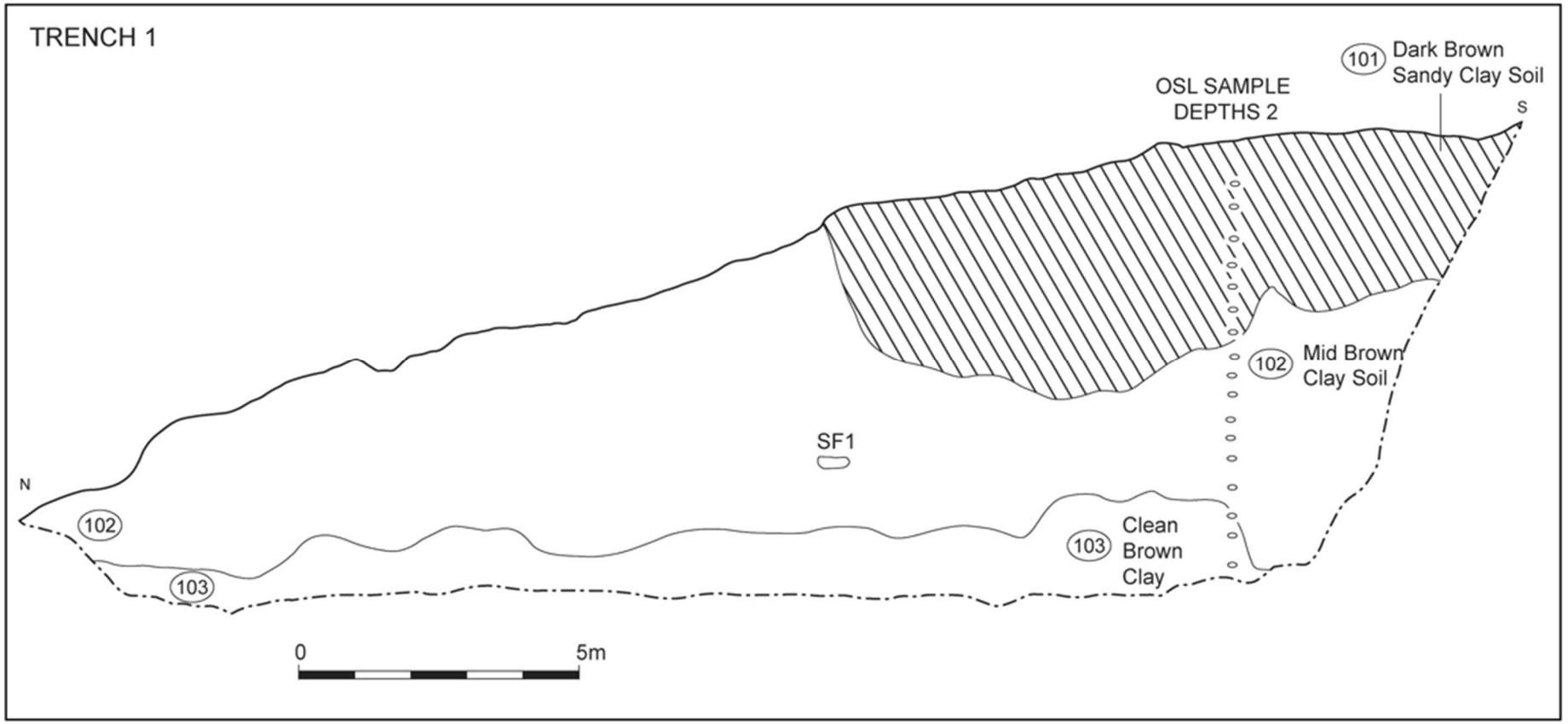

Figure 42: The west-facing section of Trench 1, showing visibly-identified archaeological contexts, OSL sample depths, and the location of a small find of pottery (SF1).

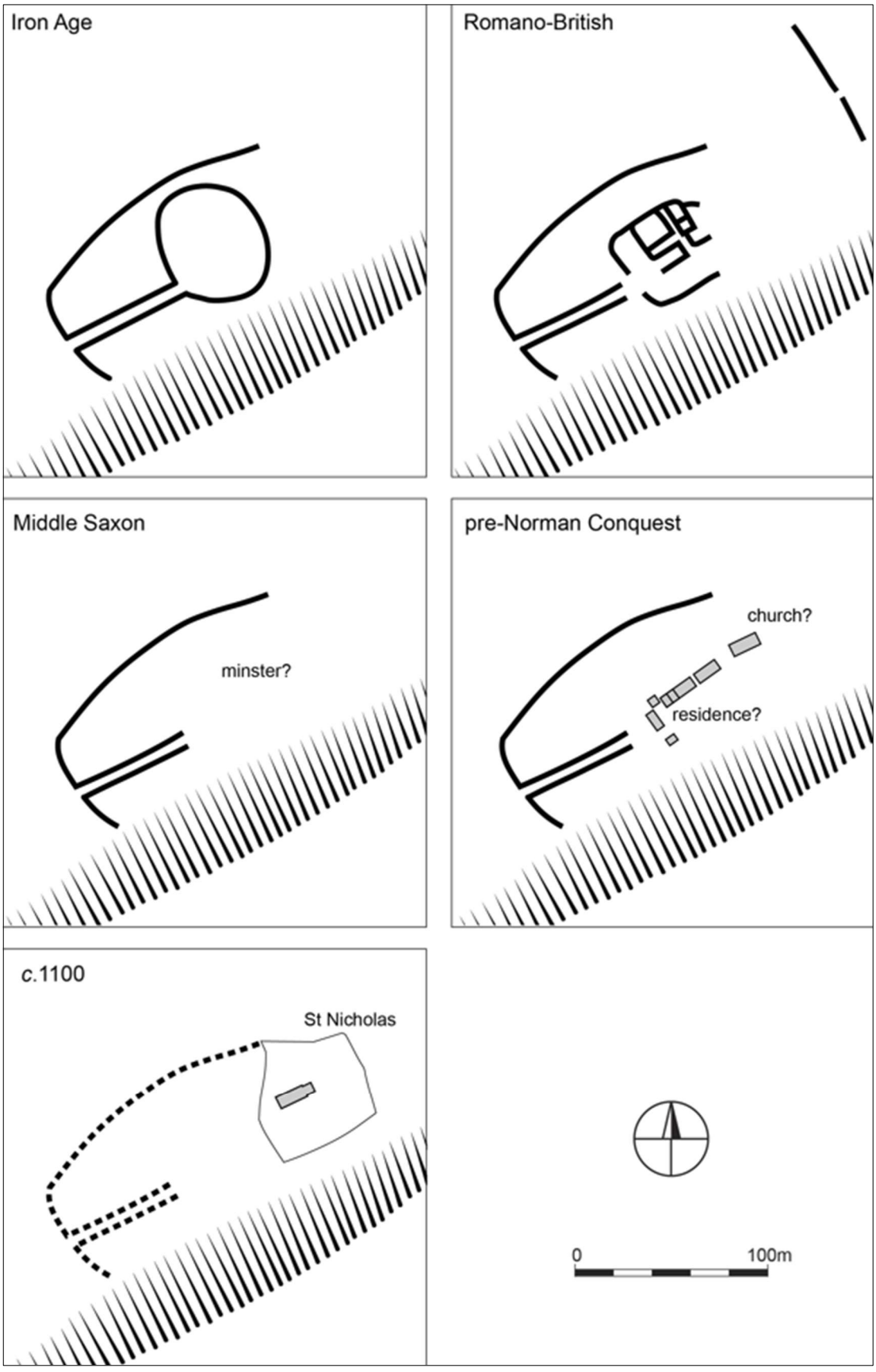

Figure 43: Conjectural phase plan of Saintbury's archaeological development.

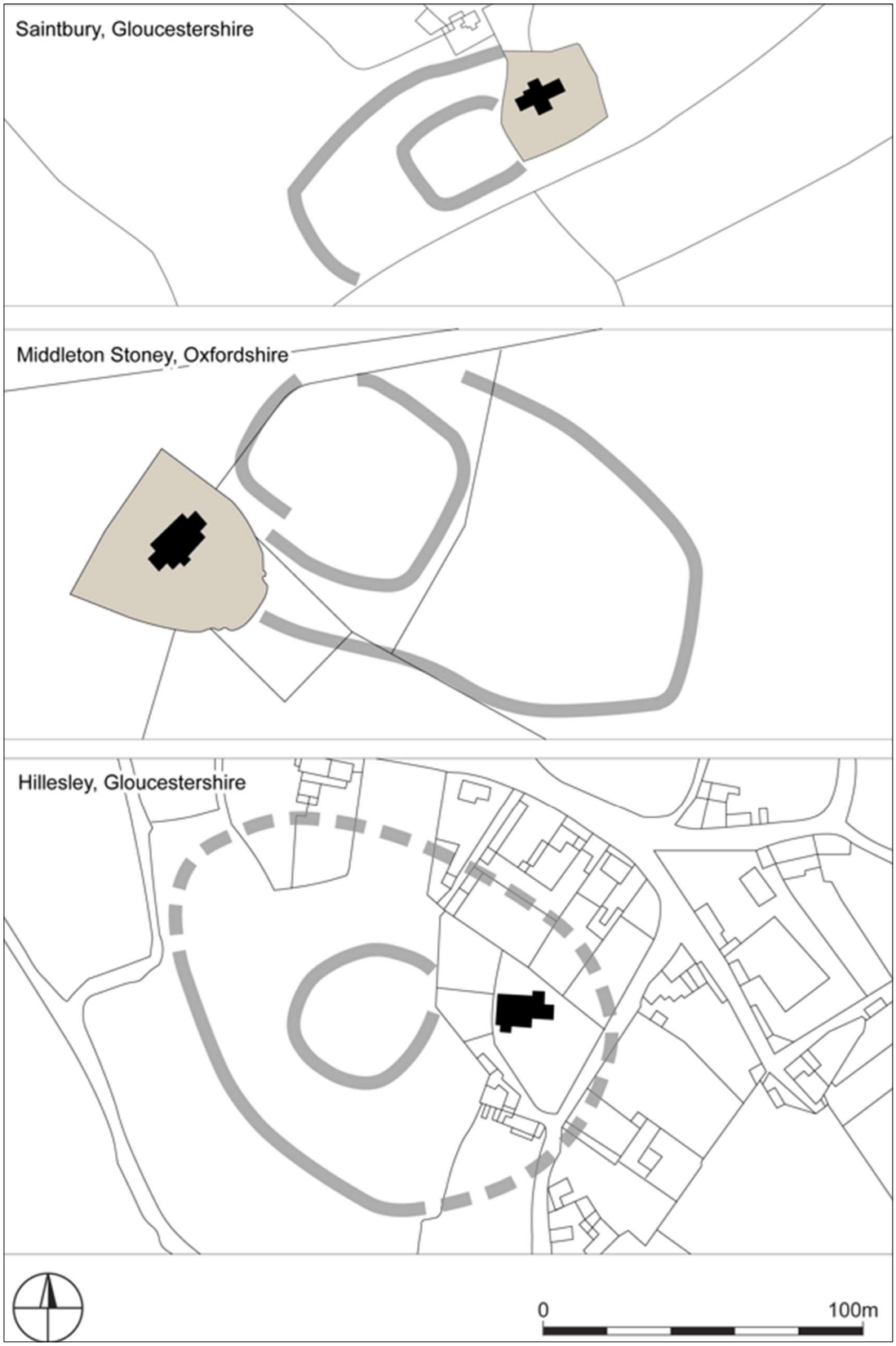
Saintbury, Gloucestershire
Middleton Stoney, Oxfordshire
Hillesley, Gloucestershire
0
100m

Figure 44: Enclosure arrangements at Saintbury, Middleton Stoney, and Hillesley, all of which have late Saxon phases and are probable lordly centres. At both Middleton Stoney and Hillesley, castles were built over earlier sites, an occurrence that did not take place at Saintbury.

APPENDIX 1: Report on the luminescence investigations at Saintbury

Tim Kinnaird, Aayush Srivastava
School of Earth and Environmental Sciences, University of St Andrews, UK

Duncan Wright, Sam Turner
School of History, Classics and Archaeology, Newcastle University, UK

Oliver Creighton
Department of Archaeology, University of Exeter, UK

Introduction

This report describes the luminescence investigations of the earthwork(s) and associated landscape features at St Nicholas Church, Saintbury. These investigations were undertaken within the wider remit of the UKRI AHRC project - *Where Power Lies: The archaeology of transforming elite centres in the landscape of medieval England c. AD 800-1200 (UKRI* AH/W001187/1).

Sampling for OSL profiling and dating (OSL-PD) took place over the 4th to 7th of September 2023. OSL was applied to constrain construction of the earthwork(s) and to date any subsequent modifications to it, and also, provide temporal constraint to landscape features in the wider landscape, including ridge and furrow. Five trenches were opened over the course of the week (fig. 1): trenches 1 and 2, sectioned the ~ NE-SW-trending earthwork; trench 3, the abutting ~ NW-SE-trending earthwork; trench 4, the system of ridge and furrow; and trench 5, the bank and ditch of a second earthwork, slightly upslope.

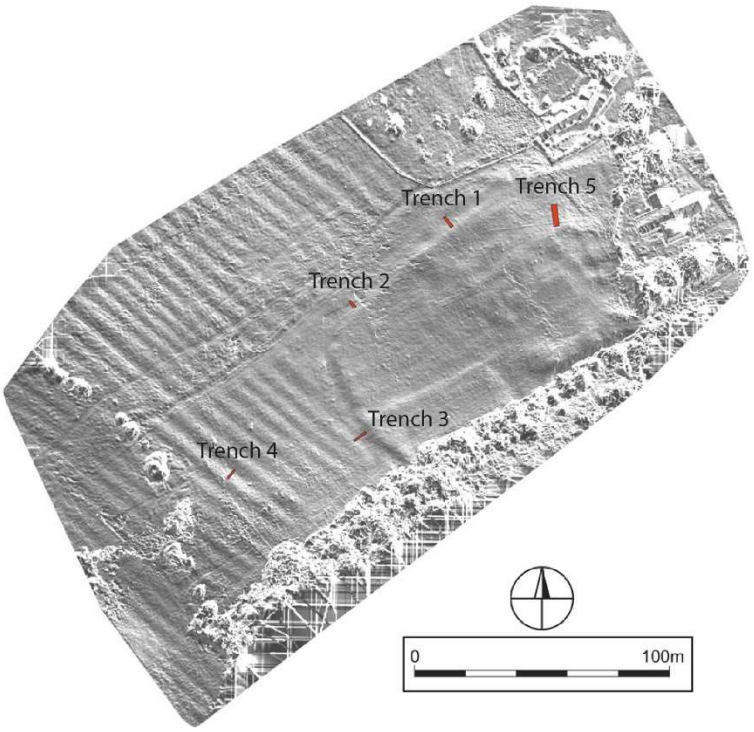

Figure 1: DTM showing the approximate locations of the 5 trenches

Methodology

The methodology utilised here is described in detail in Turner et al. (2021). It utilises a three-stage approach to luminescence investigations. The first stage concerns sample collection and OSL profiling

undertaken during excavation. The second and third stages concern more targeted analyses undertaken in the laboratory: second, to characterise the luminescence properties of prepared quartz and obtain the first approximations of apparent dose (and age); third, to determine quartz OSL depositional ages.

Stage 1: sample collection and OSL profiling

In stage 1, use is made of portable OSL equipment (Munyikwa et al. 2020) on site and in near real-time, to investigate the luminescence characteristics of bulk sediment. Figure 2 illustrates this approach. Bulk sediment is subjected to an interleaved sequence of system dark count (background), infra-red stimulated luminescence (IRSL) and OSL (Appendix A). These readings are used to calculate IRSL and OSL net signal intensities, IRSL and OSL depletion indices and IRSL:OSL ratios. In well bleached sediments, signal intensities may act as a proxy for age: lower signal intensities reflect more recent zeroing and deposition (e.g. Fig. 2, step 1A, the blue luminescence response), while higher intensities indicate sediments that were zeroed and deposited longer ago (Fig. 2, step 1A, the red response). The down-profile trends in signal intensities should respond to temporal breaks and/or stratigraphic progressions (Fig. 2, step 1B). The example shown in figure 2, step 1B is the relative luminescence sequence constructed for the sediment stratigraphy revealed in trench 2, which should encompass the earthwork and the substrate. Here, and elsewhere in the report, the sampling positions are coloured to highlight OSL signal intensity: the cooler colours reflect the lower intensities (and younger sediment), the warmer colours, the higher intensities (and older sediment).

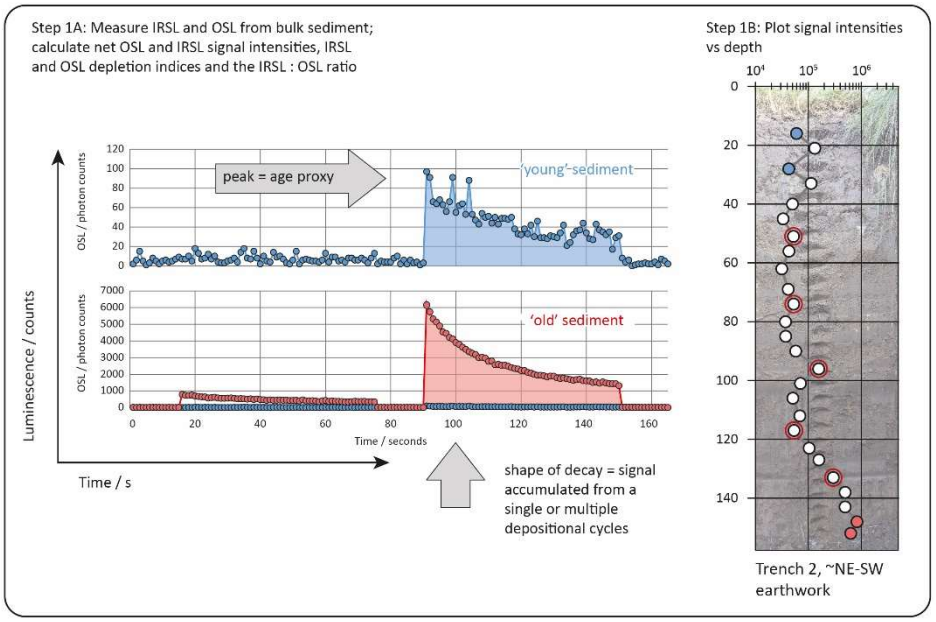

Figure 2: The methodological approach:

stage 1a, interleaved measurement sequence of dark count, IRSL and OSL, used to obtain the proxies of net signal intensities, depletion indices and the IRSL : OSL ratio

stage 1b, proxies plotted vs depth, and used to construct relaltive lumienscence stratigraphies

These field results, in combination with our archaeological and sedimentological observations, were used to position samples in the stratigraphies for dating purposes. Samples were collected from each trench. For this, steel tubes, 3.5cm in diameter, were inserted into the cleaned face of the section, extracted, and sealed. In-situ field gamma spectrometry measurements were taken from these positions using a Gamma Surveyor Vario coupled with a 19cm^3 Bismuth Germanate Oxide detector. In addition, 'bulk' samples of sediment were recovered for laboratory water content and dosimetry measurements.

Table 1 provides a list of the samples taken for OSL profiling:

Feature	Profile ID	No. of profiling samples	Depth interval sampled / cm	associated with dating sample	Significance
NE-SW earthwork	sa23-1	23	13 - 177	sa23-1 OSL1, sa23-1 OSL2	profile should encompass the bank of the earthwork and the underlying substrate; may be possible to provide TPQ and TAQ for the construction of the earthwork
NE-SW earthwork	sa23-2	28	10 - 158	sa23-2 OSL1, sa23-2 OSL2	
NW-SE earthwork	sa23-3	25	7 - 161	sa23-3 OSL1, sa23-3 OSL2	
ridge and furrow	sa23-4	22	8 - 82	sa23-4 OSL1, sa23-4 OSL2	profiles were taken through both the ridge and furrow, the juxtaposition of the two profiles should allow the ridge and furrow to be dated
NE-SW earthwork + ditch	sa23-5	35	13 - 177	sa23-5 OSL1	profiles were taken through the bank of the earthwork, and the fills of the ditch

Table 2 lists the samples collected for dating purposes:

Feature	*Field ID*	*CERSA #*	*Equivalent to profiling sample(s)*	*Depth /cm*	*Comment*
NE-SW earthwork	sa23-1 OSL1	1375	7	49	*at base of unit characterised by intensities, < 10^4 counts; base of earthwork?*
	sa23-1 OSL2	1376	15	103	*in middle of unit characterised by intensities > 10^6 count; sample positioned here, as opposed to the top of the unit, as there is a slight inflection in intensities that might indicate that sediment through 62 to 96 cm is redeposited*
	-	*1377/08	8	51	
	-	*1377/12	12	74	
	-	*1377/16	16	96	
	sa23-2 OSL1	1377	20	117	*at base of unit characterised by intensities, < 10^4 counts; base of earthwork?*
	sa23-2 OSL2	1378	23	133	*at top of unit characterised by intensities, > 10^5 counts; substrate to earthwork, TPQ for construction?*
NW-SE earthwork	sa23-3 OSL1	1379	13	87	*at base of unit characterised by intensities, < 10^4 counts; base of earthwork?*
	sa23-3 OSL2	1380	15	97	*at top of unit characterised by intensities, > 10^5 counts; substrate to earthwork, TPQ for construction?*
ridge and furrow	sa23-4 OSL1	1381	4	27	*base of furrow*
	sa23-4 OSL2	1382	15	30	*base of ridge, coherent stratigraphy*
NE-SW earthwork + ditch	sa23-5 OSL1	1383	23	64	*bank to ditch*
	-	*1383/32	32	154	*lower fill(s) of ditch*
	-	*1383/33	33	163	
	-	*1383/34	34	169	
	-	*1383/35	35	177	

Table 3 lists the gamma dose rates that were measured at each of the dating positions:

Field ID	CERSA #	*Gamma dose rates, wet / mGy a^{-1}*
sa23-1 OSL1	1375	1.16 ± 0.08
sa23-1 OSL2	1376	1.21 ± 0.08
sa23-2 OSL1	1377	1.34 ± 0.09

sa23-2 OSL2	1378	1.34 ± 0.09
sa23-3 OSL1	1379	1.35 ± 0.09
sa23-3 OSL2	1380	1.29 ± 0.09
sa23-4 OSL1	1381	1.09 ± 0.08
sa23-4 OSL2	1382	1.09 ± 0.08
sa23-5 OSL1	1383	1.10 ± 0.08

Figure 2 illustrates the distribution in OSL net signal intensities observed across the slope: the relative stratigraphies to the earthwork(s) (into substrate) are shown in the middle plots, with some broad correlations drawn from the intensities; the relative sequence to the ditch fills is shown on the left; and the stratigraphy of both the ridge and furrow on the right. The ditch is cut through the substrate, to bedrock. The ridge and furrow modifies the slope below the earthwork. These values are tabulated in Appendix A, together with the corresponding IRSL intensities, IRSL and OSL depletion indices and IRSL:OSL ratios.

The profiles through the earthwork(s) are not equivalent in time-depth: profile 1, is characterised by a depth-progression from 7.2 x 10^4 to > 1.8 x 10^6 counts; profile 2, from >3.1 x 10^4 to > 6.3 x 10^5 counts; and profile 3, from 4.4 x 10^4 to > 5.4 x 10^5 counts. Common to all though, is a transition at depth from sediment characterised by lower intensities, on the order of 10^4 counts, to sediment characterised by high intensities, > 10^5 counts. This transition occurs between 44 and 62 cm depth in profile 1, 117 and 133 cm depth in profile 2 and, 87 and 98 cm depth in profile 3. The working hypothesis was that this marked the boundary between the earthwork and substrate. Samples for dating purposes were positioned accordingly, either side of the step change in intensities.

The profiles through the ridge and furrow show similar trends, with signal-depth progressions from 8.4 x 10^4 to > 1.6 x 10^6 counts (furrow) and 7.3 x 10^4 to > 2.6 x 10^6 counts (ridge). The substrate is characterised by similar intensities, on the order of 10^6 counts. Here, though the signal-depth progression is more gradual, with only a slight inflection in gradient across the soil-substrate boundary, reflecting mixing during ploughing. The two profiles intersect at depth, potentially marking the depth of the plough in the furrow, and the base of ridge. Dating samples were positioned accordingly.

The profiles taken through the ditch are more complex, with the multiple fills characterised by discrete signal-depth progressions or signal inversions. These are indicative of change in the depositional processes, from alternating fast/slow to much slower aggradational dynamics. Fortuitously for dating, the basal fill in the axis of the ditch is characterised by lower signal intensities than observed up profile, 1.1 x 10^5 to 9.7 x10^4 counts – it likely represents a slow sedimentation, reset at deposition.

Figure 2: The distribution in OSL signal intensities across the slope: trenches 1, 2 and 3, sectioned the earthwork and substrate; trench 4, a ridge and furrow; and trench 5, the fill of a ditch

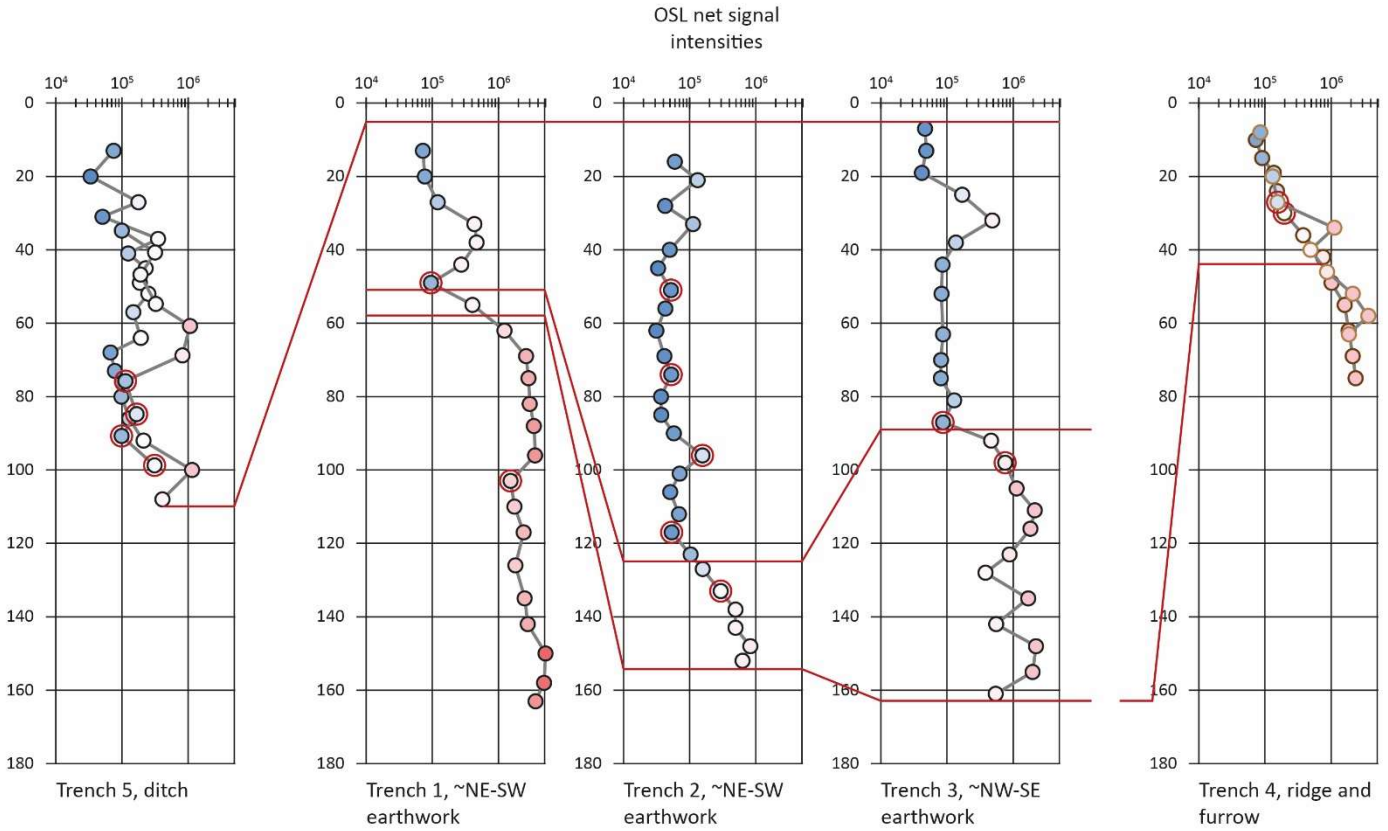

Trench 5 – Bank		Trench 5 – Ditch			Trecnh 1- ~NE-SW earthwork		Trench 2- ~NE-SW earthwork		Trench 3- ~NW-SE earthwork		Trench 4, ridge	Trench 4, furrow
sa23-5/19		sa23-5/1	sa23-5/26		sa23-1/1		sa23-2/1		sa23-3/1		SA23-4/11	SA23-4/1
sa23-5/20		sa23-5/2	sa23-5/27		sa23-1/2		sa23-2/2		sa23-3/2		SA23-4/12	SA23-4/2
sa23-5/21		sa23-5/3	sa23-5/28		sa23-1/3		sa23-2/3		sa23-3/3		SA23-4/13	SA23-4/3
sa23-5/22		sa23-5/4	sa23-5/29		sa23-1/4		sa23-2/4		sa23-3/4		SA23-4/14	SA23-4/4
sa23-5/23		sa23-5/5	sa23-5/30		sa23-1/5		sa23-2/5		sa23-3/5		SA23-4/15	SA23-4/5
sa23-5/24		sa23-5/6	sa23-5/31		sa23-1/6		sa23-2/6		sa23-3/6		SA23-4/16	SA23-4/6
sa23-5/25		sa23-5/7	sa23-5/32		sa23-1/7		sa23-2/7		sa23-3/7		SA23-4/17	SA23-4/7
		sa23-5/8	sa23-5/33		sa23-1/8		sa23-2/8		sa23-3/8		SA23-4/18	SA23-4/8
		sa23-5/9	sa23-5/34		sa23-1/9		sa23-2/9		sa23-3/9		SA23-4/19	SA23-4/9
		sa23-5/10	sa23-5/35		sa23-1/10		sa23-2/10		sa23-3/10		SA23-4/20	SA23-4/10
		sa23-5/11			sa23-1/11		sa23-2/11		sa23-3/11		SA23-4/21	
		sa23-5/12			sa23-1/12		sa23-2/12		sa23-3/12		SA23-4/21	
		sa23-5/13			sa23-1/13		sa23-2/13		sa23-3/13			
		sa23-5/14			sa23-1/14		sa23-2/14		sa23-3/14			
		sa23-5/15			sa23-1/15		sa23-2/15		sa23-3/15			
		sa23-5/16			sa23-1/16		sa23-2/16		sa23-3/16			
		sa23-5/17			sa23-1/17		sa23-2/17		sa23-3/17			
		sa23-5/18			sa23-1/18		sa23-2/18		sa23-3/18			
					sa23-1/19		sa23-2/19		sa23-3/19			
					sa23-1/20		sa23-2/20		sa23-3/20			
					sa23-1/21		sa23-2/21		sa23-3/21			
					sa23-1/22		sa23-2/22		sa23-3/22			
					sa23-1/23		sa23-2/23		sa23-3/23			
							sa23-2/24		sa23-3/24			
							sa23-2/25		sa23-3/25			
							sa23-2/26					
							sa23-2/27					

Stage 2: OSL screening and characterisation

To test the relative temporal framework outlined above, a sub-set of samples were progressed to calibrated luminescence screening and characterisation. This is stage 2 in the methodology of Turner et al. (2021), and is used to provide the first approximations of apparent dose, both in terms of magnitude and range. This is the first indication of age: low apparent doses reflect more recent zeroing and deposition (in correspondence to the low intensities in stage 1), while higher doses (the higher intensities in stage 1), indicate sediment that was deposited longer ago, or a mixing of substrate and archaeological materials.

Standard mineral preparation procedures as routinely used in the CERSA luminescence laboratories at the School of Earth and Environmental Sciences, University of St Andrews were used to extract HF-etched quartz from the samples progressed to stage 2. Luminescence sensitivities (photon counts per Gy) and stored doses (Gy) were evaluated from paired aliquots of 90-250 µm HF-etched quartz, using Risø DA-20 automatic readers (following procedures established in Burbidge et al., 2007; Kinnaird et al., 2017a,b). The readout cycles comprised a natural readout, followed by readout cycles for a nominal 1Gy test dose, 1.0, 1.9, 3.8 and 11.4 Gy regenerative doses, with further 0.9Gy test doses. A zero dose was also included, as was a repeat dose of 1.0 Gy, both with 1 Gy test doses. A 220℃ preheat held for 10s was used with 60s OSL measurements using the blue LEDs. Test doses were preheated at the same temperature as the preceding measurement, and held for the same duration.

OSL apparent doses are tabulated in table 5 for the earthwork, as sampled in trench 2, and the ditch, trench 5.

Table 5: Luminescence sensitivities (counts Gy^{-1}) and apparent doses for the sediment stratigraphies revealed in trench 2 (earthwork) and trench 5 (ditch)

Laboratory code	Depth	Apparent dose / Gy, aliquot 1	Apparent dose / Gy, aliquot 2	Sensitivity / counts Gy^{-1}, aliquot 1	Sensitivity / counts Gy^{-1}, aliquot 2		Apparent dose / Gy, mean	Sensitivity / counts Gy^{-1}, mean
CERSA1377/5	33	28.29 ± 1.51	15.40 ± 2.60	6670 ± 80	3500 ± 60		21.85 ± 6.44	5090 ± 1590
CERSA1377/6	40	2.12 ± 0.11	2.09 ± 0.19	2080 ± 50	1170 ± 30		2.10 ± 0.02	1620 ± 460
CERSA1377/7	45	4.83 ± 0.85	7.48 ± 0.91	390 ± 20	560 ± 20		6.16 ± 1.32	480 ± 90
CERSA1377/8	51	7.50 ± 2.79	2.49 ± 0.16	120 ± 10	1180 ± 30		4.99 ± 2.51	650 ± 530
CERSA1377/9	56	3.61 ± 0.16	3.87 ± 0.34	2250 ± 50	830 ± 30		3.74 ± 0.13	1540 ± 710
CERSA1377/10	62	3.89 ± 0.23	9.88 ± 0.53	1470 ± 40	2260 ± 50		6.89 ± 2.99	1870 ± 400
CERSA1377/11	69	5.93 ± 0.46	3.67 ± 0.34	1330 ± 40	750 ± 30		4.80 ± 1.13	1040 ± 290
CERSA1377/12	74	4.59 ± 0.40	4.79 ± 0.45	640 ± 30	660 ± 30		4.69 ± 0.10	650 ± 10
CERSA1377/13	80	5.21 ± 0.77	3.14 ± 0.30	290 ± 20	690 ± 30		4.17 ± 1.04	490 ± 200
CERSA1377/14	85	4.36 ± 0.44	3.91 ± 0.28	560 ± 20	1010 ± 30		4.14 ± 0.22	790 ± 220
CERSA1377/15	90	6.04 ± 0.61	5.42 ± 0.65	830 ± 30	480 ± 20		5.73 ± 0.31	650 ± 170
CERSA1377/16	96	6.87 ± 0.80	6.57 ± 1.01	510 ± 20	610 ± 20		6.72 ± 0.15	560 ± 50
CERSA1377/17	101	6.42 ± 1.40	10.36 ± 2.23	450 ± 20	460 ± 20		8.39 ± 1.97	450 ± 10
CERSA1377/18	106	10.04 ± 0.57	7.82 ± 0.34	3720 ± 60	3560 ± 60		8.93 ± 1.11	3640 ± 80
CERSA1377/19	112	7.31 ± 0.46	9.65 ± 1.66	1360 ± 40	320 ± 20		8.48 ± 1.17	840 ± 520
CERSA1377/20	117	11.2 ± 0.53	7.94 ± 0.40	4850 ± 70	2840 ± 50		9.57 ± 1.63	3840 ± 1000
CERSA1377/21	123	10.81 ± 1.02	13.02 ± 1.87	1260 ± 40	850 ± 30		11.91 ± 1.11	1050 ± 200
CERSA1377/22	127	10.96 ± 1.73	20.18 ± 4.67	360 ± 20	880 ± 30		15.57 ± 4.61	620 ± 260
CERSA1377/23	133	20.49 ± 4.46	21.75 ± 4.48	1220 ± 30	1490 ± 40		21.12 ± 0.63	1350 ± 130
CERSA1377/24	138	25.67 ± 2.26	14.33 ± 1.99	1260 ± 40	600 ± 20		20.00 ± 5.67	930 ± 330
CERSA1377/25	143	70.87±11.91	29.42±15.54	640 ± 30	410 ± 20		50.14±20.72	520 ± 120
CERSA1377/26	148	49.27 ± 4.58	55.62 ± 4.40	1460 ± 40	1730 ± 40		52.45 ± 3.17	1590 ± 130
CERSA1377/27	152	44.58 ± 4.88	19.71 ± 2.02	940 ± 30	780 ± 30		32.14±12.44	860 ± 80
CERSA1383/1	13	0.51 ± 0.03	2.79 ± 0.14	2460 ± 50	2030 ± 50		1.65 ± 1.14	2240 ± 210
CERSA1383/2	20	1.82 ± 0.14	1.94 ± 0.10	920 ± 30	1910 ± 40		1.88 ± 0.06	1420 ± 490

CERSA1383/3	27	10.16 ± 1.11	5.06 ± 0.37	2990 ± 50	1060 ± 30		7.61 ± 2.55	2030 ± 970
CERSA1383/4	31	6.29 ± 0.51	24.19 ± 5.00	670 ± 30	1060 ± 30		15.24 ± 8.95	860 ± 200
CERSA1383/5	37	12.08 ± 0.9	5.37 ± 0.24	2630 ± 50	2320 ± 50		8.73 ± 3.35	2470 ± 150
CERSA1383/6	40	5.19 ± 0.22	25.9 ± 5.08	2590 ± 50	1950 ± 40		15.54±10.36	2270 ± 320
CERSA1383/7	45	3.98 ± 0.25	4.81 ± 0.19	1240 ± 40	2740 ± 50		4.39 ± 0.42	1990 ± 750
CERSA1383/8	49	4.97 ± 0.27	6.85 ± 0.28	1150 ± 30	2360 ± 50		5.91 ± 0.94	1760 ± 610
CERSA1383/9	52	27.63 ± 6.27	25.17 ± 4.4	1460 ± 40	880 ± 30		26.4 ± 1.23	1170 ± 290
CERSA1383/10	57	6.89 ± 0.38	7.86 ± 0.71	2060 ± 50	730 ± 30		7.38 ± 0.49	1400 ± 660
CERSA1383/11	64	5.88 ± 0.38	9.00 ± 2.12	770 ± 30	480 ± 20		7.44 ± 1.56	630 ± 140
CERSA1383/12	68	6.15 ± 0.36	7.69 ± 0.40	1340 ± 40	2150 ± 50		6.92 ± 0.77	1750 ± 400
CERSA1383/13	78	5.94 ± 0.29	6.93 ± 0.36	2230 ± 50	1390 ± 40		6.44 ± 0.49	1810 ± 420
CERSA1383/14	80	6.28 ± 0.34	6.04 ± 0.40	1320 ± 40	1610 ± 40		6.16 ± 0.12	1470 ± 150
CERSA1383/15	86	4.22 ± 0.21	7.61 ± 0.94	2320 ± 50	610 ± 20		5.91 ± 1.70	1460 ± 860
CERSA1383/16	92	11.41 ± 0.62	16.71 ± 2.43	2170 ± 50	1840 ± 40		14.06 ± 2.65	2010 ± 170
CERSA1383/17	100	27.16 ± 6.48	19.64 ± 2.72	910 ± 30	570 ± 20		23.4 ± 3.76	740 ± 170
CERSA1383/18	108	18.70 ± 2.35	8.66 ± 0.57	590 ± 20	1770 ± 40		13.68 ± 5.02	1180 ± 590
CERSA1383/26	113	5.54 ± 0.44	5.47 ± 0.31	920 ± 30	1910 ± 40		5.51 ± 0.03	1420 ± 490
CERSA1383/27	119	7.64 ± 1.04	6.35 ± 0.41	2990 ± 50	1060 ± 30		6.99 ± 0.64	2030 ± 970
CERSA1383/28	125	3.08 ± 0.20	5.13 ± 0.20	670 ± 30	1060 ± 30		4.10 ± 1.03	860 ± 200
CERSA1383/29	133	16.17 ± 1.84	45.26±15.13	2630 ± 50	2320 ± 50		30.72±14.54	2470 ± 150
CERSA1383/30	139	8.10 ± 0.79	7.89 ± 0.39	2590 ± 50	1950 ± 40		8.00 ± 0.11	2270 ± 320
CERSA1383/31	147	10.07 ± 0.69	9.82 ± 0.93	1240 ± 40	2740 ± 50		9.94 ± 0.13	1990 ± 750
CERSA1383/32	154	6.33 ± 0.34	6.87 ± 0.42	1150 ± 30	2360 ± 50		6.60 ± 0.27	1760 ± 610
CERSA1383/33	163	8.71 ± 0.90	6.44 ± 0.34	1460 ± 40	880 ± 30		7.57 ± 1.14	1170 ± 290
CERSA1383/34	169	10.63 ± 1.61	6.09 ± 0.46	2060 ± 50	730 ± 30		8.36 ± 2.27	1400 ± 660
CERSA1383/35	177	7.10 ± 0.73	7.09 ± 0.33	770 ± 30	480 ± 20		7.09 ± 0.01	630 ± 140
CERSA1383/19	35	3.95 ± 0.27	4.85 ± 0.18	1020 ± 30	4190 ± 60		4.40 ± 0.45	2610 ± 1590
CERSA1383/20	42	5.40 ± 0.33	9.87 ± 0.86	2240 ± 50	950 ± 30		7.64 ± 2.23	1590 ± 650
CERSA1383/21	49	6.28 ± 1.23	8.97 ± 2.36	570 ± 20	360 ± 20		7.63 ± 1.34	470 ± 110
CERSA1383/22	53	7.82 ± 2.26	4.63 ± 0.32	280 ± 20	600 ± 20		6.22 ± 1.59	440 ± 160
CERSA1383/23	64	11.65 ± 1.46	4.78 ± 0.33	440 ± 20	850 ± 30		8.22 ± 3.43	640 ± 210
CERSA1383/24	69	13.76 ± 1.67	9.08 ± 1.17	680 ± 30	700 ± 30		11.42 ± 2.34	690 ± 10
CERSA1383/25	73	41.00 ± 6.03	27.55 ± 2.83	2460 ± 50	2030 ± 50		34.28 ± 6.73	2240 ± 210

The apparent doses are shown in figures 3 and 4: in figure 3, these are plotted versus depth; whereas in figure 4, these are overlain on the section drawing, to emphasis the spatial variation in values.

In trench 2, the down-profile trends in apparent dose largely replicate the trends observed in the field profiling dataset (fig 3.). The base of the plough soil is marked by a maxima in apparent dose, >15 Gy (corresponding with a maxima in OSL intensity). Beneath this, through the deposits constituting the bank of the earthwork, apparent doses increase with depth from ~ 2.1 to 6.6 Gy. The substrate is characterised by apparent doses that range from 10.8 to > ~20Gy. Between these, from 101 to 107 cm depth in profile, is a transitional zone – or, diffuse boundary, marked by apparent doses in the range 6.4 to 7.9 Gy. The dating samples, positioned at 117 and 133 cm depth in profile, are located in the part of the profile that might be expected to return ages that trend to geological age. Recognised this, samples from higher in the sequence, at depths of 51, 74 and 96 cm, characterised by apparent doses in the range of 2-3, 4-5 and 6-7 Gy, were progressed to dating in stage 3. These samples should encompass the full sequence to the earthwork, from construction (potentially overprinted with doses that trend to substrate-derived values), to later phasing in its construction.

A more complex distribution in apparent doses is observed in trench 5. The upper fills to the ditch <502> and <503> are characterised by heterogeneous distributions in apparent dose, ranging from ~ 4 to 27 Gy. These deposits are mixed age. Fortuitously - and replicating the earlier dataset set - the lower fill <504> is characterised by more consistent apparent dose values, 4 to 6 Gy, which might

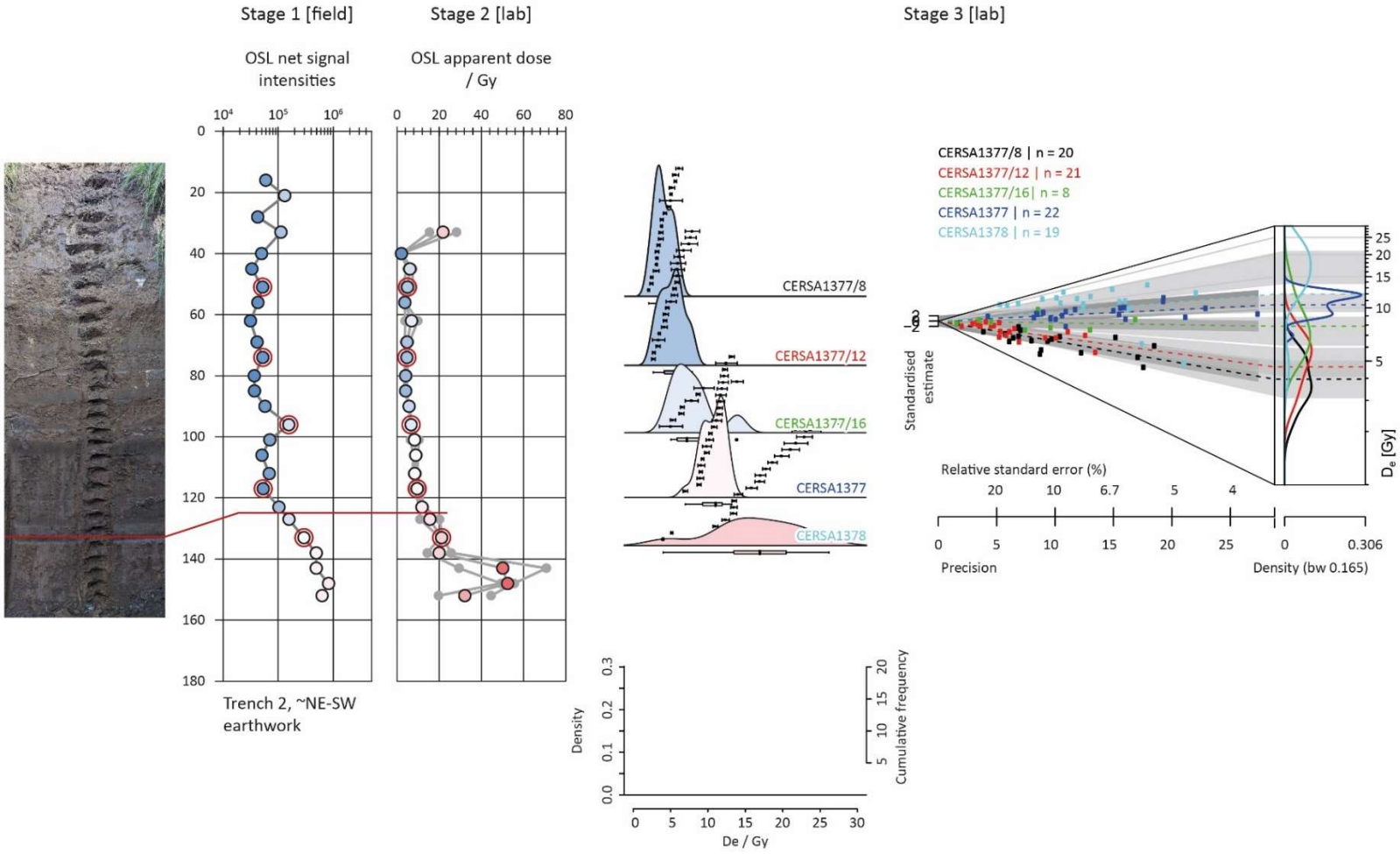

Figure 3: relative luminescence stratigraphies for the sediment revealed in trench 2; illustrating the progression from stage 1 (preliminary screening in the field), through stage 2 (laboratory characterisation) to stage 3 (quartz SAR OSL dating)

The middle plots are Kernel Density Estimate plots showing the distributions in equivalent dose for each sample, plotting these alongside the luminescence stratigraphies

The right hand plot is an Abanico plot, further illustrating the range of distributions

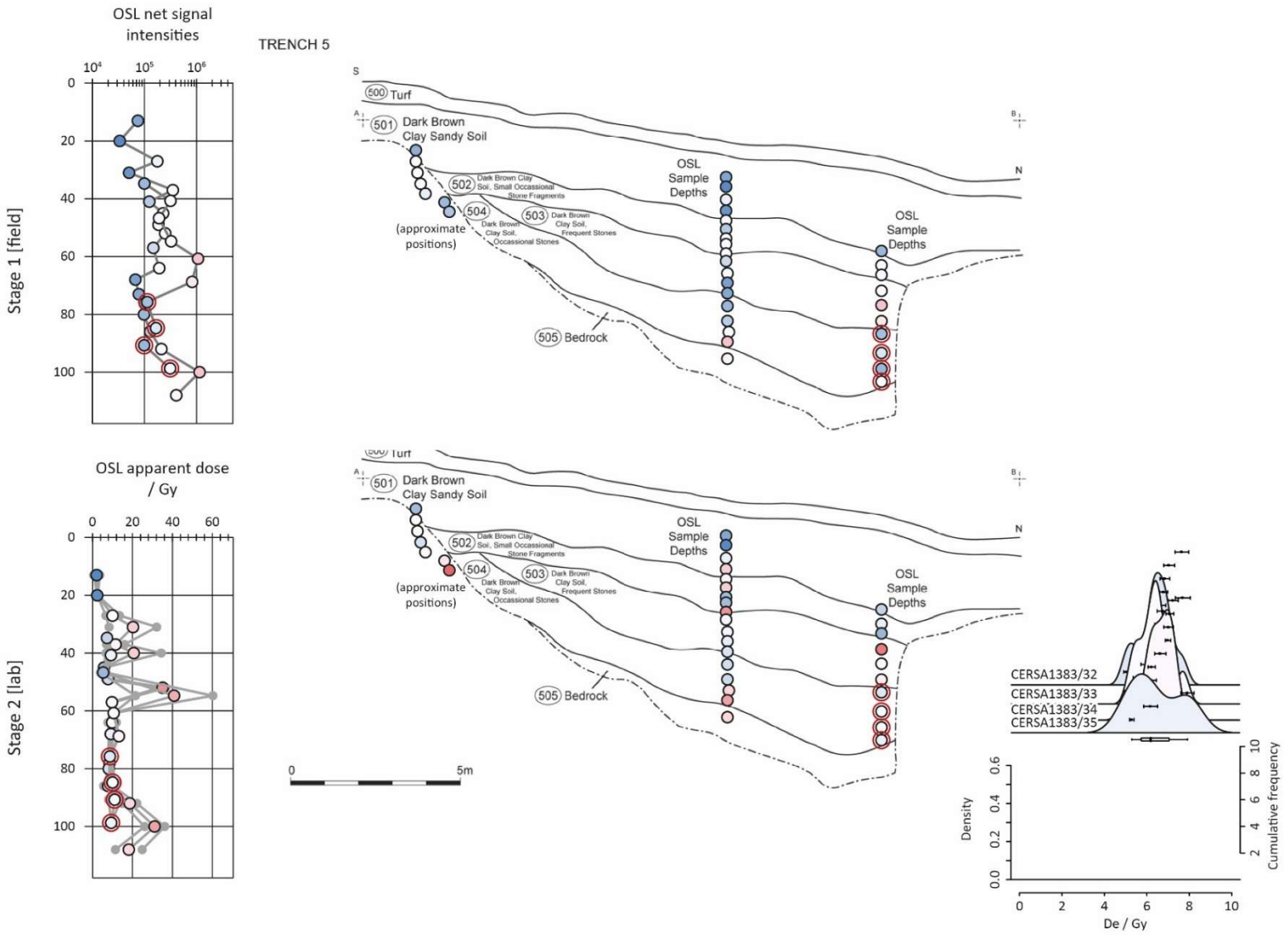

Figure 4: relative luminescence stratigraphies for the sediment revealed in trench 2; illustrating the progression from stage 1 (preliminary screening in the field), through stage 2 (laboratory characterisation) to stage 3 (quartz SAR OSL dating)

indicate that this sediment was reset at deposition. No samples had been taken from this unit for dating purposes; so, samples from the basal fill were progressed to dating.

Stage 3: Quartz SAR OSL dating

A luminescence age is the quotient of the burial dose (in Gy) over the effective environmental dose rate (in mGy a-1). It requires that the sediment was bleached prior to deposition. Here, equivalent dose (De) determinations were made on sets of 16+ aliquots using the single aliquot regenerative dose (SAR) OSL protocol. Dose rates to these sediments were assessed using the combination of in situ gamma spectrometry, and determinations of radionuclide concentrations by mass spectrometry.

Dose rate determinations. Radionuclide concentrations of ^{232}Th, ^{238}U and ^{40}K were determined from inductively coupled plasma mass spectrometry (ICP-MS; U, Th) and inductively coupled plasma optical emission spectrometry (ICP-OES; K) at X-ray Mineral Services ltd, Welshpool (Table 6). Infinite matrix α, β and γ dose rates were calculated from these using the conversion factors of Guérin et al. (2011) and adjusted for attenuation by grain size and chemical etching using the datasets of Guérin et al. (2012) and Bell (1979) respectively (Table 7).

Field and saturated water contents were determined for all samples in the laboratory (~13-16% and ~16–22%, respectively) and working values of 14–18% adopted to determine effective environmental dose rates (Ḋ). The contribution from the cosmic dose was calculated following Prescott and Hutton (1994), which takes into consideration the longitude, latitude and altitude of the profile, and the sample's depth in section. The dose rates estimates above were used in combination with the assumed burial water contents to determine the total effective dose rates for age estimation (Table 8).

Table 6: ICP-MS and ICP-OES determinations of K (%), U and Th (ppm) concentrations

Lab code / CERSA#	*Field ID*	Feature	K / %	U / ppm	Th / ppm
1375	sa23-1 OSL1	NE-SW earthwork	1.72 ± 0.10	2.04 ± 0.12	15.73 ± 0.94
1376	sa23-1 OSL2		1.39 ± 0.08	1.38 ± 0.08	16.27 ± 0.98
1377	sa23-2 OSL1		1.85 ± 0.11	2.20 ± 0.13	16.42 ± 0.99
1378	sa23-2 OSL2		1.89 ± 0.11	2.30 ± 0.14	16.09 ± 0.97
1379	sa23-3 OSL1	NW-SE earthwork	1.87 ± 0.11	2.14 ± 0.13	17.66 ± 1.06
1380	sa23-3 OSL2		1.88 ± 0.11	2.33 ± 0.14	18.34 ± 1.10
1381	sa23-4 OSL1	Ridge and furrow	2.01 ± 0.12	2.31 ± 0.14	12.09 ± 0.73
1382	sa23-4 OSL2		1.89 ± 0.11	2.40 ± 0.14	13.46 ± 0.81
1383	sa23-5 OSL1	NE-SW earthwork	2.11 ± 0.13	2.41 ± 0.14	14.74 ± 0.88

Table 7: Infinite matrix dose rates estimated from ICP-MS and ICP-OES (X-Ray Mineral Services), α and β counting (SEES) and field γ spectrometry (FGS, SEES)

Lab code/ CERSA#	ICP-MS and ICP-OES			FGS, wet / mGy a^{-1}
	α dose rate, dry /mGy a^{-1}	β dose rate, dry /mGy a^{-1}	γ dose rate, dry /mGy a^{-1}	
1375	17.29 ± 0.78	1.87 ± 0.09	1.41 ± 0.05	1.16 ± 0.08
1376	15.85 ± 0.76	1.56 ± 0.07	1.28 ± 0.05	1.21 ± 0.08
1377	18.26 ± 0.81	2.01 ± 0.09	1.49 ± 0.06	1.34 ± 0.09
1378	18.29 ± 0.81	2.04 ± 0.10	1.50 ± 0.06	1.34 ± 0.09
1379	18.99 ± 0.86	2.04 ± 0.10	1.55 ± 0.06	1.35 ± 0.09
1380	20.02 ± 0.90	2.09 ± 0.10	1.61 ± 0.06	1.29 ± 0.09
1381	15.38 ± 0.66	2.04 ± 0.10	1.34 ± 0.05	1.09 ± 0.08
1382	16.63 ± 0.72	1.99 ± 0.10	1.38 ± 0.05	1.09 ± 0.08
1383	17.61 ± 0.77	2.19 ± 0.11	1.50 ± 0.06	1.10 ± 0.08

Table 8: Effective beta and gamma dose rates following water correction. [a]Effective beta dose rate combining water content corrections with inverse grain size attenuation factors obtained Mejdahl (1979) for K, U, and Th [b] gamma dose rates reconciled from ICP-MS, µDose and field gamma spectrometry

Lab code / CERSA#	Feature	Water content / %	Cosmic dose / mGy a^{-1}	Effective dose rates, wet / mGy a^{-1}		
				β [a]	γ [b]	Ḋ
1375	sa23-1 OSL1	22 ± 11	0.18 ± 0.02	1.50 ± 0.17	1.14 ± 0.06	2.82 ± 0.19
1376	sa23-1 OSL2	21 ± 10	0.16 ± 0.02	1.27 ± 0.14	1.14 ± 0.07	2.57 ± 0.15
1377	sa23-2 OSL1	18 ± 3	0.19 ± 0.02	1.67 ± 0.09	1.23 ± 0.03	3.09 ± 0.10
1378	sa23-2 OSL2	26 ± 4	0.19 ± 0.02	1.58 ± 0.09	1.20 ± 0.03	2.97 ± 0.10
1379	sa23-3 OSL1	20 ± 3	0.17 ± 0.02	1.67 ± 0.09	1.29 ± 0.04	3.13 ± 0.10
1380	sa23-3 OSL2	19 ± 3	0.17 ± 0.02	1.72 ± 0.10	1.30 ± 0.04	3.19 ± 0.10
1381	sa23-4 OSL1	19 ± 8	0.18 ± 0.02	1.68 ± 0.15	1.11 ± 0.05	2.97 ± 0.16
1382	sa23-4 OSL2	17 ± 10	0.18 ± 0.02	1.68 ± 0.18	1.11 ± 0.05	2.97 ± 0.19
1383	sa23-5 OSL1	20 ± 2	0.18 ± 0.02	1.79 ± 0.09	1.19 ± 0.04	3.15 ± 0.10

Equivalent dose determinations and distributions. Different permutations of the assimilation of equivalent doses to obtain the burial dose were considered, including weighted combinations and statistical dose models (see Guérin et al., 2017). The weighted mean was used in age assimilations below. The distributions in equivalent dose are shown in figures 3 and 4 as Kernel Density Estimate (KDE) and Abanico plots.

Age assimilations. Table 9 lists the burial doses, environmental dose rates and corresponding depositional ages for CERSA1375-1383.

*Table 9: Burial doses, total effective environmental dose rates and corresponding depositional ages for CERSA1375-83 *likely over-estimations, on the trend to geological ages*

CERSA #	Field ID	Burial dose /Gy	Total effective dose rate / mGy a^{-1}	Age / ka	Calendar years
1375	sa23-1 OSL1	8.6 ± 3.13	2.82 ± 0.19	3.05 ± 1.13	*1030 ± 1130 BC
1376	sa23-1 OSL2	63.27 ± 4.36	2.57 ± 0.15	24.61 ± 2.24	-
1377/08	-	3.52 ± 0.33	3.09 ± 0.1	1.14 ± 0.11	AD 890 ± 110
1377/12	-	4.14 ± 0.43	2.97 ± 0.1	1.40 ± 0.15	AD 630 ± 150
1377/16	-	7.24 ± 0.93	3.13 ± 0.1	2.32 ± 0.31	290 ± 310 BC
1377	sa23-2 OSL1	10.08 ± 0.45	3.09 ± 0.1	3.26 ± 0.18	*1240 ± 180 BC
1378	sa23-2 OSL2	6.93 ± 3.31	2.97 ± 0.1	2.33 ± 1.12	310 ± 1120 BC
1379	sa23-3 OSL1	7.67 ± 0.96	3.13 ± 0.1	2.45 ± 0.32	430 ± 320 BC
1380	sa23-3 OSL2	19.11 ± 3.36	3.19 ± 0.1	6.00 ± 1.07	*3980 ± 1070 BC
1381	sa23-4 OSL1	0.99 ± 0.39	2.97 ± 0.16	0.33 ± 0.13	AD 1690 ± 130
1382	sa23-4 OSL2	2.27 ± 0.46	2.97 ± 0.19	0.77 ± 0.16	AD 1260 ± 160
1383	-	6.15 ± 0.18	3.15 ± 0.1	1.95 ± 0.09	AD 70 ± 90
1383/32	-	6.03 ± 0.29	3.15 ± 0.1	1.91 ± 0.11	AD 110 ± 110
1383/33	-	6.37 ± 0.24	3.15 ± 0.1	2.02 ± 0.10	AD 1 ± 100
1383/24	-	6.41 ± 0.33	3.15 ± 0.1	2.03 ± 0.12	10 ± 120 BC

Discussion and conclusions

The work has progressed well through stage 1 to stage 2, then on to luminescence dating. The key findings from each of these stages are reiterated here and the overall conclusions summarised.

Stage 1. A relative temporal framework was established for the sediments comprising the earthwork, and the underlying substrate. The profiles taken through the earthwork (into substrate) were not equivalent in time-depth across the site. However, each profile did share one similarity - a transition

at depth from sediment characterised by intensities on the order of 10^4 counts, to sediment characterised by intensities, 10^5 -10^6 counts. This 'transition' occurred at different depths across the earthwork(s): between 44 and 62 cm depth in profile 1, 117 and 133 cm depth in profile 2 and, 87 and 98 cm depth in profile 3. There are a couple of explanations to this: 1.) the earthwork was built across an uneven slope and at construction it might have been necessary to fill local depressions to provide a uniform foundation (this would account for the greater thickness of sediments characterised by x10^4 counts in trench 2); 2.) the lower part of the earthwork was constructed from shods of the substrate, that were rapidly stacked with minimal exposure to daylight (the slight inflection in signal intensities between 96 and 103 cm depth in profile 1, might be evidence of this). Likely, it is a combination of the two. The working hypothesis was that the sediment characterised by intensities in the range x10^4 counts indicated the earthwork, and the sediment that returned intensities > x10^5 counts, the substrate.

This hypothesis was strengthened when the investigations turned to the ridge and furrow, sectioned in trench 4. Here, there was a clear differentiation between the organic, silty loams forming the plough soil, and the compact, greyed clay loams constituting the substrate. The substrate was characterised by intensities > 10^5 counts. The signal-depth progression across this boundary is more gradual, with only a slight inflection in gradient across the boundary, which reflects mixing during ploughing. The profiles characterising the ridge and the furrow intersect at depth, indicating the base of the furrow, and the corresponding depth in the ridge. In terms of relative age, this sediment was characterised by lower signal intensities than that observed in the earthwork: the system of ridge and furrow is younger, as expected.

The investigation then considered the ditch, cut into the slope behind the earthwork(s) sampled in trenches 1 and 2. When sectioned, the ditch was found to contain 3-4 fills - <501> (potentially a drape), <502>, <503> and <504>, characterised by heterogeneous distributions in intensity, with discrete signal-depth progressions and inversions. This is indicative of the change in depositional process, from alternating fast/slow to much slower aggradational dynamics. The basal fill <504>, in the axis of the ditch, was characterised by lower signal intensities than observed up profile, and it was hoped that this reflected a slower sedimentation and a resetting of the luminescence signals at deposition. Importantly though, excluding a few outliers (representing discrete horizons carrying large residuals), the ditch fills are characterised by intensities <10^5 counts: in terms of relative age, the fill to the ditch post-dates construction of the earthwork, and pre-dates the system of ridge and furrow.

Stage 2. The apparent dose distributions observed for the sediment comprising the earthwork, the underlying substrate (trench 2) and the fills to the ditch (trench 5), strengthened the argument for the spatial and temporal relationships outlined above. Further, this phase of the investigations highlighted that the full range of archaeologically significant doses was not represented in the samples collected for dating purposes, and a number of additional samples were progressed to dating: from higher stratigraphic levels in the bank of the earthwork, and from the basal fill of the ditch.

Stage 3. The distribution in depositional ages is complex: from individual ages trending towards the geological, > 24 ka (CERSA1376), through those that represent a mixing of substrate-derived and archaeologically-significant ages (CERSA1375, 1377-1378, 1380), to those that provide temporal constraint on the construction of the earthwork(s) and additional features across the landscape (CERSA1377/8, 1377/12, 1377/16, 1379, 1381-1382, 1383/32, 1383/33, 1383/34).

The consistency between the stage 1 and stage 2 datasets, and the spatial (and temporal) correlations observed in the OSL signal intensities across the investigated sediment stratigraphies, suggest the following chronological sequence:

- a phase of soil formation, with some zeroing of the luminescence, at 3.26 ± 0.18 ka (1230 ± 180 BC)
- construction of earthwork(s) between 2.38 ± 0.22 ka (360 ± 220 BC) and 1.91 ± 0.11 ka (AD 110 ± 110). *Terminus Ante Quem* is provided by the weighted combination of the ages obtained for <504>, the basal fill of the ditch, which is cut into the slope above the earthwork(s). The earlier constraint is provided by the weighted combination of ages obtained for the sediment at the base of the earthwork in trenches 2 and 3.
- continued management of the earthwork(s) into the 7th and 9th centuries AD (1.40 ± 0.15 ka (AD 630 ± 150) and 1.14 ± 0.11 ka (AD 890 ± 110), respectively)
- development of the ridge and furrow between the 13th and 17th centuries AD (0.77 ± 0.16 ka (AD 1260 ± 160 and 0.33 ± 0.13 (AD1690 ± 130), respectively)

References

Bell, W.T., 1979. 'Attenuation factors for the absorbed radiation dose in quartz inclusions for thermoluminescence dating', *Ancient TL*, 8(2), p.12.

Bøtter-Jensen, L., Andersen, C.E., Duller, G.A. and Murray, A.S., 2003. 'Developments in radiation, stimulation and observation facilities in luminescence measurements', *Radiation Measurements*, 37(4-5), p.535-541.

Duller, G.A.T., 2003. 'Distinguishing quartz and feldspar in single grain luminescence measurements', *Radiation Measurements*, 37(2), p.161-165.

Guérin, G., Mercier, N. and Adamiec, G., 2011. 'Dose-rate conversion factors: update', *Ancient TL*, 29(1), p.5-8.

Guérin, G., Mercier, N., Nathan, R., Adamiec, G. and Lefrais, Y., 2012. 'On the use of the infinite matrix assumption and associated concepts: a critical review', *Radiation Measurements*, 47(9), p.778-785.

Kinnaird, T. C., Bolòs, J., Turner, A. and Turner, S., 2017a. 'Optically-stimulated luminescence profiling and dating of historic agricultural terraces in Catalonia (Spain)', *Journal of Archaeological Science*, 78, p.66-77.

Kinnaird, T. C., Dawson, T., Sanderson, D. C. W., Hamilton, D., Cresswell, A. and Rennel, R., 2017b, 'Chronostratigraphy of an eroding complex Atlantic round house, Baile Sear, Scotland', *Journal of Coastal and Island Archaeology*, 14(1), p.46-60.

Kinnaird, T.C., Turner, S., Castle, M. and Gaskell, D. 2023. Report on phase 1 of the luminescence investigations at ARCH EX14. Unpublished report to Headland Archaeology, August 2023Kolb, T., Tudyka, K., Kadereit, A., Lomax, J., Poręba, G., Zander, A., Zipf, L. and Fuchs, M., 2022. 'The µDose system: determination of environmental dose rates by combined alpha and beta counting – performance tests and practical experiences', *Geochronology*, 4(1), p.1-31.

Murray, A.S. and Wintle, A.G., 2000. 'Luminescence dating of quartz using an improved single-aliquot regenerative-dose protocol', *Radiation Measurements*, 32(1), p.57-73.

Murray, A.S. and Wintle, A.G., 2003. 'The single aliquot regenerative dose protocol: potential for improvements in reliability', *Radiation Measurements*, 37(4-5), p.377-381.

Prescott, J.R. and Hutton, J.T., 1994. C'osmic ray contributions to dose rates for luminescence and ESR dating: large depths and long-term time variations', *Radiation measurements*, 23(2-3), p.497-500.

Srivastava, A., Kinnaird, T.C., Sevara, C., Holcomb, J. and Turner, S. 2023. 'Dating agricultural terraces in the Mediterranean using luminescence: recent progress and challenges', *Land* 12(3), 716.

Tudyka, K., Miłosz, S., Adamiec, G., Bluszcz, A., Poręba, G., Paszkowski, Ł. and Kolarczyk, A., 2018. 'µDose: A compact system for environmental radioactivity and dose rate measurement', *Radiation Measurements*, 118, p.8-13.

Turner, S., T. Kinnaird, G. Varinlioğlu, T.E. Şerifoğlu, D. Athanassoulis, E. Koparal, V. Demirciler, K. Ødegård, J. Bolòs, J.C. Sánchez-Pardo, J. Crow, M. Jackson, F. Carrer, D. Sanderson, A. Turner. 2021. 'Agricultural terraces in the Mediterranean: intensive construction during the later Middle Ages revealed by landscape analysis with OSL-PD', *Antiquity* 95 (381), 773-790.

Appendix A: Stage 1, OSL profiling

Natural luminescence signals were measured following an interleaved sequence of system dark count (background), infra-red stimulated luminescence (IRSL) and OSL. From this IRSL and OSL net signal intensities, IRSL and OSL depletion indices and IRSL : OSL ratios were calculated (Turner et al. 2021).

Table A-1: Net signal intensities, depletion indices and IRSL:OSL ratios for profiles 1 through 5

Feature	Field ID	Depth*	IRSL signal intensities / counts	IRSL depletion	OSL signal intensities / counts	OSL depletion	IRSL : OSL ratio
	sa23-1/1	13	8210 ± 100	1.30 ± 0.03	71990 ± 270	1.26 ± 0.01	0.1141 ± 0.0014
	sa23-1/2	20	15960 ± 130	1.35 ± 0.02	77040 ± 280	1.30 ± 0.01	0.2072 ± 0.0019
	sa23-1/3	27	22690 ± 160	1.32 ± 0.02	120860 ± 350	1.44 ± 0.01	0.1878 ± 0.0014
	sa23-1/4	33	90720 ± 300	1.43 ± 0.01	435840 ± 660	1.52 ± 0.01	0.2082 ± 0.0008
	sa23-1/5	38	105390 ± 330	1.34 ± 0.01	469960 ± 690	1.48 ± 0.01	0.2243 ± 0.0008
	sa23-1/6	44	58620 ± 250	1.30 ± 0.01	275880 ± 530	1.55 ± 0.01	0.2125 ± 0.001
	sa23-1/7	49	20410 ± 150	1.27 ± 0.02	95160 ± 310	1.34 ± 0.01	0.2145 ± 0.0017
	sa23-1/8	55	110720 ± 340	1.32 ± 0.01	404270 ± 640	1.37 ± 0.01	0.2739 ± 0.0009
	sa23-1/9	62	309010 ± 560	1.32 ± 0.01	1239400 ± 1120	1.49 ± 0.01	0.2493 ± 0.0005
	sa23-1/10	69	734080 ± 860	1.38 ± 0.01	2630350 ± 1630	1.51 ± 0.01	0.2791 ± 0.0004
	sa23-1/11	75	810630 ± 900	1.35 ± 0.01	2856610 ± 1700	1.49 ± 0.01	0.2838 ± 0.0004
	sa23-1/12	82	861620 ± 930	1.35 ± 0.01	2989860 ± 1740	1.51 ± 0.01	0.2882 ± 0.0004
	sa23-1/13	88	1281700 ± 1140	1.40 ± 0.01	3459860 ± 1870	1.20 ± 0.01	0.3704 ± 0.0004
	sa23-1/14	96	1058040 ± 1030	1.35 ± 0.01	3607750 ± 1910	1.57 ± 0.01	0.2933 ± 0.0003
	sa23-1/15	103	420900 ± 650	1.35 ± 0.01	1529900 ± 1240	1.46 ± 0.01	0.2751 ± 0.0005
	sa23-1/16	110	500420 ± 710	1.35 ± 0.01	1755690 ± 1330	1.46 ± 0.01	0.285 ± 0.0005
	sa23-1/17	117	674150 ± 820	1.32 ± 0.01	2416810 ± 1560	1.45 ± 0.01	0.2789 ± 0.0004
	sa23-1/18	126	462060 ± 680	1.30 ± 0.01	1810290 ± 1350	1.48 ± 0.01	0.2552 ± 0.0004
	sa23-1/19	135	676100 ± 830	1.35 ± 0.01	2506220 ± 1590	1.50 ± 0.01	0.2698 ± 0.0004
	sa23-1/20	142	755890 ± 870	1.36 ± 0.01	2782100 ± 1670	1.50 ± 0.01	0.2717 ± 0.0004
	sa23-1/21	150	1389820 ± 1180	1.37 ± 0.01	5181610 ± 2280	1.46 ± 0.01	0.2682 ± 0.0003
	sa23-1/22	158	1340910 ± 1160	1.37 ± 0.01	4921340 ± 2230	1.57 ± 0.01	0.2725 ± 0.0003
	sa23-1/23	163	1029660 ± 1020	1.36 ± 0.01	3650710 ± 1920	1.53 ± 0.01	0.282 ± 0.0003
	sa23-2/1	10	-	-	-	-	-
	sa23-2/2	16	9650 ± 110	1.40 ± 0.03	59150 ± 250	1.59 ± 0.01	0.1631 ± 0.0019
	sa23-2/3	21	18970 ± 140	1.49 ± 0.02	131170 ± 370	1.31 ± 0.01	0.1447 ± 0.0012
	sa23-2/4	28	6000 ± 90	1.36 ± 0.04	41990 ± 210	1.46 ± 0.01	0.1429 ± 0.0022
	sa23-2/5	33	22020 ± 150	1.35 ± 0.02	111770 ± 340	1.64 ± 0.01	0.197 ± 0.0015
	sa23-2/6	40	3440 ± 70	1.40 ± 0.05	49510 ± 230	1.36 ± 0.01	0.0694 ± 0.0015
	sa23-2/7	45	4430 ± 80	1.28 ± 0.04	33080 ± 190	1.48 ± 0.02	0.1338 ± 0.0025
		51					
	sa23-2/9	56	6720 ± 90	1.24 ± 0.03	42550 ± 210	1.60 ± 0.02	0.158 ± 0.0023
	sa23-2/10	62	4650 ± 80	1.24 ± 0.04	31070 ± 180	1.51 ± 0.02	0.1498 ± 0.0026
	sa23-2/11	69	5820 ± 90	1.31 ± 0.04	41210 ± 210	1.45 ± 0.01	0.1413 ± 0.0022
	sa23-2/12	74	10170 ± 110	1.33 ± 0.03	52220 ± 230	1.51 ± 0.01	0.1948 ± 0.0022
	sa23-2/13	80	5050 ± 80	1.22 ± 0.04	36550 ± 190	1.55 ± 0.02	0.1381 ± 0.0023
	sa23-2/14	85	5670 ± 80	1.22 ± 0.03	36650 ± 200	1.52 ± 0.02	0.1547 ± 0.0024
	sa23-2/15	90	5600 ± 80	1.32 ± 0.04	57010 ± 240	1.44 ± 0.01	0.0982 ± 0.0015
	sa23-2/16	96	34120 ± 190	1.35 ± 0.02	154390 ± 400	1.67 ± 0.01	0.221 ± 0.0014
	sa23-2/17	101	11270 ± 110	1.33 ± 0.03	69980 ± 270	1.68 ± 0.01	0.161 ± 0.0017
	sa23-2/18	106	7450 ± 90	1.25 ± 0.03	50350 ± 230	1.57 ± 0.01	0.148 ± 0.002
	sa23-2/19	112	10420 ± 110	1.35 ± 0.03	68070 ± 260	1.51 ± 0.01	0.1531 ± 0.0017
	sa23-2/20	117	8340 ± 100	1.27 ± 0.03	52760 ± 230	1.60 ± 0.01	0.1581 ± 0.002
	sa23-2/21	123	21660 ± 150	1.31 ± 0.02	102320 ± 320	1.56 ± 0.01	0.2117 ± 0.0016
	sa23-2/22	127	31970 ± 180	1.31 ± 0.01	155760 ± 400	1.48 ± 0.01	0.2052 ± 0.0013
	sa23-2/23	133	68140 ± 260	1.39 ± 0.01	292040 ± 540	1.70 ± 0.01	0.2333 ± 0.001
	sa23-2/24	138	123730 ± 360	1.32 ± 0.01	488940 ± 700	1.52 ± 0.01	0.2531 ± 0.0008
NE-SW earthwork	sa23-2/25	143	125390 ± 360	1.31 ± 0.01	489550 ± 700	1.45 ± 0.01	0.2561 ± 0.0008

	sa23-2/26	148	218600 ± 470	1.36 ± 0.01	819100 ± 910	1.48 ± 0.01	0.2669 ± 0.0006
	sa23-2/27	152	163230 ± 410	1.33 ± 0.01	624050 ± 790	1.49 ± 0.01	0.2616 ± 0.0007
	sa23-2/28	158	-	-	-	-	-
NW-SE earthwork	sa23-3/1	7	5390 ± 80	1.27 ± 0.04	46520 ± 220	1.35 ± 0.01	0.1158 ± 0.0018
	sa23-3/2	13	8210 ± 100	1.26 ± 0.03	48310 ± 220	1.35 ± 0.01	0.17 ± 0.0021
	sa23-3/3	19	5840 ± 80	1.21 ± 0.03	41630 ± 210	1.29 ± 0.01	0.1403 ± 0.0021
	sa23-3/4	25	43390 ± 210	1.36 ± 0.01	168530 ± 410	1.34 ± 0.01	0.2575 ± 0.0014
	sa23-3/5	32	111240 ± 340	1.37 ± 0.01	481300 ± 700	1.53 ± 0.01	0.2311 ± 0.0008
	sa23-3/6	38	36760 ± 190	1.39 ± 0.01	135230 ± 370	1.42 ± 0.01	0.2718 ± 0.0016
	sa23-3/7	44	22550 ± 150	1.40 ± 0.02	85090 ± 290	1.43 ± 0.01	0.265 ± 0.002
	sa23-3/8	52	12800 ± 120	1.26 ± 0.02	82100 ± 290	1.28 ± 0.01	0.1559 ± 0.0015
	sa23-3/9	63	16370 ± 130	1.33 ± 0.02	86280 ± 300	1.49 ± 0.01	0.1897 ± 0.0017
	sa23-3/10	70	14590 ± 130	1.42 ± 0.02	80710 ± 290	1.41 ± 0.01	0.1808 ± 0.0017
	sa23-3/11	75	18800 ± 140	1.31 ± 0.02	80110 ± 290	1.40 ± 0.01	0.2346 ± 0.002
	sa23-3/12	81	30150 ± 180	1.34 ± 0.02	127440 ± 360	1.48 ± 0.01	0.2366 ± 0.0015
	sa23-3/13	87	16270 ± 130	1.28 ± 0.02	86910 ± 300	1.33 ± 0.01	0.1872 ± 0.0016
	sa23-3/14	92	126310 ± 360	1.33 ± 0.01	462480 ± 680	1.45 ± 0.01	0.2731 ± 0.0009
	sa23-3/15	98	198220 ± 450	1.31 ± 0.01	754950 ± 870	1.48 ± 0.01	0.2626 ± 0.0007
	sa23-3/16	105	304260 ± 560	1.30 ± 0.01	1124340 ± 1070	1.4 ± 0.01	0.2706 ± 0.0006
	sa23-3/17	111	589640 ± 770	1.34 ± 0.01	2125910 ± 1460	1.52 ± 0.01	0.2774 ± 0.0004
	sa23-3/18	116	518380 ± 720	1.36 ± 0.01	1822440 ± 1360	1.52 ± 0.01	0.2844 ± 0.0004
	sa23-3/19	123	232260 ± 490	1.34 ± 0.01	880280 ± 940	1.53 ± 0.01	0.2638 ± 0.0006
	sa23-3/20	128	106120 ± 330	1.33 ± 0.01	379360 ± 620	1.5 ± 0.01	0.2797 ± 0.001
	sa23-3/21	135	463940 ± 680	1.33 ± 0.01	1681770 ± 1300	1.5 ± 0.01	0.2759 ± 0.0005
	sa23-3/22	142	127580 ± 360	1.34 ± 0.01	550780 ± 750	1.62 ± 0.01	0.2316 ± 0.0007
	sa23-3/23	148	618120 ± 790	1.35 ± 0.01	2217420 ± 1490	1.5 ± 0.01	0.2788 ± 0.0004
	sa23-3/24	155	497460 ± 710	1.31 ± 0.01	1971810 ± 1410	1.48 ± 0.01	0.2523 ± 0.0004
	sa23-3/25	161	123820 ± 360	1.38 ± 0.01	544480 ± 740	1.7 ± 0.01	0.2274 ± 0.0007
Ridge and furrow (adjacent to Trench 3)	sa23-4/1	8	10810 ± 110	1.29 ± 0.03	84320 ± 290	1.30 ± 0.01	0.1282 ± 0.0014
	sa23-4/2	15					
	sa23-4/3	20	24290 ± 160	1.37 ± 0.02	129590 ± 360	1.53 ± 0.01	0.1874 ± 0.0013
	sa23-4/4	27	30920 ± 180	1.33 ± 0.02	154040 ± 400	1.44 ± 0.01	0.2007 ± 0.0013
	sa23-4/5	34	313530 ± 560	1.38 ± 0.01	1110500 ± 1060	1.58 ± 0.01	0.2823 ± 0.0006
	sa23-4/6	40	118910 ± 350	1.37 ± 0.01	486010 ± 700	1.60 ± 0.01	0.2447 ± 0.0008
	sa23-4/7	46	224160 ± 480	1.36 ± 0.01	864940 ± 930	1.57 ± 0.01	0.2592 ± 0.0006
	sa23-4/8	52	466050 ± 690	1.37 ± 0.01	2114150 ± 1460	1.72 ± 0.01	0.2204 ± 0.0004
	sa23-4/9	58	807860 ± 900	1.38 ± 0.01	3632470 ± 1910	1.76 ± 0.01	0.2224 ± 0.0003
	sa23-4/10	63	398750 ± 640	1.35 ± 0.01	1850570 ± 1370	1.68 ± 0.01	0.2155 ± 0.0004
	sa23-4/11	10	10060 ± 110	1.32 ± 0.03	72530 ± 270	1.31 ± 0.01	0.1388 ± 0.0016
	sa23-4/12	15	17590 ± 140	1.32 ± 0.02	90860 ± 300	1.40 ± 0.01	0.1936 ± 0.0017
	sa23-4/13	19	27960 ± 170	1.33 ± 0.02	135560 ± 370	1.41 ± 0.01	0.2062 ± 0.0014
	sa23-4/14	24	32440 ± 180	1.30 ± 0.01	152070 ± 390	1.44 ± 0.01	0.2133 ± 0.0013
	sa23-4/15	30	44270 ± 220	1.29 ± 0.01	195640 ± 450	1.45 ± 0.01	0.2263 ± 0.0012
	sa23-4/16	36	92570 ± 310	1.31 ± 0.01	378960 ± 620	1.62 ± 0.01	0.2443 ± 0.0009
	sa23-4/17	42	195560 ± 450	1.34 ± 0.01	754240 ± 870	1.58 ± 0.01	0.2593 ± 0.0007
	sa23-4/18	49	260310 ± 510	1.30 ± 0.01	1013860 ± 1010	1.47 ± 0.01	0.2568 ± 0.0006
	sa23-4/19	55	382670 ± 620	1.35 ± 0.01	1604720 ± 1270	1.63 ± 0.01	0.2385 ± 0.0004
	sa23-4/20	62	473930 ± 690	1.35 ± 0.01	1847230 ± 1370	1.60 ± 0.01	0.2566 ± 0.0004
	sa23-4/21	69	518620 ± 720	1.35 ± 0.01	2129630 ± 1470	1.64 ± 0.01	0.2435 ± 0.0004
	sa23-4/22	75	552320 ± 750	1.38 ± 0.01	2360760 ± 1540	1.71 ± 0.01	0.234 ± 0.0004
	sa23-4/23	82	-	-	-	-	-
NE-SW earthwork and ditch	sa23-5/1	13	9700 ± 110	1.32 ± 0.03	74170 ± 280	1.45 ± 0.01	0.1308 ± 0.0015
	sa23-5/2	20	2730 ± 60	1.31 ± 0.05	33370 ± 190	1.46 ± 0.02	0.0817 ± 0.002
	sa23-5/3	27	23580 ± 160	1.27 ± 0.02	176760 ± 420	1.38 ± 0.01	0.1334 ± 0.001
	sa23-5/4	31	6930 ± 90	1.29 ± 0.03	50300 ± 230	1.40 ± 0.01	0.1378 ± 0.0019
	sa23-5/5	37	66380 ± 260	1.34 ± 0.01	350860 ± 600	1.5 ± 0.01	0.1892 ± 0.0008
	sa23-5/6	41	15320 ± 130	1.29 ± 0.02	123530 ± 360	1.45 ± 0.01	0.124 ± 0.0011

	sa23-5/7	45	36410 ± 200	1.32 ± 0.01	227900 ± 480	1.45 ± 0.01	0.1598 ± 0.0009
	sa23-5/8	49	27880 ± 170	1.35 ± 0.02	185330 ± 430	1.58 ± 0.01	0.1504 ± 0.001
	sa23-5/9	52	41490 ± 210	1.35 ± 0.01	250020 ± 500	1.53 ± 0.01	0.1659 ± 0.0009
	sa23-5/10	57	29970 ± 180	1.31 ± 0.02	146980 ± 390	1.42 ± 0.01	0.2039 ± 0.0013
	sa23-5/11	64	36130 ± 190	1.34 ± 0.01	191150 ± 440	1.71 ± 0.01	0.189 ± 0.0011
	sa23-5/12	68	9560 ± 110	1.23 ± 0.03	66750 ± 260	1.51 ± 0.01	0.1432 ± 0.0017
	sa23-5/13	73	12610 ± 120	1.31 ± 0.02	77830 ± 280	1.57 ± 0.01	0.1619 ± 0.0016
	sa23-5/14	80	18340 ± 140	1.37 ± 0.02	97560 ± 320	1.51 ± 0.01	0.188 ± 0.0016
	sa23-5/15	86	20620 ± 150	1.30 ± 0.02	127850 ± 360	1.43 ± 0.01	0.1613 ± 0.0013
	sa23-5/16	92	48790 ± 230	1.31 ± 0.01	210410 ± 460	1.47 ± 0.01	0.2319 ± 0.0012
	sa23-5/17	100	276280 ± 530	1.38 ± 0.01	1139090 ± 1070	1.60 ± 0.01	0.2425 ± 0.0005
	sa23-5/18	108	100330 ± 320	1.33 ± 0.01	405810 ± 640	1.45 ± 0.01	0.2472 ± 0.0009
	sa23-5/19	35	13900 ± 130	1.31 ± 0.02	86170 ± 300	1.44 ± 0.01	0.1613 ± 0.0016
	sa23-5/20	42	38810 ± 200	1.32 ± 0.01	189690 ± 440	1.63 ± 0.01	0.2046 ± 0.0012
	sa23-5/21	49	41170 ± 210	1.35 ± 0.01	230960 ± 480	1.67 ± 0.01	0.1783 ± 0.001
	sa23-5/22	57	50000 ± 230	1.40 ± 0.01	254500 ± 510	1.87 ± 0.01	0.1965 ± 0.001
	sa23-5/23	64	36120 ± 200	1.36 ± 0.01	176070 ± 420	1.55 ± 0.01	0.2051 ± 0.0012
	sa23-5/24	69	18100 ± 140	1.32 ± 0.02	99180 ± 320	1.47 ± 0.01	0.1825 ± 0.0015
	sa23-5/25	73	24990 ± 160	1.29 ± 0.02	118070 ± 350	1.46 ± 0.01	0.2116 ± 0.0015

Appendix B: Stage 2, laboratory OSL characterisation and screening

Natural luminescence signals were measured following an interleaved sequence of system dark count (background), infra-red stimulated luminescence (IRSL) and OSL. From this IRSL and OSL net signal intensities, IRSL and OSL depletion indices and IRSL : OSL ratios were calculated (Turner et al. 2021).

Table B-1: Apparent doses (Gy) and sensitivities (counts Gy^{-1}) for profiles 1 through 5